Analysis, Design, and Implementation of a Formula SAE Cooling System

by
Zachary Theroff

A THESIS

submitted to

Oregon State University

University Honors College

in partial fulfillment of
the requirements for the
degree of

Honors Baccalaureate of Science in Mechanical Engineering
(Honors Scholar)

Presented May 31, 2016
Commencement June 2016

AN ABSTRACT OF THE THESIS OF

Zachary Theroff for the degree of Honors Baccalaureate of Science in Mechanical Engineering presented on May 31, 2016. Title: Analysis, Design, and Implementation of a Formula SAE Cooling System.

Abstract approved:

_____

Robert K. Paasch

This project consists of the analysis, design, and manufacturing of the 2016 cooling system for Global Formula Racing's combustion vehicle. Several water configurations were examined, using computational fluid dynamics (CFD) to estimate airflow and heat transfer calculations in MATLAB to estimate heat rejection through each concept. Data used to perform calculations was collected in previous years, both during vehicle testing and dynamometer testing. A configuration was selected based on these results and the diffuser and ducts were designed to implement the radiators chosen. Sensors were added to the system in order to determine the effectiveness of the thermal management of the system at various points in the cooling loops. Recommendations for system improvement and expansion are provided for future iterations of the cooling system for both the combustion and electric vehicles. Details of the manufacturing steps are provided in an appendix both as documentation of what was accomplished and as a guide for future students.

Key Words: Cooling, Radiator, Analysis, Formula SAE

Corresponding e-mail address: zachary.theroff@gmail.com

Analysis, Design, and Implementation of a Formula SAE Cooling System

by
Zachary Theroff

A THESIS

submitted to

Oregon State University

University Honors College

in partial fulfillment of
the requirements for the
degree of

Honors Baccalaureate of Science in Mechanical Engineering
(Honors Scholar)

Presented May 31, 2016
Commencement June 2016

Honors Baccalaureate of Science in Mechanical Engineering project of Zachary Theroff presented on May 31, 2016.

APPROVED:

Robert K. Paasch, Mentor, representing Mechanical Engineering

Nancy Squires, Committee Member, representing Mechanical Engineering

Brian M. Fronk, Committee Member, representing Mechanical Engineering

Toni Doolen, Dean, University Honors College

I understand that my project will become part of the permanent collection of Oregon State University, University Honors College. My signature below authorizes release of my project to any reader upon request.

Zachary Theroff, Author

Contents

1. Project Description 3
1.1 Introduction 3
1.2 Rules and Constraint Analysis 3
1.3 Requirements 7
2. Current State Analysis and Benchmarking 9
2.1 Current State Analysis 9
2.1.1 Current State 9
2.1.2 SWOT Analysis 23
2.2 Benchmarking 23
2.2.1 Thermal Considerations 23
2.2.2 Mass Considerations 31
3. Design Analysis 33
3.1 Radiator Set-up and Plumbing 33
3.2 Diffuser - General Design Considerations 40
3.3 Ducting - Converging Duct Discussion 41
4. Design Selected 42
4.1 Rationale for Selection 42
4.1.1 Radiator Selection 43
4.1.2 Diffuser 45
4.1.3 Jack Bar 49
4.1.4 Ducts 50
4.1.5 Plumbing 53
4.1.6 Other Parts 56
4.2 Technical Specification 57
5. Testing 64
5.1 Tests Completed to Date 64
5.1.1 Forces 64
5.1.2 Cooling 64
5.2 Tests to Complete 68
6. Conclusion 68
6.1 Project Reflection 68
6.2 Key Areas of System Improvement 69
7. Acknowledgments 70

8. Works Cited....70
Appendix A: Manufacturing....73
A.1 Part Drawings....73
A.2 Manufacturing Plan....75
A.3: Implementation....84
A3.1 Aerodynamic Cooling Elements....84
A3.2 Water Plumbing Elements....114
A3.3 Oil Plumbing Elements....127
A3.4 Other Parts....131
Appendix B: Code....148
B.1 Heat Transfer Calculations for Radiator Configurations....148

1. Project Description

1.1 Introduction

Formula SAE (FSAE) provides a proving ground for schools around the globe to compete with small formula vehicles. These cars are constructed and driven by the students of each university in a series of events that not only test speed, but several other performance quality characteristics as well. Points can be earned by having a quick time, but it is just as important to have a design that that is efficient and marketable, a fact that Global Formula Racing (GFR) takes very seriously. In taking advantage of the way scores are determined in these competitions, the goal is not simply to have the fastest car at competition. Rather, GFR approaches the competitions to earn the most points. By leveraging the tools available to GFR for simulation and point calculation, the effect on score can be traced from tweaks made to various parts of the vehicle.

Global Formula Racing is a collaborative team, with students at Oregon State University and Germany's Duale Hochschule Baden-Württemberg-Ravensburg (DHBW-R) working to create two vehicles, one powered by an electric motor (the eCar) and one powered by a combustion engine (the cCar). Both cars must operate at peak operating condition, which is where this project comes in. The cooling system for the cCar must strike a middle ground between keeping the car from overheating while not keeping the car too cool. Overcooling would result in poor engine performance and efficiency, hindering the success of the car in several competition events, especially the endurance event. Excessive cooling is also indicative of superfluous equipment, resulting in a system that is unnecessarily heavy. Running the vehicle too hot comes with a slew of problems, too, including thinning of oil and damage to the engine. Therefore calculations must be carefully executed to ensure that a reasonable operating temperature can be achieved quickly and maintained over the course of the most grueling events.

This project can be split into two distinct parts. First, the cooling system of the cCar was selected based upon the cooling requirements of the vehicle, acting as a continuation of the 2014 Heat Transfer report by Andrew Vandenbrink [1]. The cCar uses two loops, one for water cooling the engine and one for the engine's oil lubricant. The second portion of this project is the design and manufacturing of aerodynamic parts, including cooler ducting and a diffuser, as well as all necessary mounting. This phase of the project involved getting sufficient airflow through the radiators to hit the desired operating temperatures while mitigating drag and lift forces.

This project will serve to not only provide the cooling system for the cCar (as well as duct and diffuser design for the eCar) in the 2016 Formula SAE year, but also give reference for future heat transfer analysis of the vehicle, including modeling the cCar's engine as a heat source and finding ways to dissipate that heat in an efficient manner. This project should help GFR adapt to the newest design of the car that utilizes side wings in finding better cooling methods.

1.2 Rules and Constraint Analysis

Unless otherwise specified, all indented text in this section comes straight from the 2016 FSAE rules [2].

> **T2.1 Vehicle Configuration**
> The vehicle must be open-wheeled and open-cockpit (a formula style body) with four (4) wheels that are not in a straight line.

Definition of "Open Wheel" – Open Wheel vehicles must satisfy all of the following criteria:

a. The top 180 degrees of the wheels/tires must be unobstructed when viewed from vertically above the wheel.
b. The wheels/tires must be unobstructed when viewed from the side.
c. No part of the vehicle may enter a keep-out-zone defined by two lines extending vertically from positions 75mm in front of and 75mm behind, the outer diameter of the front and rear tires in the side view elevation of the vehicle, with tires steered straight ahead. This keep-out zone will extend laterally from the outside plane of the wheel/tire to the inboard plane of the wheel/tire. See the figure "Keep Out Zones" below.
d. Must also comply with the dimensions/requirements of Article 9 Aerodynamic devices.

This rule helps define the general size and dimension constraints of the vehicle. These restrictions affect the locations available for placing the coolers, especially for investigations in placing the coolers between the wheels on the car's sides. This rule is illustrated in the below Figure 1.1.

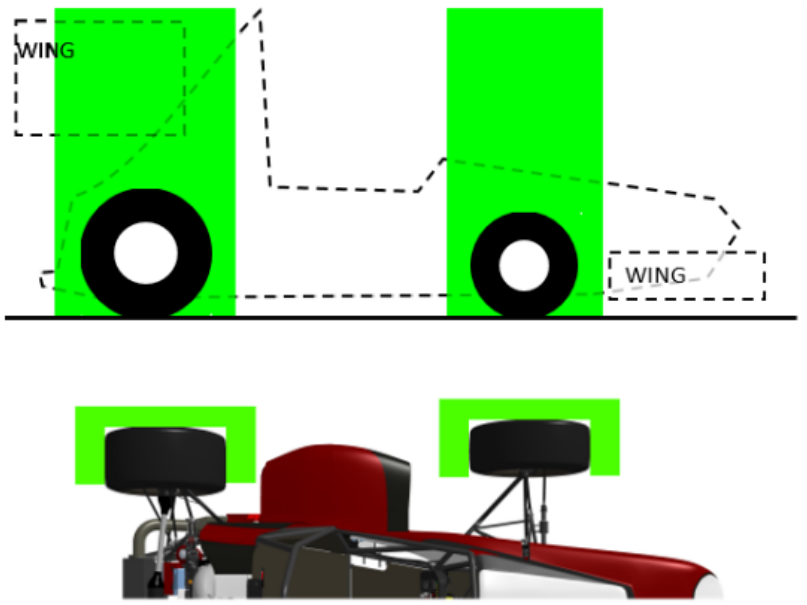

Figure 1.1: The keep-out zones, dictated by the green boxes and defined in the preceding paragraph [2].

Firewall

T4.5.1 A firewall must separate the driver compartment from all components of the fuel supply, the engine oil, the liquid cooling systems and any high voltage system (PART EV - EV1.1). It must protect the neck of the tallest driver. It must extend sufficiently far upwards and/or rearwards such that any point less than 100 mm (4 ins.) above the bottom of the helmet of the tallest driver shall not be in direct line of sight with any part of the fuel system, the cooling system or the engine oil system.

When implementing any cooling features, it is important to be mindful of where the operator will be. Any cooling lines and components needed to be safely tucked away to prevent harm to the driver.

T6.6 Jacking Point

T6.6.1 A jacking point, which is capable of supporting the car's weight and of engaging the organizers' "quick jacks", must be provided at the rear of the car.

T6.6.2 The jacking point is required to be:

a. Visible to a person standing 1 meter (3 feet) behind the car.
b. Painted orange.
c. Oriented horizontally and perpendicular to the centerline of the car
d. Made from round, 25 – 29 mm (1 – 1 1/8 inch) O.D. aluminum or steel tube
e. A minimum of 300 mm (12 inches) long
f. Exposed around the lower 180 degrees (180°) of its circumference over a minimum length of 280 mm (11 in)
g. The height of the tube is required to be such that:
    i. There is a minimum of 75 mm (3 in) clearance from the bottom of the tube to the ground measured at tech inspection.
    ii. With the bottom of the tube 200 mm (7.9 in) above ground, the wheels do not touch the ground when they are in full rebound.
h. Access from the rear of the tube must be unobstructed for at least 300mm of its length

The jacking point rules above place some restrictions on the design and implementation of a rear diffuser for the coolers. As with T2.1, these rules help define the space available for part placement on the vehicle. As the diffuser mounts to the bottom rear of the vehicle, the jack bar was installed as a component of the diffuser.

T8.1 Coolant Fluid Limitations
Water-cooled engines must only use plain water. Electric motors, accumulators or HV electronics can use plain water or oil as the coolant. Glycol-based antifreeze, "water wetter", water pump lubricants of any kind, or any other additives are strictly prohibited.

T8.1 above states that only plain water may be used for water-cooled engines. Additionally, other components, such as electric motors or accumulators, may use oil. This rule is important to defining the working fluid of the cooling of the engine.

T8.2.1 Any cooling or lubrication system must be sealed to prevent leakage.

T8.2.1 dictates that there can be no leaks in the cooling system. This is discussed further under T8.5.1 and T8.5.2 below.

T8.2.2 Separate catch cans must be employed to retain fluids from any vents for the coolant system or engine lubrication system. Each catch-can must have a minimum volume of ten (10) percent of the fluid being contained or 0.9 liter (one U.S. quart) whichever is greater. NOTE: Motorcycle engine/gearbox combinations must comply with T8.2.2.
T8.2.3 Any vent on other systems containing liquid lubricant, i.e., a differential or gearbox, must have a catch-can with a minimum volume of ten (10) percent of the fluid being contained or 50ml, whichever is greater.
T8.2.4 Catch cans must be capable of containing boiling water without deformation, and be located rearwards of the firewall below the driver's shoulder level, and be positively retained, i.e. no tie-wraps or tape.
T8.2.5 Any catch can on the cooling system must vent through a hose with a minimum internal diameter of 3 mm (1/8 inch) down to the bottom levels of the Frame.

Rules T.8.2.2 through T.8.2.5 deal with the catch cans required for the vehicle. Volume is defined as the greater of 10% of fluid circulating or 0.9 liters for engine coolant system or the greater of 10% of fluid circulating or 50ml for other liquid lubricants on the vehicle. The rules specifically state that the catch cans

must be able to contain boiling water (or water at approximately 100°C). It should be noted, though, that hot oil may need to be contained as well, which is estimated to be up to 110°C, despite not specifically mentioned in the rules. As the water and lubrication loops contain fluid well below 9 liters each, the catch cans were designed to hit the 0.9 liter capacity mark.

> **T8.5.1 Tilt Test - Fluids** During technical inspection, the car must be capable of being tilted to a forty-five degree (45°) angle without leaking fluid of any type.
> **T8.5.2** The tilt test will be conducted with the vehicle containing the maximum amount of fluids it will carry during any test or event.

The tilt test is part of the technical inspection. The test involves rotating the vehicle up to 45°, at which point any leaking fluids will result in the team not being able to compete. For this reason it is absolutely critical that no leaks be present. This largely involves having plumbing with good fittings and no structural issues such as cracks in the pipes.

> **T9.2 Location – *Front Mounted Devices***
> **T9.2.1** In plan view, no part of any aerodynamic device, wing, under tray or splitter can be:
> a. Further forward than 700 mm (27.6 inches) forward of the fronts of the front tires
> b. Wider than the outside of the front tires measured at the height of the hubs.
> **T9.3 *Location Rear Mounted Devices:***
> **T9.3.1** In plan view, no part of any aerodynamic device, wing, undertray or splitter can be:
> a. Further rearward than 250 mm (9.8 inches) rearward of the rear of the rear tires
> b. Further forward than a vertical plane through the rearmost portion of the front face of the driver head restraint support, excluding any padding, set (if adjustable) in its fully rearward position (excluding undertrays).
> c. Wider than the inside of the rear tires, measured at the height of the hub centerline.
> **T9.3.2** In side elevation, no part of the rear wing or aerodynamic device (including end-plates) may be higher than 1.2 meters above the ground when measured without a driver in the vehicle

T9.2 deals with restrictions on the front end of the vehicle while T9.3 discusses keep-out zones relating to the rear of the vehicle. Both sets of rules help continue to define the area available for implementing aerodynamic devices (including the ducting and, if used, rear diffuser for the cooling components). Special care was taken to keep the rear diffuser from extending too far rearward or outward.

> **T9.5.1** All forward facing wing edges including wings, end plates, Gurney flaps, wicker bills and undertrays that could contact a pedestrian must have a minimum radius of 5 mm (0.2 inches) for all horizontal edges and 3mm (0.12 inches) for vertical edges (end plates). The 3/5mm radius requirements must be achieved with permanently affixed components and with specific design intent to meet this radius requirement.

T9.5.1 does not restrict the high level design so much as it states a necessary feature to be present on the parts. Should a part be located such that it could contact someone while the vehicle is in operation, a radius of 5mm (horizontal edge) or 3mm (vertical edge) must be added. Unless a judge specifically calls into question the design, this rule does not apply to the elements used on the 2016 car.

> **T9.7.1** All aerodynamic devices must be designed such that the mounting system provides adequate rigidity in the static condition and such that the aerodynamic devices do not oscillate or move excessively when the vehicle is moving. In Technical Inspection this will be checked by pushing on the aerodynamic devices in any direction and at any point.

NOTE: The following should be seen as guidance as to how this rule will be applied but actual conformance will be up to technical inspectors at the respective competitions. The overall aim is to reduce the likelihood of wings detaching from cars whilst they are competing.

1. If any deflection is significant, then a force of approximately 200N can be applied and the resulting deflection should not be more than 25mm and any permanent deflection less than 5mm.
2. If any vehicle on track is observed to have large, uncontrolled movements of aerodynamic devices, then officials will have the right to Black Flag the car for inspection and the car may be excluded from that run and until any issue identified is rectified.

T9.7.1 adds a required strength and rigidity aspect to any aerodynamic features. Design features and material selection helped to prevent this from becoming an issue for the cooling system.

1.3 Requirements

Design Parameters and Points

One of the factors contributing to the continued success of GFR is its focus on points rather than focusing strictly on speed. A tool used to make design choices is equating design decisions to a point change [3]. Table 1.1 summarizes some of those changes below using parameters from the 2012 cCar. According to the table, by increasing various parameters by specified values, the points received over the course of a competition can be predicted. These trends are important to making design choices for the vehicle.

Table 1.1: Design parameters and their impact on competition points [3].

cCar	GFR12c Baseline						
1 kg vehicle mass		**Acceleration**	**Skidpad**	**Autocross**	**Endurance**	**Fuel**	**Total**
FSAE	*% Faster*	*-0.082*	*-0.055*	*-0.093*	*-0.093*		
	Points	-0.171	-0.141	-0.413	-0.725	-0.054	**-1.503**
FSG / FSA	*% Faster*	*-0.082*	*-0.055*	*-0.093*	*-0.093*		
	Points	-0.171	-0.195	-0.429	-1.087	-0.092	**-1.973**
1 N-m engine torque		**Acceleration**	**Skidpad**	**Autocross**	**Endurance**	**Fuel**	**Total**
FSAE	*% Faster*	*0.771*	*0.000*	*0.166*	*0.166*		
	Points	1.606	0.000	0.758	1.329	-0.693	**3.000**
FSG / FSA	*% Faster*	*0.771*	*0.000*	*0.166*	*0.166*		
	Points	1.606	0.000	0.788	1.995	-2.340	**2.049**
10 mm CG height		**Acceleration**	**Skidpad**	**Autocross**	**Endurance**	**Fuel**	**Total**
FSAE	*% Faster*	*0.167*	*-0.158*	*-0.258*	*-0.258*		
	Points	0.356	-0.406	-1.159	-2.033	0.000	**-3.242**
FSG / FSA	*% Faster*	*0.167*	*-0.158*	*-0.258*	*-0.258*		
	Points	0.356	-0.556	-1.205	-3.052	0.000	**-4.457**
10 N downforce		**Acceleration**	**Skidpad**	**Autocross**	**Endurance**	**Fuel**	**Total**
FSAE	*% Faster*	*0.000*	*0.075*	*0.112*	*0.112*		
	Points	0.000	0.194	0.504	0.885	0.011	**1.594**
FSG / FSA	*% Faster*	*0.000*	*0.075*	*0.112*	*0.112*		
	Points	0.000	0.265	0.524	1.328	-0.053	**2.064**
10 N drag		**Acceleration**	**Skidpad**	**Autocross**	**Endurance**	**Fuel**	**Total**
FSAE	*% Faster*	*-0.154*	*0.000*	*-0.035*	*-0.035*		
	Points	-0.336	0.000	-0.149	-0.262	-0.635	**-1.382**
FSG / FSA	*% Faster*	*-0.154*	*0.000*	*-0.035*	*-0.035*		
	Points	-0.318	0.000	-0.165	-0.417	-0.635	**-1.535**

Cooling Requirements

Because engines operate more efficiently at hotter temperature, the engine should be allowed to heat up as quickly as possible. Excessive temperatures will be harmful to the car, so the cooling system should only allow the car to reach a desired maximum. The 2016 cCar water loop should keep the water between 90℃ and 100℃, while the oil should be allowed to reach temperatures no higher than 115℃, based on discussion with cPowertrain technical lead Eric Bramlett. The system in place for the cCar activates a fan on the radiator once the engine reaches 105℃, switching off once the temperature reaches 95℃. The 2015 eCar is also equipped with a fan to enhance cooling, as shown in Section 2.1. The 2016 system was designed to keep the engine operating at temperature sufficiently high for proper efficiency while keeping the temperature low enough to mitigate the chance of overheating.

Aerodynamic Requirements

As can be seen in Table 1.1, mass, downforce, and drag are the most influential parameters on competition points, with downforce being almost twice as sensitive as drag. While the system's function is to keep the engine at a desired operating temperature, these are the areas that will result in loss or gain of points.

Downforce and drag are especially critical to note. Because cooling ducts contain radiators, there is almost certainly going to be high pressure within the ducts. With a relative low pressure above the duct, the car would experience a lift force (or, in other words, a negative downforce). The duct design aims to limit any lift force. Additionally, radiators with higher surface area will result in higher skin friction drag, which impacted the selected configuration. That said, there are far more points to be received from increasing downforce versus drag, so it will be important to remain mindful of the effect of a design on both these aspects.

Other Design Requirements

Mass and center of gravity should be addressed before proceeding. The cooling system needs to be as light as possible but still able to execute its function. This is where overcooling becomes a significant issue. While keeping the engine too cool can be somewhat detrimental to performance, it also means that there is unnecessary weight on the car. An example would be the fan used to cool the water; ideally, the design would not need such a part. Finally, controlling the location of the cooling components can keep the center of gravity of the car low, retaining as many points as possible associated with events that benefit from center of gravity height. Considering the density of water and the weight of the cooling elements and radiators, the coolers' positions in the x-y plane was selected to keep the weight tight and reduce moment of inertia about the yaw axis.

2. Current State Analysis and Benchmarking

2.1 Current State Analysis

2.1.1 Current State

2013-2014 Performance Comparison

The cooling system has gone through considerable changes, even in just the past few years. The 2013 car design utilized a new front wing system. This helped generate better front downforce, but the sidepods, in which the radiators were situated, did not receive enough air, stifling heat transfer and causing the engine to overheat [4]. Moving to 2014, GFR was able to dedicate more personnel to redesign the sidepods, allowing for better ducting to tap into the air flowing around the car and side wings. However, this design proved to be too effective in cooling, corresponding to inefficient engine performance and unnecessary weight.

Table 2.1: Performance characteristics of the 2014 GFR sidepods vs the 2013 GFR sidepods [4].

Performance Characteristic	GFR 2014	GFR 2013	% Improvement
Weight (no endplate)	211.13 g	444.4 g	52%
Weight (including endplate)	1,007 g	444.4 g	127%
Mass Flow Rate	0.465 kg/sec	0.05 kg/sec	830%
Total Vehicle Downforce	1176.6 N	844.2 N	39%
Total Vehicle Drag	423.2 N	396.2 N	7%
Side-Pod Downforce	-10 N	-31 N	-68%
Side-Pod Drag	-0.8 N	-0.2 N	300%

Table 2.1 above shows the result of Austin Volk's 2014 sidepod project. Of interest is the huge increase in mass flow rate of air, up 830% to 0.465 kg/s. This is a vast improvement over 2013's 0.05 kg/s. However, due to the addition of side wings in 2015, this sidepod design could not be built upon further; for the 2015 year, the coolers were moved to the back of the car.

2015

Cooling System - General Design

Moving to 2015, a critical change to the rules made it necessary to redesign several aspects of the aerodynamic devices on the cars. The 2014 cars were able to capitalize on large rear wing designs to take advantage of point gains from large amounts of downforce. However, moving to 2015, the rules regarding rear wings were changed to restrict size significantly. To counter these rule changes, the 2015 cars were built with side wings to recoup some of the lost downforce. This was not a perfect solution, though, as the sidepods needed a new place to take in air. The cooling system in 2015 was moved to the rear of the vehicle, placed on a diffuser. Due to the difficulty in air reaching the radiators in this location, there was room for improvement for the cooling system. While functional, the system did not perform at as high a level as the 2014 cCar.

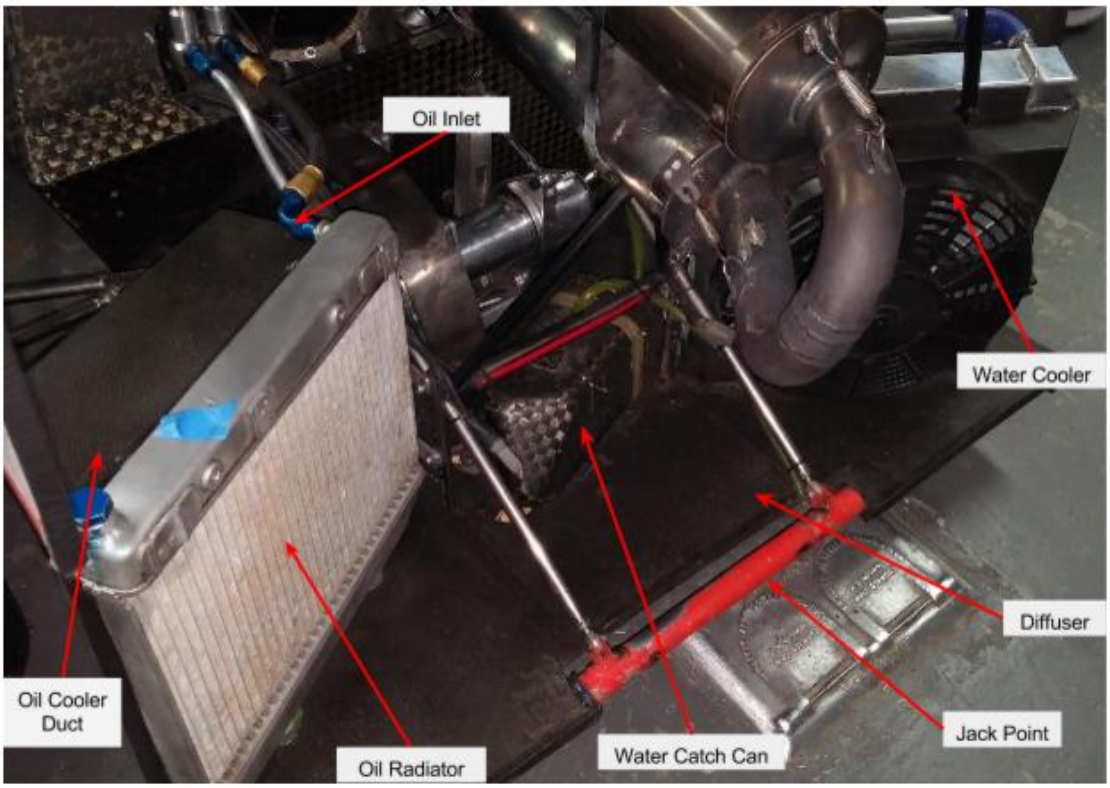

Figure 2.1: Rear diffuser and various components.

Water Cooling System

The water cooler was positioned on the right side, with the oil cooler sitting on the left side. Figure 2.2 below shows the water cooling system in detail. Hot water enters the top-left of the radiator and cool water exits at the bottom-right. The yellow tubing seen at the top right of the right image allows steam or otherwise overflowing water to exit the radiator and run to a catch can (not pictured) when the system reaches an excessively high pressure determined by the radiator cap. The left portion of Figure 2.2 clearly shows where the rear duct and front duct meet on the radiator. Air enters the front of the ducting and exits past a fan (shown in Figure 2.3). The fan is triggered when the system reaches a specified temperature, approximately 105℃. The fan then turns off once the engine reaches roughly 95℃.

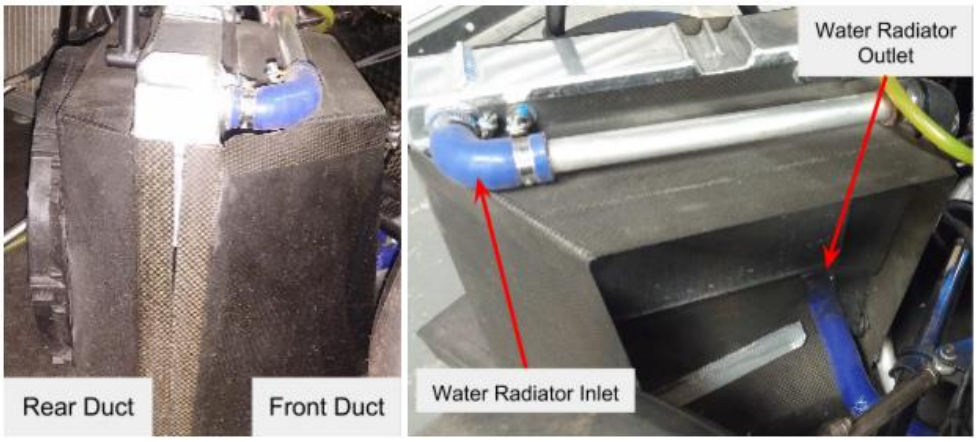

Figure 2.2: Right cooling duct side view showing radiator between rear and front ducts (left), air intake view (right).

When it comes to analyzing the heat transfer of a system such as this, there are two primary aspects to consider: air flowing through the radiator fins and water flowing through the radiator tubes. All else equal, the more air flowing through the fins per second corresponds to an increase in the heat dissipation of the system. This is because fresh, cool air is moving across the fins faster, replacing the air that is whisking away energy via convection and can be seen in the following equation:

$$C = c_p \dot{m} \qquad \text{Eq. (2.1)}$$

where $c_p$is the specific heat capacity of the fluid in question [J/kg*K] and $\dot{m}$is the mass flow rate of the fluid in [kg/s]. $C$is known as the heat capacity rate and helps relate a fluid's change in temperature to the energy transferred to or from said fluid, as in the equation:

$$q = CdT \qquad \text{Eq. (2.2)}$$

where $q$is heat transferred in [W] and $dT$is the change in the fluid's temperature in [K]. With a higher heat capacity rate, the same heat can be transferred for a lower change in temperature. Conversely, more heat can be transferred for similar temperature difference. What is important to note is that increasing the mass flow rate of air keeps the air cooler as it passes through the radiator, resulting in an overall lower fluid temperature at a given point along the fins of the radiator. This enhances the ability of the radiator to reject heat as the temperature difference remains as high as possible. To think of the process qualitatively, with slower airflow, the fluid stagnates and heats up faster, increasing temperature and diminishing the effectiveness of the fluid as the fluid temperature approaches fin temperature. Determining the airspeed through the coolers is not particularly easy, however, as airspeed is related to car speed, which is especially difficult to consider during turns and cornering. In addition, when the car stops, there is effectively no forced convection through the radiator. Typically, the cars use the previously mentioned fan to assist with cooling when airflow is insufficient. This fan can be better seen in the below image. Fan operation should be limited as it uses valuable energy from the car's battery. Otherwise, the battery may become too depleted to restart the engine during the endurance event's driver change or become unable to supply other systems with electricity.

The fluid in the cooling loops may be allowed to reach relatively high pressures. Inspection of the radiator cap showed a pressure rating of around 2 bar, about twice atmospheric pressure. In other words, if the pressure at the cap reaches 2 bar, the radiator will begin to pass water through the previously mentioned yellow tubing into a catch can; it is critical to limit how much water leaves the system to prevent the catch can from overflowing.

Figure 2.3: Right cooling duct exhaust, showing fan and fan shroud, as well as the diffuser upon which the cooling components sit.

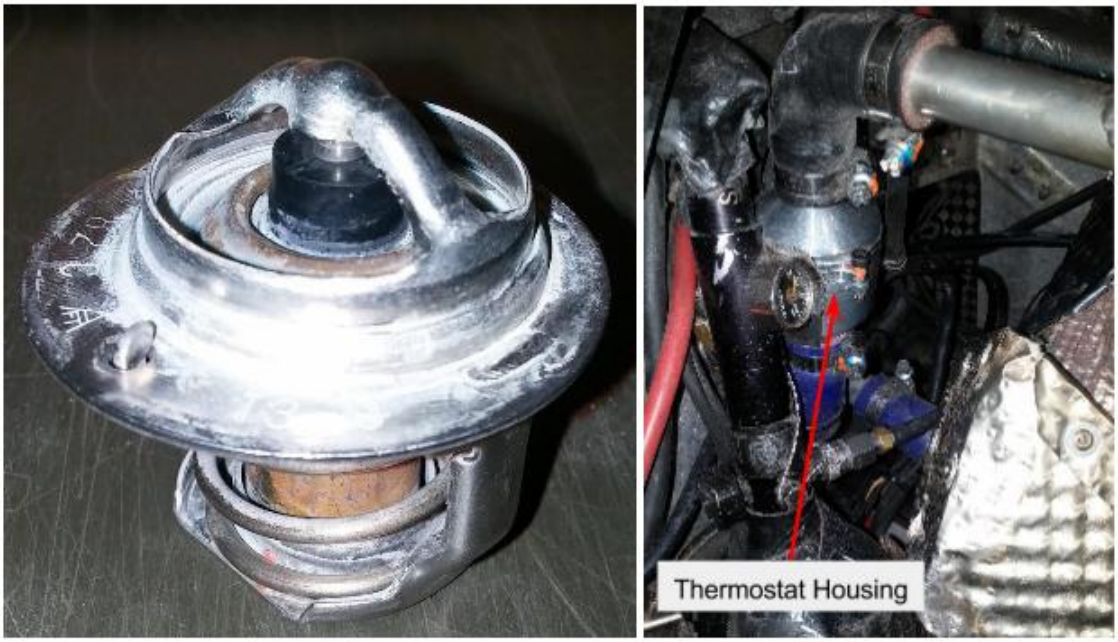

Figure 2.4: The thermostat (left) and where it was located in its housing in the 2015 cCar (right).

The flow of water can be loosely controlled using a device known as a thermostat, pictured above. This type of thermostat uses wax. The idea of a thermostat is to block the flow of the coolant, typically while the engine is initially heating up. This allows the engine to quickly reach its desired operating temperature, improving performance. This particular thermostat has a wax element that melts when the engine gets up to temperature, at which point the thermostat opens up, allowing fluid to flow. The 2015 cCar uses a thermostat rated to melt at about 82-83℃. As can be seen in the Figure 2.4 image on the right, the thermostat is housed in the engine bay, but not directly on the engine.

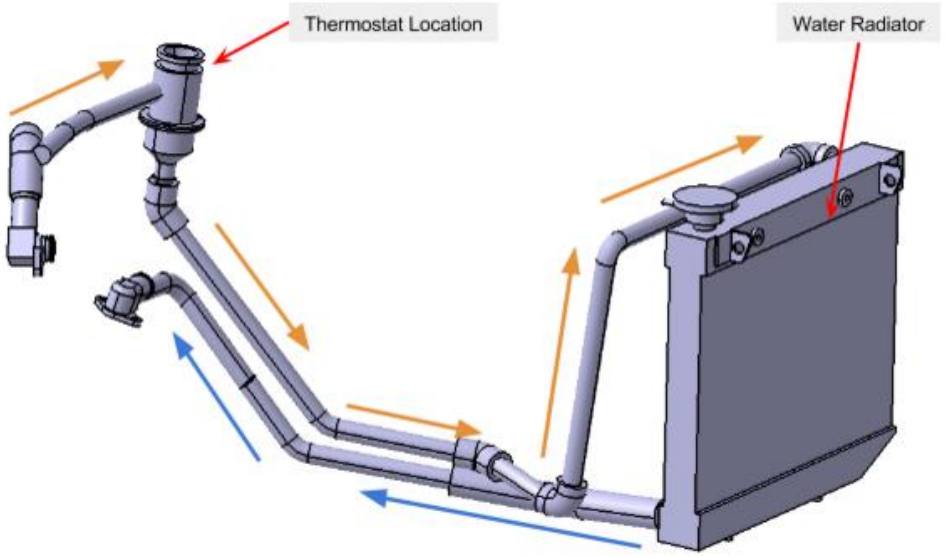

Figure 2.5: Water loop CATIA models from the2015 cCar model; orange arrows track incoming hot water, while blue arrows show the direction of flow of the cooled water.

The general design of the water cooling loop can be seen in the above CATIA model. The hot water enters the radiator at the top (after passing by the thermostat), then returns to the engine (not pictured) from the bottom of the radiator. This allows gravity to do part of the work of moving the fluid; pumping up through the narrow banks of tubes in the radiator would be unnecessary work. The capabilities of the system are further explored in Section 2.2, including the heat rejected from the engine to the water and flow rate of water as a rough function of engine speed in rotations per minute [rpm]. For now, it should be noted that based on MoTeC data, the engine pump manages to hit a volumetric flow rate of approximately 70 liters per minute at the high end.

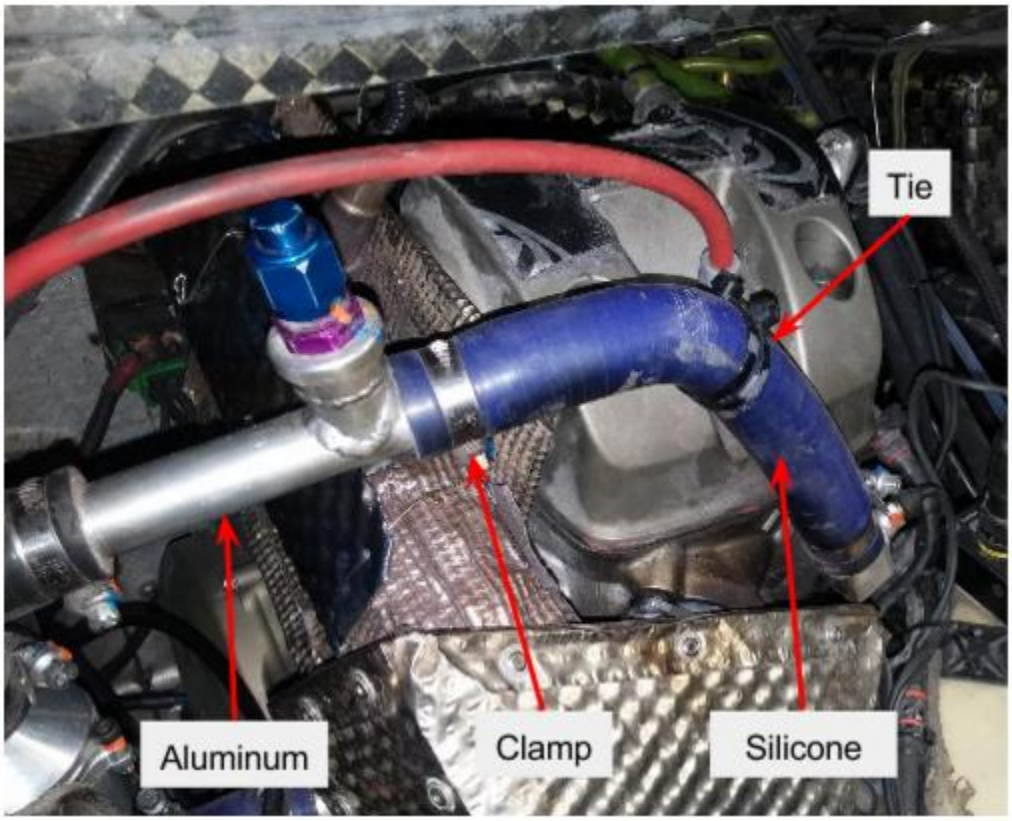

Figure 2.6: Various plumbing parts (this section of pipe is at engine water outlet).

The plumbing consists mostly of aluminum and, when connections are needed, silicone tubing. The silicone has an inner diameter of 19mm, roughly ¾", matching the aluminum's outer diameter of 0.75". The aluminum has a wall thickness of 0.035", resulting in an inner diameter of approximately 0.68".

Oil Cooling System

The cooling of the oil lubricant for the engine works in a very similar manner to the water cooler and is subject to some of the same heat transfer constraints. However, taking a look at the below image shows an interesting difference.

Figure 2.7: Rear of the left (oil) radiator.

As can be seen in Figure 2.7, the oil radiator does not have a fan attached. This is because during 2015 cCar testing, the fan was deemed unnecessary as it did not add any benefit to the cooling capabilities. It was therefore removed to reduce weight, along with the rear duct.

Figure 2.8: Oil lines with anti-siphon valves.

Figure 2.8 above shows another interesting feature of the oil lines visible near the oil radiator: anti-siphon valves. These valves help reduce the risk of oil flowing unpredictably, such as when the car stops and a temperature gradient affects the pressure in the line. Without the valves, the oil might flow back into the

engine, making it difficult to start. The lines attached to the valve connect to the oil catch can (not pictured).

The oil cooling system for 2015 did not use a thermostat.

Ducts

Ducts are used to facilitate the airflow through the radiators, bringing in another factor to help balance the cooling of the car. The 2015 duct designs were not tested for flow rate of air through the ducts. However, Table 2.2 below shows the estimated performance based on simulation results.

Table 2.2: Simulation results of the 2015 sidepod/ducts design and 2014 sidepod [5].

Sidepod	**2015 Ducts**	**2014 Sidepod**
Inlet Area (m^2)	0.075	0.12
Outlet Area (m^2)	0.051	0.076
Velocity Ratio	1.47	2.02
Mass (Kg)	0.41	0.53
Downforce (N)	*-0.2*	*-12*
Drag (N)	*0.06*	*-0.4*
Mass Flow Rate (Kg/s)	*0.44*	*0.45*
L/D	*2.24*	*2.78*
Total Downforce (N)	*674.1*	*1176.6*
Total Drag (N)	*301.4*	*423.2*
Downforce Points	*121.54*	*212.14*
Drag Points	*-44*	*-24.84*
Net Points	*77.54*	*187.3*

Table 2.2 shows that the 2015 duct design was estimated to have a slight decrease in mass flow rate of air (0.44 kg/s vs 0.45 kg/s) compared to the 2014 sidepods, but with much improved downforce (-0.2 N compared to 2014's -12 N; negative downforce indicates upward direction, or lift). These numbers are only estimates, though; without physical testing, it is unclear which design performed better.

The ducts were designed to be mirror images of each other, which would serve to simplify the design process somewhat. Again, because the oil radiator did not need a fan, only the front duct was used on the cCar's oil cooler in 2015, as seen in Figure 2.9. The shape of the ducts also allowed for rather simple manufacturing: laser cut sheet metal was bent into the desired shape and made carbon layup simple [5].

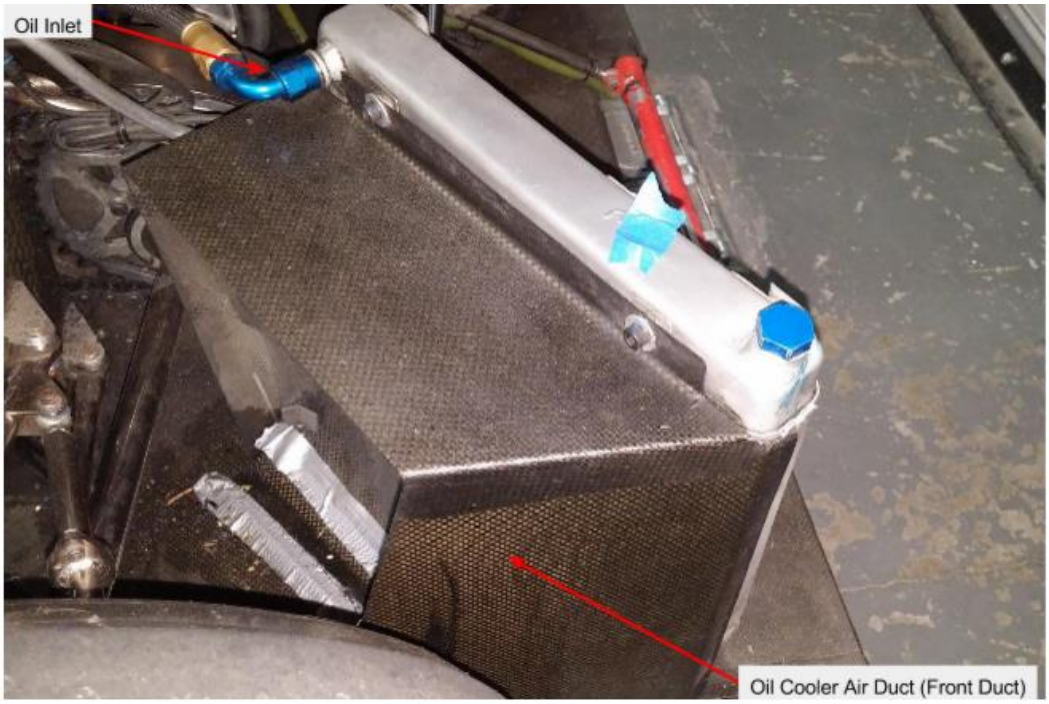

Figure 2.9: The left (oil cooler) duct.

Radiators


Figure 2.10: Third-party radiator for Honda TRX 450R ATV (image retrieved from AliExpress [6]).

The 2015 cCar originally used two Honda TRX450R stock radiators, similar to the radiator pictured above (one for the water loop and one for the oil loop). However, as the Germany competition approached, the team swapped the water cooler for a thicker aftermarket radiator. The benefits of the swap were dubious as there seemed to be no performance improvement, according to comments from several team members.

During design, oil-specific radiators were considered, but to keep with simple packaging, water radiators were selected. It should be noted that there is a risk of the radiators bowing outward, as seen below in Figure 2.11, due to the high pressure in the oil loop. If a radiator is not designed for a certain fluid, this may be a risk.

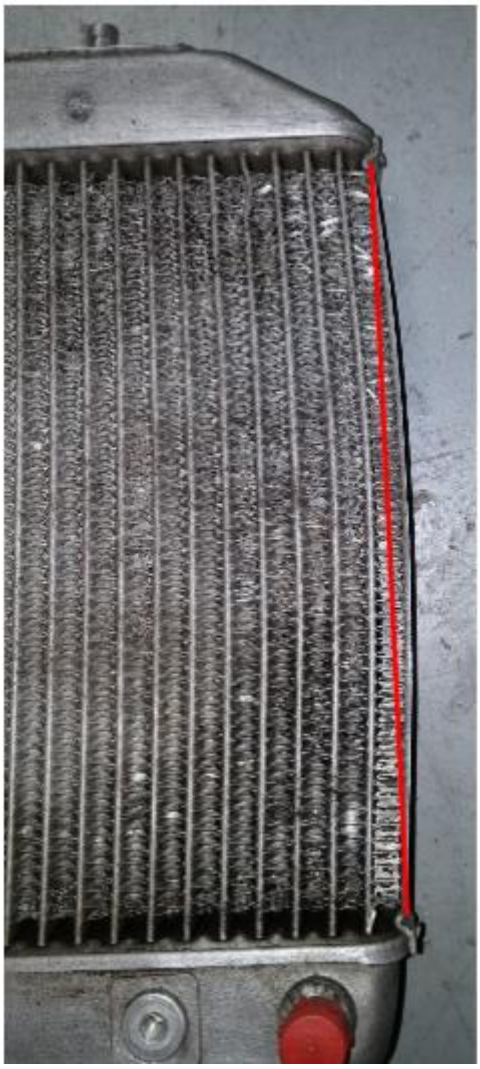

Figure 2.11: Picture of radiator used in an oil loop; red line added to illustrate the magnitude of the bowing.

Diffuser

The diffuser is worthy of note. The 2014 car did not use one, but due to the cooler placement issue previously discussed, the 2015 cars required one, such that everything could fit on top as seen in Figure 2.1. The diffuser CAD model can also be seen below in Figure 2.12.

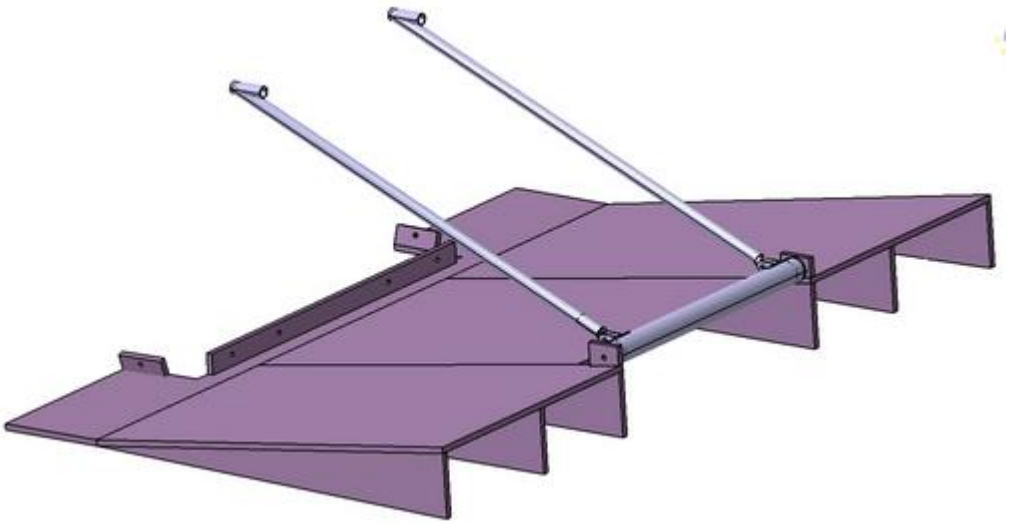

Figure 2.12: 2015 diffuser CAD model [5].

The 2015 sidepod team claimed that the diffuser CFD simulations showed approximately 25N of downforce generation by the diffuser. As with the ducts, no physical testing was performed. However, if this were the case, it should be noted that 25N of downforce is paltry compared to what other components generate (the rear wing generates several hundred newtons of downforce, depending on speed). At 0.579 kg [5] for the cCar diffuser, without serving the function as a place to store radiators, it is difficult to make a favor in case of the diffuser. A note on the weight: while the report claims the diffuser weighed in at 0.579 kg, including all components for mounting, a value of close to 1 kg was found using the Composite Weight Calculator [7] for the diffuser plate alone. The source of the discrepancy is unclear.

Other Components

The fans, though important to increasing airflow and thereby improving the cooling capacity of the radiators, are rather large. The fans used have a diameter of 10” and weigh roughly 1 kg [8]. Data on the capabilities of the fans are shown below in Table 2.3.

Table 2.3: The mass flow rate capabilities of the 10” fans based on various static pressures [8].

Tensione di prova 13 V cc - *Test voltage 13 V DC*

Pressione statica *Static pressure* mm H_2O	Portata *Airflow* m^3/h	Corrente assorbita *Current input* A
0	1100	6,4
2,5	1000	6,4
5	900	6,4
7,5	800	6,4
10	650	6,4
12,5	400	6,5
15	230	6,5
17,5	0	6,5

Static pressure: 1 mm H_2O = 0,04 in. H_2O
Airflow: 1 m^3/h = 0,59 cfm

Catch cans can be seen in Figure 2.13 (for water) and Figure 2.14 (for oil). While the water catch can is located near the radiators, the oil catch can is tucked in the engine bay on the left side of the vehicle. The catch cans are the same size, once again, aiding in simplicity by reusing designs. This design was also used on the 2014 cCar (according to Eric Bramlett, one of the catch cans was actually taken off the 2014 car to be used on the 2015 cCar).

Figure 2.13: The catch can for the water radiator, mounted between the oil and water radiators and ducts on the diffuser.

Figure 2.14: Engine bay showing location of the oil catch can and water line for reference.

eCar Differences

The focus thus far has been around the cCar's cooling components. I contacted Connor Torris for information on the eCar as he was, at the time of writing, in Germany advising for the electric car. He contributed the below images, Figure 2.15 and Figure 2.16.

Figure 2.15: The rear of the eCar showing the water radiators, rear duct, and fan, as well as some of the plumbing (photo from Connor Torris).

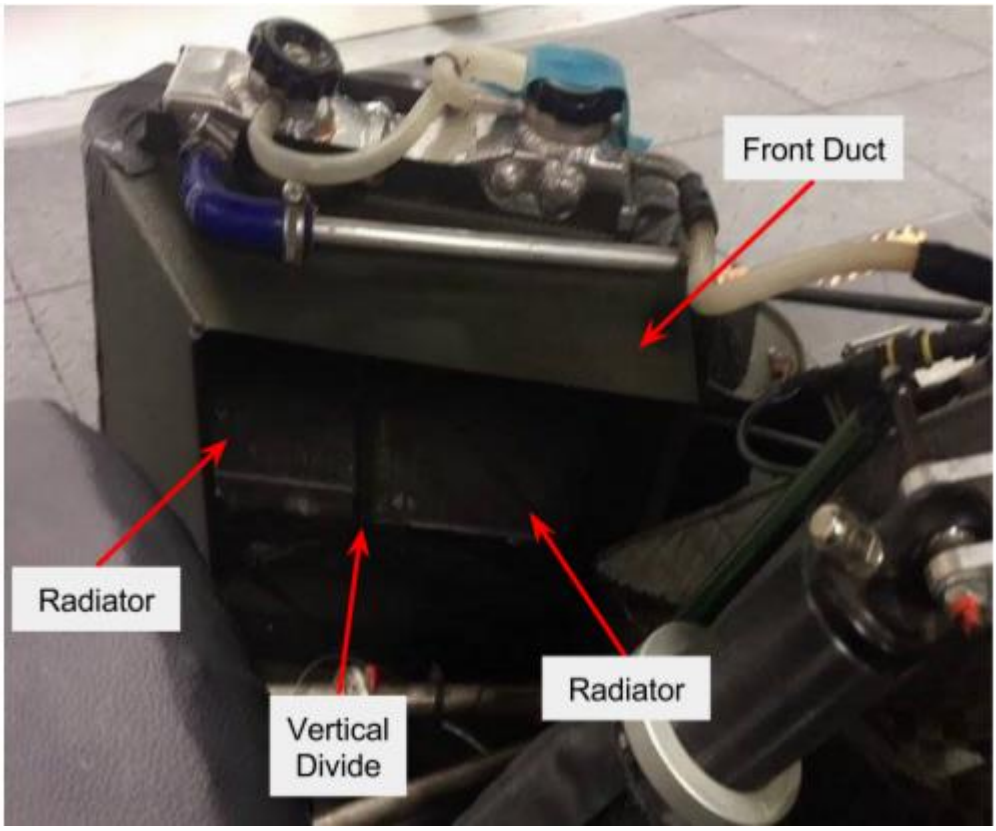

Figure 2.16: The water radiators and cooling duct from the front for the eCar (photo from Connor Torris).

The eCar capitalizes on the lack of need for an oil cooler by using just one ducting and radiator package, with some differences. Like the cCar, it is mounted on the right side on the diffuser. However, it uses two radiators of roughly half the width of the cCar's radiators. This allows both to fit into the same ducting

design side by side. In Figure 2.16, the location labeled “Vertical Divide” shows where the two radiators touch. In previous years the eCar used two loops, one for controllers and one for the motors; in 2015, battery cooling was added to the controller loop [9]. The plumbing for the eCar is also significantly different compared to the 2015 cCar. As hinted at above, though, the duct (and diffuser) designs matched between the two cars.

2015 cCar Cooling Performance - FSAE Michigan

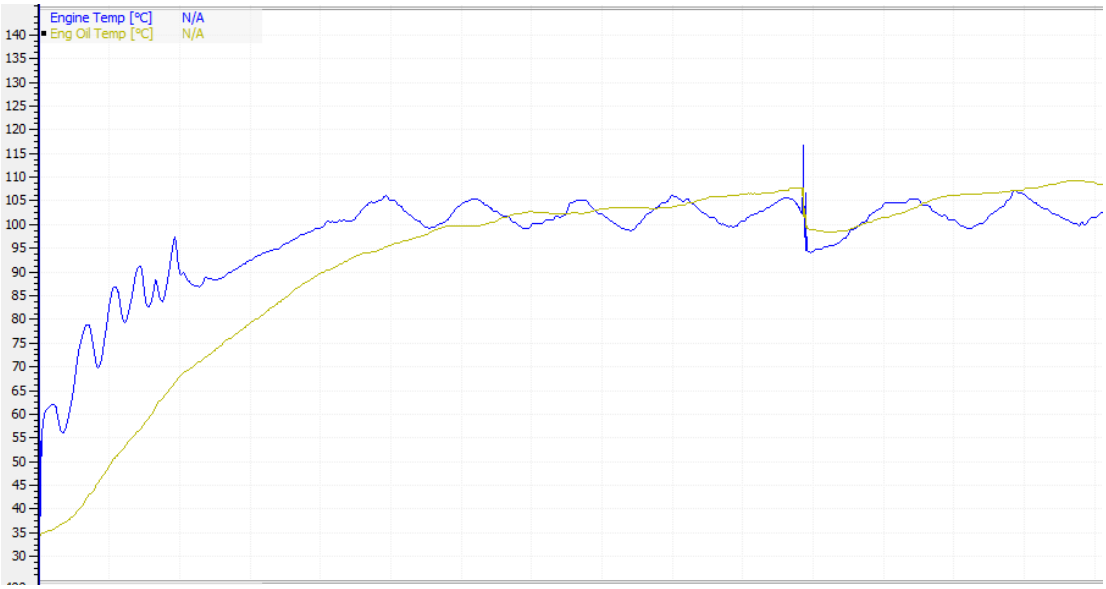

Figure 2.17: Plot showing the temperature data for the engine water (blue line) and the oil (tan line) from the FSAE Michigan 2015 competition (cCar; endurance event).

The above plot shows temperature data for the combustion car at the 2015 Formula SAE competition in Michigan for roughly the first half of the endurance event. The blue line corresponds to engine/water temperature and the tan line corresponds to oil temperature. The spot where the engine temperature spikes then immediately drops is located halfway through the event when the driver changes.

Some interesting features are apparent in the plot, especially with regards to engine temperature. As the engine is heating up, the temperature oscillates quite a bit before stabilizing on its final rise to about 105°C, at which point the fan turns on until the temperature decreases to about 99°C. Once the engine reaches this temperature the fan deactivates and the temperature begins to rise back to 105°C. This process repeats until the driver change, at which point the car is stopped, halting the flow of coolant through the lines and air through the radiators, resulting in the temperature spike.

The oscillations around operating temperature are overall a good sign, indicating that the fan was sufficient to keep the engine from overheating, while not having to be run constantly. There is certainly room for improvement, such as finding a way to reduce the duration the fan operates or, optimally, smoothing out the oscillations entirely around 100°C.

The oil loop seems to approach approximately 110°C almost asymptotically. Depending on the specific oil used, temperatures that high could pose issues with the fluid properties of the oil, altering the heat transfer capabilities. As with engine temperature, there is a “sweet spot” for oil; higher temperature causes it to thin out, making it easier to flow through the pipes. However, in the case of GFR’s oil selection, operating

temperatures around 110℃ would be fine for the fluid flow.

2.1.2 SWOT Analysis

Strengths

- Oil cooling
    - The 2015 car had sufficient oil cooling from running the car normally to drop any need for a fan for the oil radiator.
- Experience with heat transfer
    - Coursework in Applied Heat Transfer and Thermal Fluids Sciences Laboratory enhanced understanding of the cooling system, assisting with analysis.

Weaknesses

- Rear position of coolers
    - Positioning the coolers at the rear of the vehicle keeps them out of the way of other aerodynamic features, but restricts airflow to the radiators.
- Software experience
    - Lack of experience in CATIA (GFR's CAD software) and Star-CCM+ (GFR's CFD software) resulted in additional time spent learning programs.
- Car mechanics experience
    - Car-specific needs required additional time to develop an understanding of how the system interacts with other components, especially with packaging requirements.

Opportunities

- Radiator style change
    - Due to the strength of the oil system, there were several options to change to different radiator styles, explored in Section 3.

Threats

- Coordinating globally
    - Working with a school in Germany required constant cooperation and communication in order to function properly.
- Rule changes
    - Formula SAE rules, being subject to change, must be watched carefully, even after the car is built, to ensure a rules-compliant vehicle.
- Ambient conditions
    - A target operating condition does not encapsulate all potential conditions, and one year's air quality and temperature may differ from another's.

2.2 Benchmarking

2.2.1 Thermal Considerations

To analyze the cooling capabilities of the 2015 cCar radiators and estimate the performance of other options in Section 3 of this paper, $\epsilon - NTU$(effectiveness - Number of Transfer Units) analysis was performed, assuming constant fluid properties evaluated at the average fluid temperature. Following are a list of variables and equations:

Variable	Description	Units
q	Heat transfer rate	W
$\dot{m}$	Mass flow rate	kg/s
c_p	Specific heat at constant pressure	kg/J*K
dT	Temperature difference of fluid ($T_{final} - T_{initial}$)	K
D_h	Hydraulic diameter	m
A_c	Cross sectional area of a pipe	m^2
P	Wetted perimeter of a pipe	m
v	Fluid velocity	m/s
Q	Volumetric flow rate of a fluid	m^3/s
N_{tube}	Number of tubes across the radiator	(Unitless)
Re_D	Reynolds number, flow in a pipe	(Unitless)
Re_L	Reynolds number, flow across a flat plate	(Unitless)
ρ	Fluid density	kg/m^3
μ	Fluid dynamic viscosity	kg/m*s
f	Darcy friction factor	(Unitless)
Nu_D	Nusselt number, internal pipe flow	(Unitless)
Nu_L	Nusselt number, external flow	(Unitless)
Pr	Prandtl number	(Unitless)
h	Convective heat transfer coefficient	W/m^2*K
k	Conductive heat transfer coefficient of fluid	W/m*K
W_{fin}	Fin width	m
UA	Overall heat transfer coefficient	W/K
m	Intermediate coefficient for finding efficiency of fin	1/m
L_c	Adjusted fin length, accounting for angle	m
k_{alum}	Conductivity of the radiator's solid portion (aluminum)	W/m*K
H_{fin}	Fin thickness	m
η	Efficiency for a fin	(Unitless)

η_o	Efficiency of the external surface	(Unitless)
A_{ext}	Heat transfer area seen by airflow (external radiator surface area)	m^2
A_{int}	Heat transfer area seen by water (total internal surface area)	m^2
C	Heat transfer rate of a fluid	W/K
C_r	Ratio of the minimum to maximum C	(Unitless)
q_{max}	Theoretical maximum heat transfer in heat exchanger based on the maximum temperature difference of fluids	W
$T_{h,i}$	Temperature of the hot fluid (water) at inlet	K
$T_{c,i}$	Temperature of the cool fluid (air) at inlet	K
NTU	Number of transfer units, used to find effectiveness of heat exchanger	(Unitless)
ϵ	Radiator effectiveness	(Unitless)

Governing Equations – From Bergman et al. [10]

$$q = \dot{m} c_p dT \quad \text{Eq. (2.3)}$$

$$D_h = \frac{4 * A_c}{P} \quad \text{Eq. (2.4)}$$

$$v = \frac{Q}{A_c * N_{tube}} \quad \text{Eq. (2.5)}$$

$$Re_D = \frac{\rho * v * D_h}{\mu} \quad \text{Eq. (2.6)}$$

$$Re_L = \frac{\rho * v * L}{\mu} \quad \text{Eq. (2.7)}$$

$$f = 0.790 ln(Re_D - 1.64)^{-2} \quad \text{Eq. (2.8)}$$

$$Nu_D = \frac{(f/8)(Re_D - 1000) * Pr}{1 + 12.7 * (f/8)^{(1/2)} * (Pr^{(2/3)} - 1)} \quad \text{Eq. (2.9)}$$

$$Nu_L = 0.664 * {Re_L}^{(1/2)} * Pr^{(1/3)} \quad \text{Eq. (2.10)}$$

$$h_{water} = \frac{Nu_D * k}{D_h} \quad \text{Eq. (2.11)}$$

$$h_{air} = \frac{Nu_L * k}{W_{fin}} \quad \text{Eq. (2.12)}$$

$$UA = \frac{1}{1/(\eta_o * h_{air} * A_{ext}) + 1/(h_{water} * A_{int})} \quad \text{Eq. (2.13)}$$

$$m = (\frac{2h_{air}}{k_{alum}H_{fin}})^{1/2} \quad \text{Eq. (2.14)}$$

$$\eta = \frac{tanh(mL_c)}{mLc} \quad \text{Eq. (2.15)}$$

$$\eta_o = 1 - \frac{N_{fin}A_{fin}}{A_{air}} * (1 - \eta) \quad \text{Eq. (2.16)}$$

$$C = \dot{m} * c_p \quad \text{Eq. (2.17)}$$

$$C_r = \frac{C_{min}}{C_{max}} \quad \text{Eq. (2.18)}$$

$$q_{max} = C_{min} * (T_{h,i} - T_{c,i}) \quad \text{Eq. (2.19)}$$

$$NTU = \frac{UA}{C_{min}} \quad \text{Eq. (2.20)}$$

$$\epsilon = 1 - e^{[(\frac{1}{C_r}NTU^{0.22})(e^{(-C_rNTU^{0.78})}-1)]} \quad \text{Eq. (2.21)}$$

$$q_{rejected} = \epsilon * q_{max} \quad \text{Eq. (2.22)}$$

Summary of Analysis

The calculations performed are very similar to what was performed by Carl et al. [11], with some adjustments made for the particular radiator style used. To begin the analysis of the cooling system, the engine heat output was investigated using data collected during the 2015 competition year in addition to dynamometer test data from 2014. The dynamometer data was required as flow rates are needed to depict the flow characteristics of the water. In order to use this information in conjunction with competition data, the dynamometer data was used to develop an equation relating the engine speed in rpm to the volumetric flow rate of the water in the system:

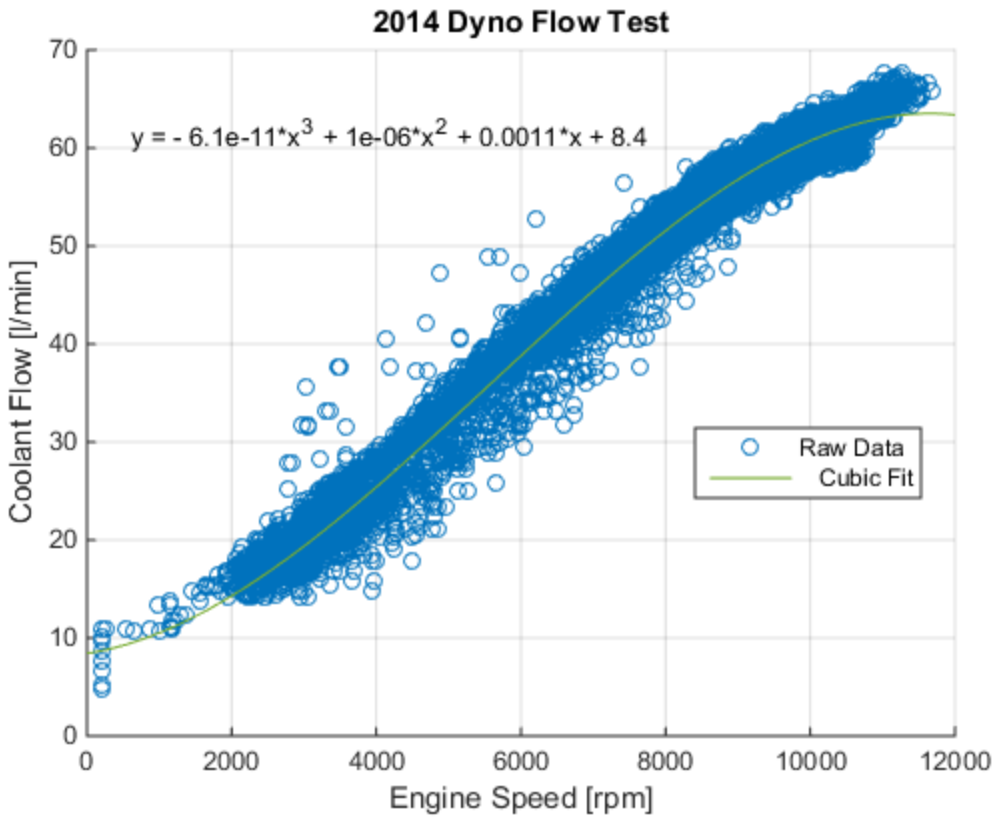

Figure 2.18: Dynamometer test data correlating water flow rate in liters per minute to engine rpm.

Figure 2.18 above shows a plot of the raw data taken from the dynamometer flow meter test performed in November 2013 for the 2014 cCar. A cubic fit was applied, as it follows the data reasonably well. Using the equation generated, an approximate relationship between engine speed and water flow rate was established to be applied on the 2015 cCar competition data.

The analysis for the heat transfer into the system used data from the 2015 cCar's endurance events at both Germany and Austria. These events had temperature data at the inlet and outlet of the engine, allowing for Equation 2.3 to easily be applied once the mass flow rate had been calculated using the relationship from Figure 2.18 and converted to mass flow rate using the density of water (approximately 970 kg/m^3 at temperature and pressure considered).

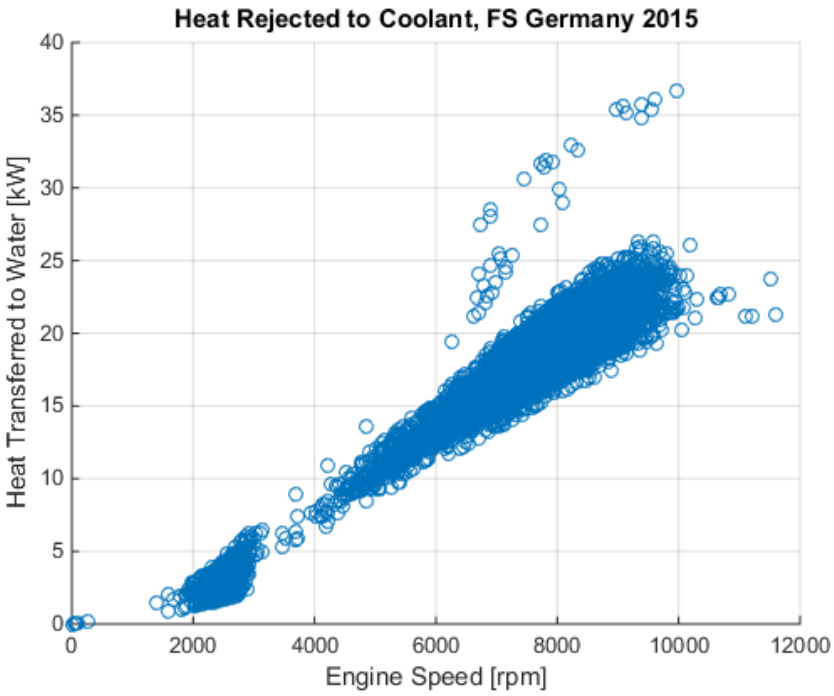

Figure 2.19: Heat rejected from engine using data from FS Germany 2015 Endurance Event.

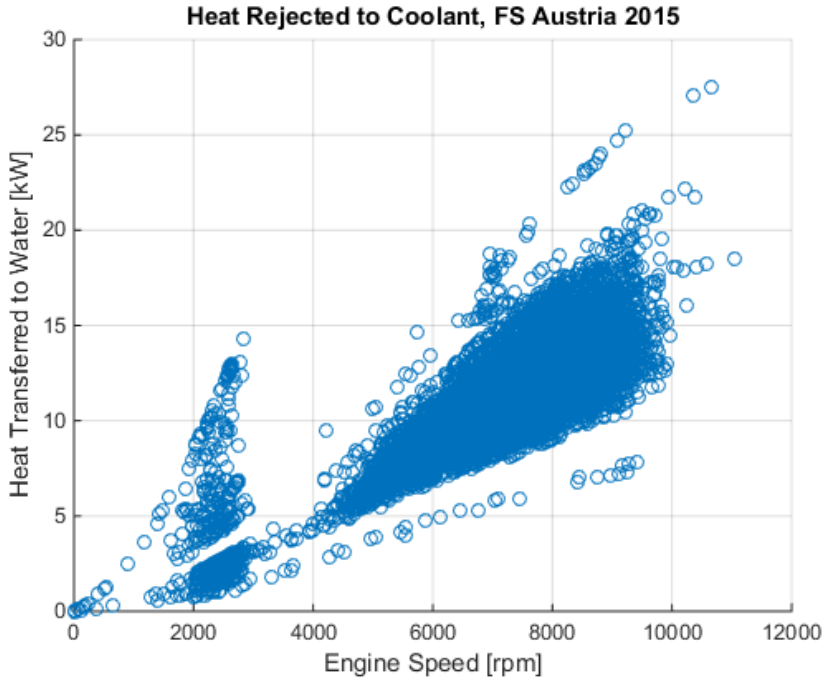

Figure 2.20: Heat rejected from engine using data from FS Austria 2015 Endurance Event.

The above figures showed that the engine typically rejects around 10-20 kW, with some sporadic data points strewn about. Many of these are due to the disruption in the cooling performance when the pump shuts off during the driver swap in the middle of the event, or possibly due to lack of airflow at zero velocity.

With the analysis of the heat entering the water in mind, analysis of the 2015 cCar radiator set up continued with considering the heat leaving the water as it passes through the radiator. Several measurements were taken of the radiators used and are tabulated below.

Table 2.4: Measurements taken from a TRX 450 radiator using calipers and counting tubes and fins.

Tubes		**Fins**	
Number of Tubes	31	Number of Fins Per Tube	288
Tube Width, W	0.023 m	Fin Width, W	0.023 m
Tube Thickness, H	0.0045 m	Fin Thickness, H	0.00014 m
Tube Length, L	0.23 m	Fin Length, L	0.006 m

In Table 2.4, it should be noted what the dimensions correspond to. The "Width" values correspond to the depth of the core. In other words, the widest dimension of the tube and the distance the air travels across the fins to pass through the radiator. Assuming the fins span the full width of the tubes, this number should be the same for both tube and fin. Thickness values are the smallest measurement of the feature. For tubes, this would be the smaller dimension of the cross section while for fins this is simply the thickness. For tubes, the length is the distance the water travels as it passes down the radiator, while fin length is the distance between tubes in the radiator. NOTE ON FIN LENGTH: To simplify radiator analysis, the fins of the radiator, while in reality are at an angle, are treated as straight. As such, the length used in calculations is half the measured length between radiator tubes (L/2), as done in [11]. Keep in mind that the TRX 450 radiator is a single core (air passes one bank of tubes) radiator, while the paper mentioned uses a double core radiator.

With the geometry of the 2015 cCar radiators known, the necessary information to solve the heat transferred from water to air could be solved. This process was split into first analyzing the water, then running the calculations for air, and finally tying everything together. Following the equations described at the beginning of this section the process begins with determining the hydraulic diameter of the tubes and water velocity through each tube. With that information, the Reynolds number in the pipe could be calculated with Equation 2.6. Depending on the number determined here, the flow can either be described as "laminar" ($Re<5000$) or "turbulent" ($Re>5000$). Discussion on flow regimes is outside the scope of this paper. What is important is to use the correct correlation for finding the Nusselt number. For the laminar region, interpolation was used to find a Nusselt number based on information found in [10]. For non-circular cross sections, the Nusselt number depends on the ratio of tube width/tube thickness. In the case of the TRX 450 radiator, this ratio comes to about 5.11, resulting in a Nusselt number of around 4.96 (assuming uniform wall temperature of the tubes). The table of Nusselt numbers is not included in this paper as special permissions are required. See page 553 of the text if more information is desired. If the flow is determined to be turbulent, however, Equation 2.9 must be used in conjunction with Equation 2.8 to find the Darcy friction factor. With this information, the convective heat transfer coefficient can be found for water using Equation 2.11.

Analysis for air follows much the same procedure, with some slight variation to factor in the flow being external. The first difference is that the air calculations do not make use of a hydraulic diameter. Rather, the width of the fins (in other words, the distance the air travels over the fins) is used for the Reynolds number. This means a different equation is used for the Nusselt number. Fortunately, the speed of the vehicle does not come close to causing turbulence for the flow, which occurs at a Reynolds number of approximately 5E5. Thus a single equation is used: Equation 2.10. The convective heat transfer coefficient is also different, instead using Equation 2.12.

The last major step to complete is determining the overall heat transfer coefficient, UA. This requires some additional work; the external area (area seen by air) and internal area (area seen by water) of the radiator are simple to calculate, but finding $\eta_o$is a bit more involved. The reason it is needed is to help compensate for modeling the radiator fins as rectangular, orthogonal fins on a flat plate. The efficiency is found using Equation 2.14, 2.15, and 2.16. With the overall heat transfer coefficient calculated, the number of transfer units can be found using Equation 2.20 and, from there, finding the effectiveness is trivial with equation 2.21. The heat rejected by the 2015 cCar water radiator can be easily determined using Equation 2.19 to first find the theoretical maximum heat transfer and plugging in the result to Equation 2.22. The results of this analysis are shown in the plots below.

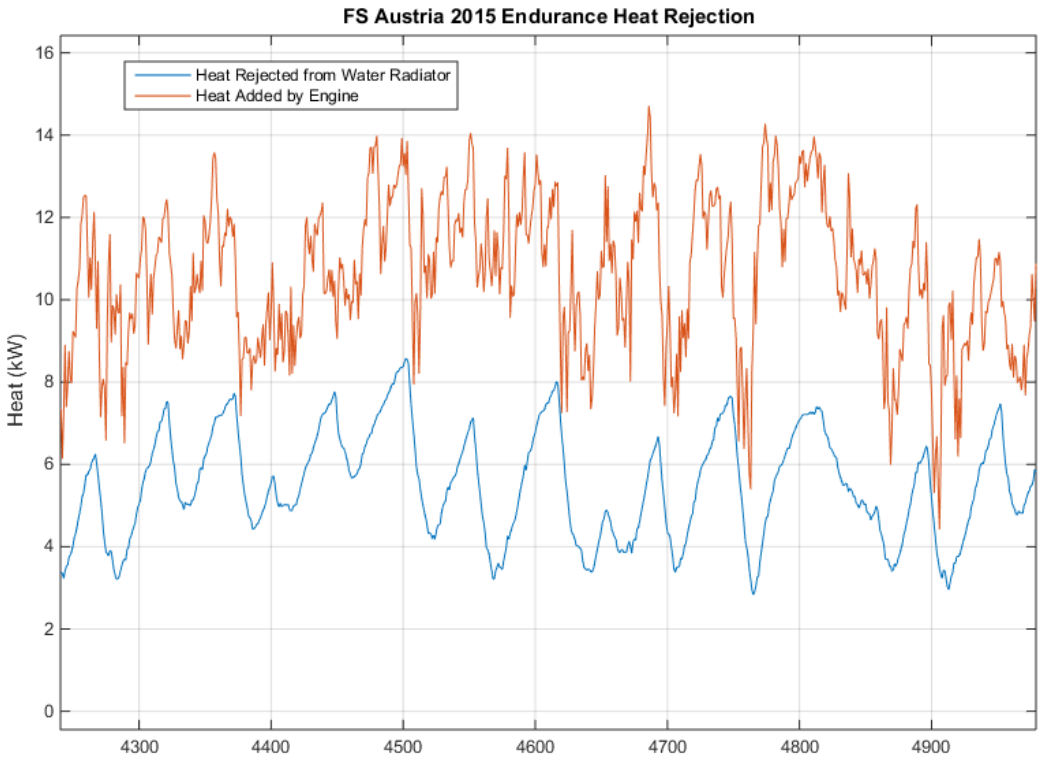

Figure 2.21: Endurance data from FS Austria 2015 showing heat rejected by radiator and heat added to water by engine.

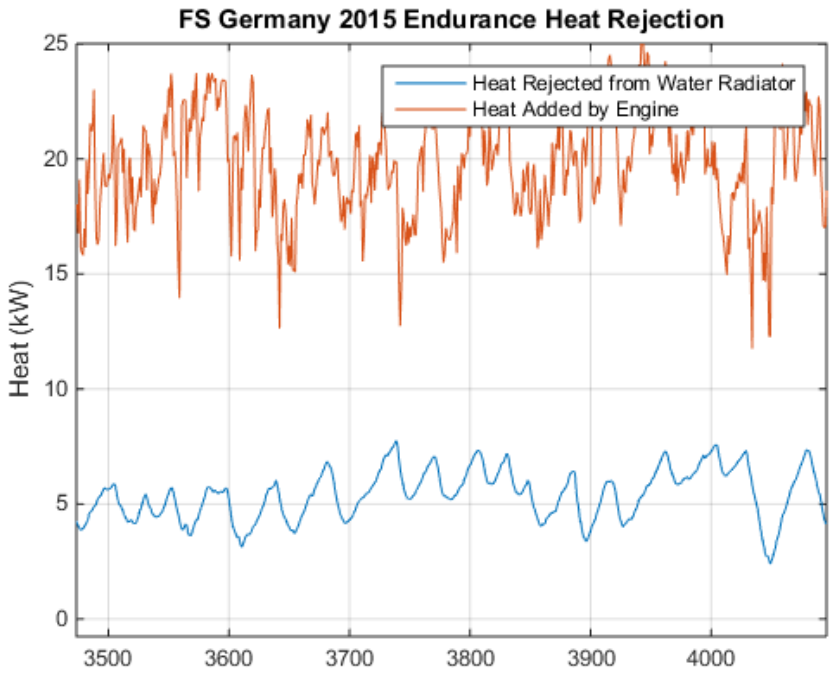

Figure 2.22: Endurance data from FS Germany 2015 showing heat rejected by radiator and heat added to water by engine.

Figures 2.21 and 2.22 show that the heat added to the engine is quite a bit higher than the heat rejected by the engine. However, there are several potential reasons for this. The analysis does not account for the enhanced airflow of the system when the fans are on. Rather, the air speed is determined using CFD data (see Section 3 for more information) and applying a factor of car speed/CFD speed (65kph) to scale the air flow rate. Additionally, the actual radiator analysis makes numerous assumptions, including fully developed flow, smooth tubes, and various geometry-related approximations. Using the above plots to make a statement about the amount of heat transfer rejected would be suspect. Rather, this data will be used in Section 3 to compare radiator set ups.

For the MATLAB code used to run the calculations to compose the above graphs, Appendix B.

More complex investigations of the cooling can be done in similar fashion to Dube et al., who implemented a numerical approach to assessing variations of a front-mounted cooling package [12].

2.2.2 Mass Considerations

Another aspect important for describing the quality of a system is its weight. An overly heavy vehicle will be negatively impacted in competition. Thus finding ways to decrease the system mass is key in design.

Table 2.5: Water line weights for 2013 and 2014 cCars [13].

	2013		2014	
Engine Cooling System				
Water Radiator Mass (g)	1100		1025	
Coolant Tubing (Hard and Silicone Lines)				
Outlet to Swirl Pot	Aluminum Hard Line-340mm	55.3g	Outlet to Thermostat	174.3g

	Silicone Line-165mm 4 Hose Clamps	54.9g 84g		
Swirl Pot to Radiator	Aluminum Hard Line-705mm Silicone Line-207mm 4 Hose Clamps	114.9g 68.9g 84g	Thermostat to Radiator	251.7g
Radiator to Inlet	Aluminum Hard Line-660mm Silicone Line-105mm 4 Hose Clamps	107.6g 35.0g 84g	Radiator to Inlet	202.1g
Total System Weight	1788.6g		1652.1g	
Number of Connections	6		8	

Table 2.6: Water line weights for 2015 cCar; weights were measured using available spares and lengths were estimated using CATIA models and some physical measurements of the car.

Engine Cooling System: Water			
	Weight, Each [g]	**Quantity**	**Total Weight [g]**
Water Radiator	1031	1	1031
Hose Clamps (ea)	14	16	224
	Measured Weight per mm [g]	**Length Used [mm]**	**Total Weight [g]**
Aluminum [3/4" OD]	0.127	1889	239.903
Silicone Tubing [3/4" ID]	0.380	590	224.200
Total Weight [g]			1719.103

The above tables show that, over the past three years, the weight of the water cooling system has remained fairly consistent, with the minimum weight being 1.67 kg in 2014 and the maximum weight being 1.79 kg in 2013. It should be noted that the weight measurements do not include fluid weight. Without more information about the length and dimensions of the pipes, it is difficult to factor that amount into the overall weight of the systems.

There is a very key point to take away from this: the weight of the silicone tubing compared to aluminum pipe. While silicone tubing is nice as it is flexible, it is around three times heavier per unit length than aluminum and should only be used when absolutely necessary, such as connection points to ports and tight joints where bends in aluminum are insufficient. Limiting the number of connections would also serve to reduce the number of hose clamps in the system.

Table 2.7: Oil line weights for 2013 and 2014 cCars [13].

	2013		2014	
Engine Oil System				
Oil Radiator Mass (g)	400		1025	
Oil Tubing (Hard and Silicone Lines)				
Outlet to Swirl Pot	Aluminum Hard Line-520mm Silicone Line-610mm	34.7g 186.5g	Outlet to Thermostat	521.2g

	6 Hose Clamps	126g		
Lines Bridging Coolers	Aluminum Hard Line-80mm Silicone Line-285mm 4 Hose Clamps	114.9g 68.9g 84g	Thermostat to Radiator	94.9g
Cooler to Inlet	Aluminum Hard Line-720mm Silicone Line-530mm 6 Hose Clamps	48.0g 160.3g 126g	Cooler to Inlet	287.3g
Oil Catch Can	Aluminum Hard Line-170mm Silicone Line-115mm 4 Hose Clamps	11.3g 27.0g 84g	Oil Catch Can	81.1g
Total System Weight	1356.2		2009.5	
Number of Connections	10		6	

Table 2.8: Oil line weights for 2015 cCar; weights measured by hand except in the case of the oil catch can, as the catch can was reused from the 2014 cCar (based on discussion with Eric Bramlett).

Oil Cooling System			
	Weight, Each [g]	**Quantity**	**Total Weight [g]**
Water Radiator	1031	1	1031
Hose Fittings	23	2	46
Oil Catch Can	81.1	1	81.1
	Measured Weight per mm [g]	**Length Used [mm]**	**Total Weight [g]**
Aluminum oil hardline	0.0670	[Data needed]	N/A
Braided softline, 12mm OD	0.0777	[Data needed]	N/A
Braided softline, 7mm OD	0.0490	[Data needed]	N/A
Total Weight, not including lines [g]			1158.1

There is missing data in the length of the hard and softline materials used. However, it is arguably more important to understand the weight on a per-millimeter basis anyway, as comparison between otherwise equivalent materials is more direct. As in the water loop, the right material for the job makes all the difference. In the case of oil, though, things are a bit more difficult. The oil gets to a higher temperature and its properties generate a need for special equipment. Special braided cable is sometimes necessary, especially if the line flows near something sensitive to high temperature and extra insulation is needed.

Aerodynamic elements were designed as a means of packaging the cooling system and nothing more. That is, only slight consideration was given to downforce and drag points from CFD. The focus was on limiting weight and moving the system as far forward on the car as possible.

3. Design Analysis

3.1 Radiator Set-up and Plumbing

This section deals with the radiator and plumbing options for the water cooling loop, the primary design investigation for the 2016 cCar cooling system. The following options were considered for the car before deciding on Option C.

Option A: 2015 cCar setup - single TRX 450 radiator

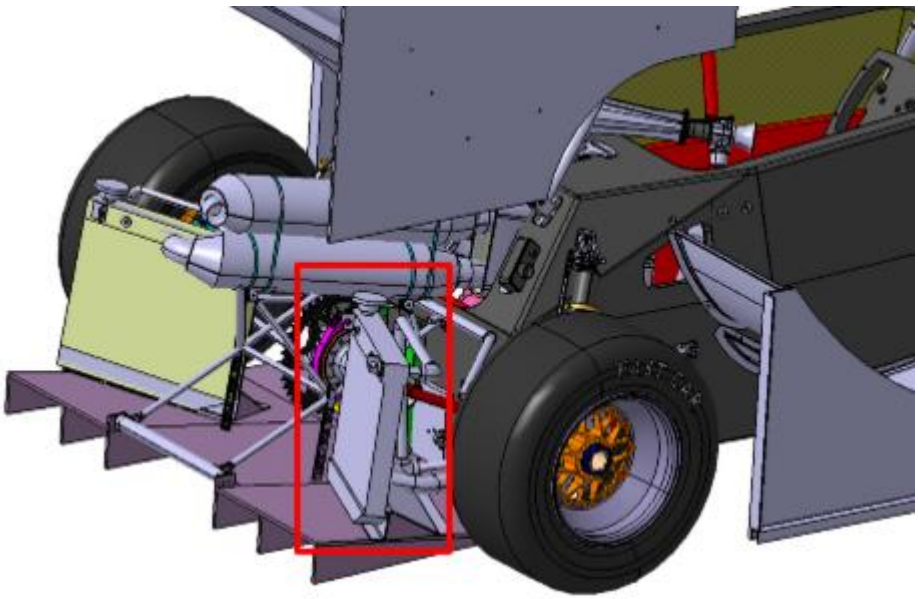

Figure 3.1: Water radiator location on diffuser of 2015 cCar; image from CAD model.

As stated previously, the 2015 cCar saw the coolers moved to the rear of the vehicle, placed on a diffuser. Due to the side wings and wheels, air has trouble reaching the radiators in this spot. Performance of this radiator was touched upon in benchmarking in Section 2.2.1.

Options B and C: Two CRF 450 Radiators

The following options, B and C, both use CRF 450 radiators that are smaller than the 2015 cCar radiators. The 2015 cCar uses TRX 450 radiators, which have cross sectional areas of roughly 325mm by 230mm for an overall area of about 0.0748 square meters. The CRF 450 radiators come in a few different sizes, based on product year and whether it is mounted on the left or right of the motorcycle. The "left-side" radiator from 2005-2008 CRF 450 bikes can be seen in Figure 3.2, left image. This particular radiator has a cooling area of about 236mm by 117mm for a total cross sectional area of around 0.0276 square meters. The corresponding right-side radiator from this series of bikes has a cooling area of about 220mm by 117mm for a total area of 0.0257 square meters. Both CRF 450 radiator cooling areas were measured from physical radiators. Where B and C differ is with plumbing options.

Figure 3.2: Left CRF 450 radiator (image retrieved from [14]).

Figure 3.3: Right side CRF 450 radiator, 2005-2008 bike model; photo of radiator purchased for 2016 cCar.

Option B: Two CRF 450 radiators, plumbed in parallel

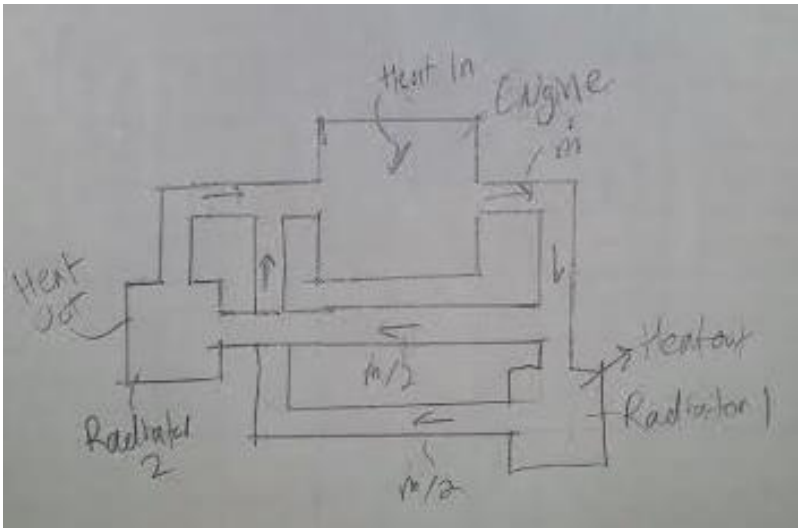

Figure 3.4: Schematic of plumbing to two radiators with parallel plumbing.

This option investigates the cooling capabilities of two small radiators plumbed in parallel. The idea with the plumbing is that it maximizes the temperature difference between ambient air and water; if the radiators are plumbed in series, the temperature of the water drops slightly as it passes the first radiator. However, this design also splits the flow into two parts. Assuming the total mass flow rate of water through the engine is the same for a series and parallel set up, approximately half the water flows through each radiator, hindering the heat transfer capacity of the water. The plumbing is somewhat more difficult than a series loop as well, as it would require fittings to split the flow and attention to detail would be necessary to ensure balanced flow, based on the "path of least resistance."

Option C: Two CRF 450 radiators, plumbed in series

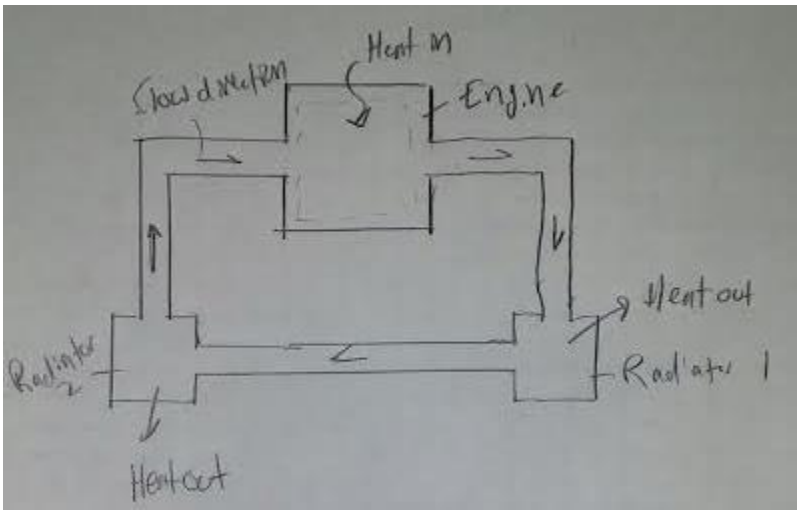

Figure 3.5: Schematic of plumbing to two radiators with series plumbing.

This option reverses the pros and cons of the parallel schematic. The water temperature will drop after the first radiator resulting in a lower heat rejection at the second radiator. However, the mass flow rate of water will be much higher in both radiators. In order to determine if the temperature drop or mass flow rate win out in this design versus parallel, calculations were performed, discussed further in this section.

Option D: Single go-kart radiator

Figure 3.6: Go-kart radiator for TaG racing kart (image from expired eBay listing [15]).

This concept is similar to Option A, with the dimensions being different. The radiator size is somewhere between that of the CRF 450 radiators and the TRX 450 radiators.

Option E: Two CRF 450 radiators mounted on vehicle side

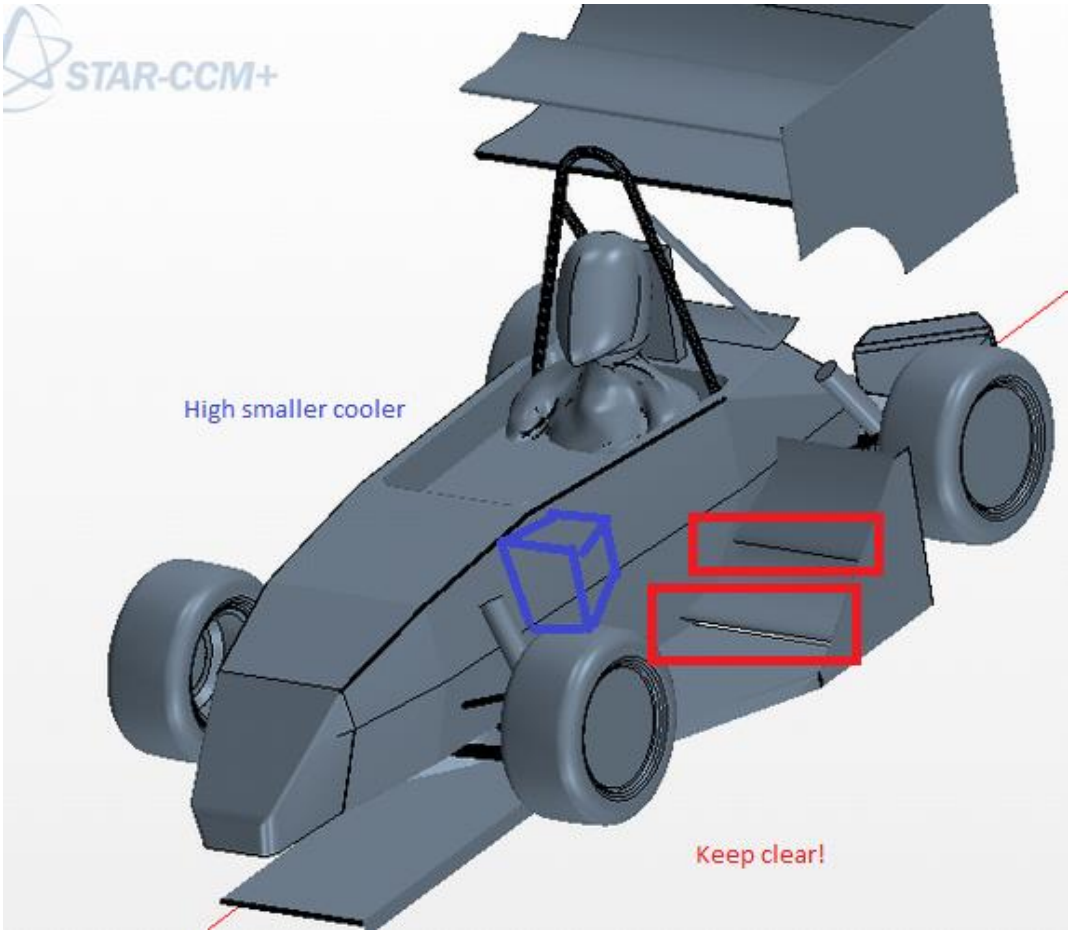

Figure 3.7: Concept image from Phillip Arscott's 2016 Aero Predevelopment [16].

This concept investigates the airflow benefits of mounting the coolers on the sides of the vehicle, behind the front wheels.

Radiator Analysis

Phillip Arscott ran CFD simulations that have been tabulated below. These simulations were used to run heat transfer calculations for the different concepts.

Table 3.1: CFD results for Radiator Concepts A-E (from "Aero Run/Ran" spreadsheet [17]).

Concept	CFD Code	Area [m^2]	Mass Flow of Air [kg/s]	Cooler DF Points	Cooler DR Points	Aero Net Points
A	GFR16_HB_ALv6_Mid_75 _15 2 flaps_Triangle V2.3	0.07475	.37	-1.2	0.6	83.25

B,C	GFR16_HB_ALv6_CL_1	.039	.22	-2.6	-0.3	85.02
D	GFR16_HB_ALv6_CL_3	.057368	.39	-1.6	0	85.48
E	GFR16_HB_ALv6_CL_2	.039	.38	-6.4	1	80.67

Table 3.1 shows the CFD results for the radiator concepts pursued. The net points were roughly the same for all runs, with the side mounted coolers having a slightly lower amount compared to the rest. For B, C, and E, the mass flow rate of air is effectively doubled, as the CFD simulation gives results for only one radiator (half the car is simulated) and it can be assumed at this point that a radiator on the other side of the car would experience the same flow rate of air. Because Option E was the only concept with a net points score noticeably below the others, the concept was dropped at this point.

The heat transfer calculations followed the same procedure outlined in Section 2.2.1, with the two radiator concepts having slight modifications: the series plumbing concept requires summing the heat transfer at both radiators while the parallel concepts have the heat transfer analysis run for a single radiator with half the flow rate calculated, then doubling the resulting heat output.

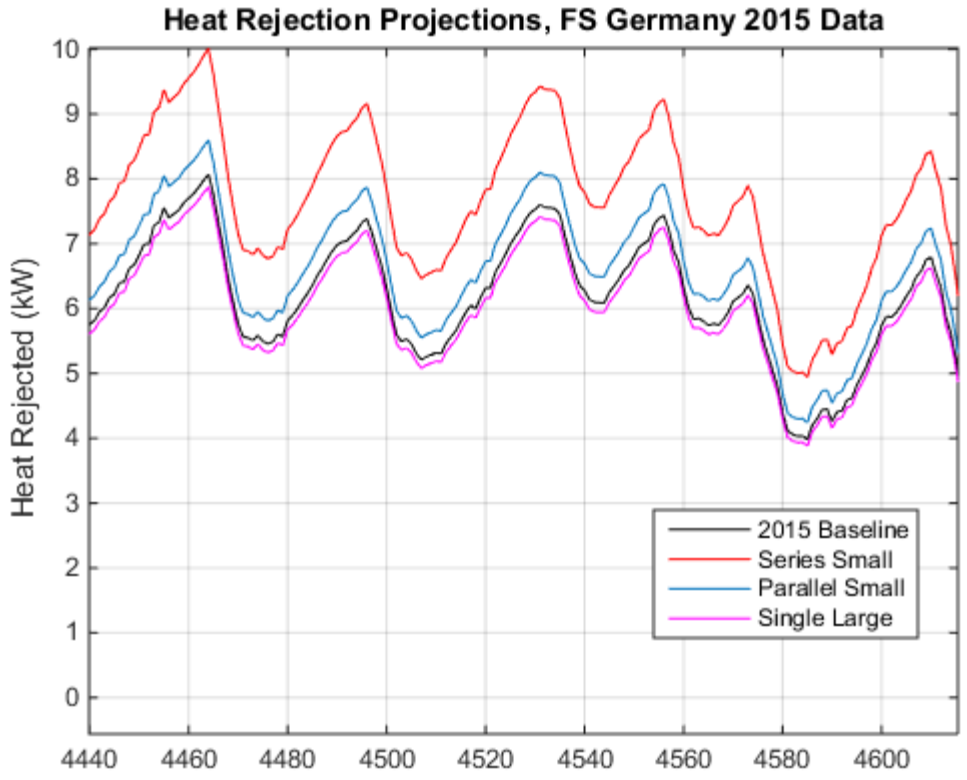

Figure 3.8: Heat rejection estimates using FS Germany 2015 data for Concepts A-D.

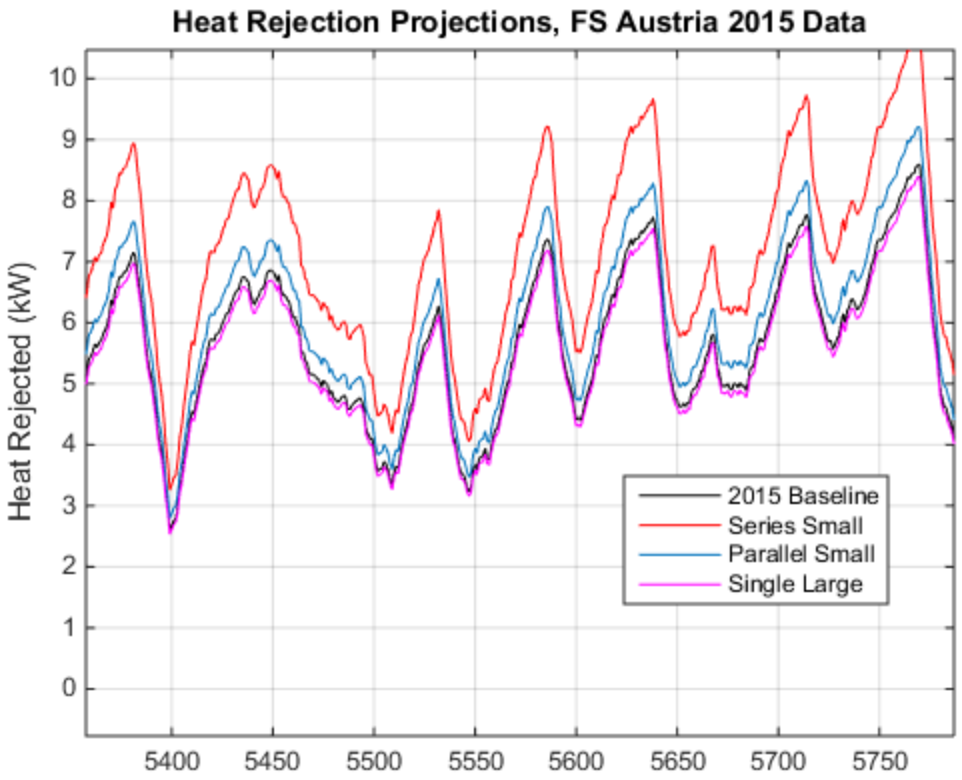

Figure 3.9: Heat rejection estimates using FS Austria 2015 data for Concepts A-D.

Figures 3.8 and 3.9 show the results of the heat transfer equations applied to the radiator concepts for FS Germany 2015 and FS Austria 2015 data, respectively. The legends correspond to concepts as follows: Concept A: 2015 Baseline; Concept B: Parallel Small; Concept C: Parallel Series; Concept D: Single Large. In both cases, the data suggested that the heat rejection quantities are scaled up or down a roughly consistent amount. The series setup for small radiators seems to be superior to the rest, with approximately 24% greater heat rejection compared to 2015 cCar baseline. The x-axis corresponds to a subset of MoTeC data points only and is arbitrary. Several assumptions were made in this analysis, including equivalent mass flow rate of water, regardless of the plumbing (half mass flow rate through each radiator in parallel), which may be a limiting factor for Concept C due to pressure drop across two small radiators versus a single large radiator.

The reason for the huge increase in cooling with the series setup (red line) is in part due to the Reynolds number being far higher due to higher velocity water in the radiators. Once in the turbulent region, Equation 2.9 comes into play. The faster the water travels through the radiator (as a result of higher engine RPM pumping more water), the higher the Reynolds number. The Nusselt number then rises as well, resulting in better heat transfer from water to radiator.

Another thing to keep in mind with the two-radiator set ups is the weight: even if the two radiators are approximately the same weight of a single larger radiator, the additional plumbing connecting the radiators will very likely result in a heavier cooling loop. Based on the tabulated pipe and fitting weights in Table 2.6, and factoring in the additional volume of water, the estimated weight gain of plumbing alone is approximately 500g, shown below in Table 3.2. However, as will be seen in Section 3.2, a possible remedy for this would be shifting the radiators forward, which would move them closer to the engine, decreasing

the inlet and outlet length sections. Other ways to lower the weight of this particular section would be to make the path more direct, lower overall length, reducing necessity for silicone line, and, if connections are removed, reducing the numbering of clamps. Additionally, if thinner wall pipes are used in the future, the weight of the lines can be reduced as water has a lower density than aluminum (water: approximately 1kg/m^3; aluminum: 2.7kg/m^3 [18]). This only takes into account weight of the water loop; by using a smaller radiator for the water system, a smaller radiator for the oil loop can be used, which drastically drops weight of the system, both due to raw radiator weight and decreased fluid volume required.

Table 3.2: Table showing estimates for connecting line weights (series connection).

Item	Amount	Weight
Hardline (aluminum)	766mm	112.6g
Softline (silicone)	300mm	114g
Clamps	11	148.5g
Water	0.25 liters	240g
Total Weight	*501g*	

Note: this table was composed based on the design for a line used for the in-series loop as Concept C had been selected. A parallel setup would have different values for additional system weight.

Table 3.3: Decision matrix and plumbing style concepts.

Criterion	Weight	(A) 2015 Baseline	(B) 2X Rear Mounted, Small, Parallel Plumbing	(C) 2X Rear Mounted, Small, Series Plumbing	(D) Alt. Large Cooler
Cooling	50%	5	6	8	4
Small Size	10%	2	7	7	7
Ease of Mounting	20%	3	5	5	6
Ease of Plumbing	10%	7	3	5	7
Weight	10%	3	6	6	4
Total	100%	4.3	5.6	6.8	5

The above table shows weights for design criteria and values associated for concepts A-D, ultimately leading to a selection of Concept C.

3.2 Diffuser - General Design Considerations

A goal for the car this year, according to Phil Arscott, was to shift the center of gravity forward. To do so, the diffuser was shortened and the coolers moved as far forward as possible without causing issues with suspension elements.

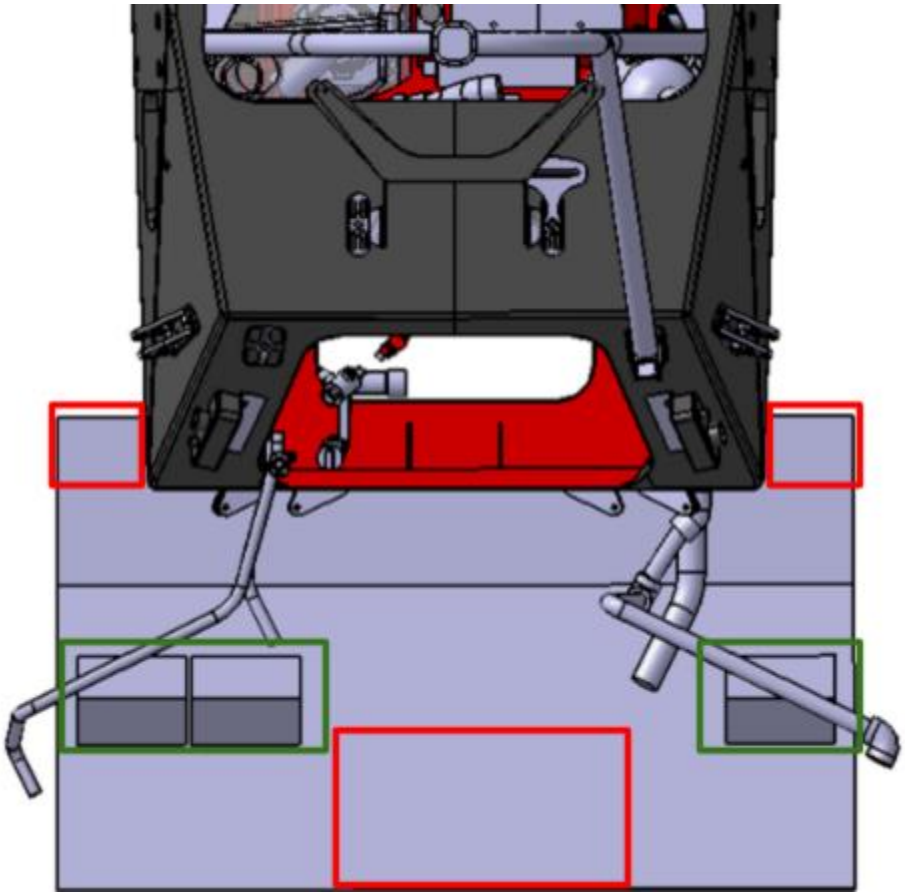

Figure 3.10: Rear diffuser, top view, rough model.

Figure 3.10 shows a rough model of the diffuser for the 2016 cars. Red rectangles show zones that were investigated for material removal. Note that the two red squares near the chassis are spots where the 2015 diffusers mount to the chassis. To validate if removal of this area is acceptable, the bolts holding the diffuser in were removed and a force applied to the jack bar (which would be located at the bottom of the bottom red rectangle, but was not modeled yet). The 2015 car was jacked with no issue, so these portions of the diffuser were removed from the model. A small portion of the red rectangle at the bottom of the image was removed to make room for the jack bar. Green rectangles denote cooler locations. The two coolers on the left are one water cooler (leftmost) and one oil cooler. The other water cooler that was mounted to the diffuser appears on the right side. The coolers are small enough to be packaged such that they face straight forward. The 2015 cCar plumbing can be seen around the new coolers, included for a visual representation of where the 2015 cCar radiators were. The plumbing is angled the same way the coolers were, and positioned rearward from the cooler representations shown in the figure. Other differences between the image and the final design are the diffuser was shortened until it extended only an inch rearward of the coolers and the angle (not visible, other than the bend axis) was removed, resulting in a short, flat plate.

3.3 Ducting - Converging Duct Discussion

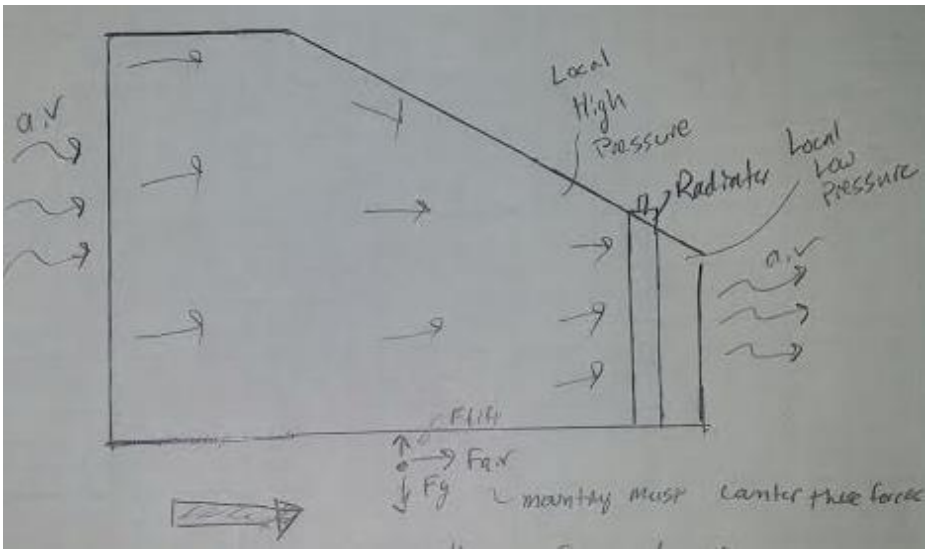

Figure 3.11: Sketch of a converging duct; air enters left side, passes through radiator near right side, after the area has decreased.

The 2015 cCar uses ducts that remain roughly the same size throughout in terms of cross sectional area. The 2016 design uses a ducting system that converges slightly, resulting in a drop in static pressure as seen in:

$$(P_s + \frac{\rho v^2}{2})_1 = (P_s + \frac{\rho v^2}{2})_2 \quad \text{Eq. (3.1)}$$

Bernoulli's equation states that, along a streamline, the total pressure remains constant. The $P_s$term is the static pressure portion in Pa. The other term consists of ρ, or the fluid density, and v, or the fluid velocity, in kg/m^3 and m/s, respectively. The subscript 1 and 2 refer to two different points along the streamline. This equation can be applied as long as the flow is steady, incompressible, and there are no viscous losses [19].

The converging duct design has risks involved. While it seems like a good idea to capture more air and speed it up, it is also possible that the air will recirculate if the pressure across the radiator is not enough to drive airflow through. While testing has shown the current design to work fine, future iterations should look into using a diverging duct to help increase static pressure at the inlet side of the coolers.

4. Design Selected

4.1 Rationale for Selection

In the interest of time, the design selection consisted primarily of the following criteria:

- Optimize engine cooling (water-side) for maximum system heat rejection.
- Keep system weight down.
- Move center of gravity of car forward.

While traditional aerodynamic factors such as downforce and drag were considered, they were not the

primary deciding factors in the design. Furthermore, the oil system was subject to minimal analysis based on the fact that it performed extremely well in 2015; as long as only minor sacrifices were made, it was assumed that the oil system would work as intended.

The analysis in the coming 4.1.X sections follows the design process through the project chronologically.

4.1.1 Radiator Selection

The first step in the design of the cooling system was to analyze the cooling capabilities of the different cooler layouts. Based on the analysis covered in Section 3.1, Option C was selected. As a reminder, this design utilizes two small radiators for the water loop plumbed in series. A third CRF 450 radiator was to be used for the oil system, placed next to the left water radiator. Figure 3.8 was copied below and given the new figure number of 4.1 for convenience. This plot, in conjunction with Figure 3.9, was the primary factor in selecting this design: in these plots, the use of two CRF 450 radiators plumbed in series had about 24% increased heat rejection over the 2015 single-radiator concepts. Do note that this data uses some very key assumptions, the most important of which is mass flow rate of water through the engine being equivalent in all setups. This will need to be validated. It is very likely there will be a diminished flow rate as flowing through the smaller radiator will result in higher pressure drops across each of the coolers. However, in the interest of time, this analysis was neglected in favor of the equal-flow rate assumption. When the competition season is over, a flowmeter can be added to the cCar to help determine if the assumption was reasonable.

Enhanced heat rejection was not the only factor in this decision. There are also weight savings to be had as the radiators for the CRF 450 all weigh about 550 grams each, while a TRX 450 radiator was measured at roughly 1050 grams. Having three CRF 450 radiators (two water, one oil) means about 1650 grams while two TRX 450 radiators (one water, one oil) as was used in 2015 totals about 2100 grams, a savings of about 450 grams for the 2016 cCar.

Packaging the new coolers is also simpler as they are not nearly as wide as the TRX radiators. Two of the radiators placed side by side only take up 240mm widthwise, compared to a single TRX's 325mm of space consumption. As such, the radiators can be placed facing straight forward, both simplifying the duct design to follow and allowing air to travel straight through the radiator, rather than being forced to change direction as it passes through the fins.

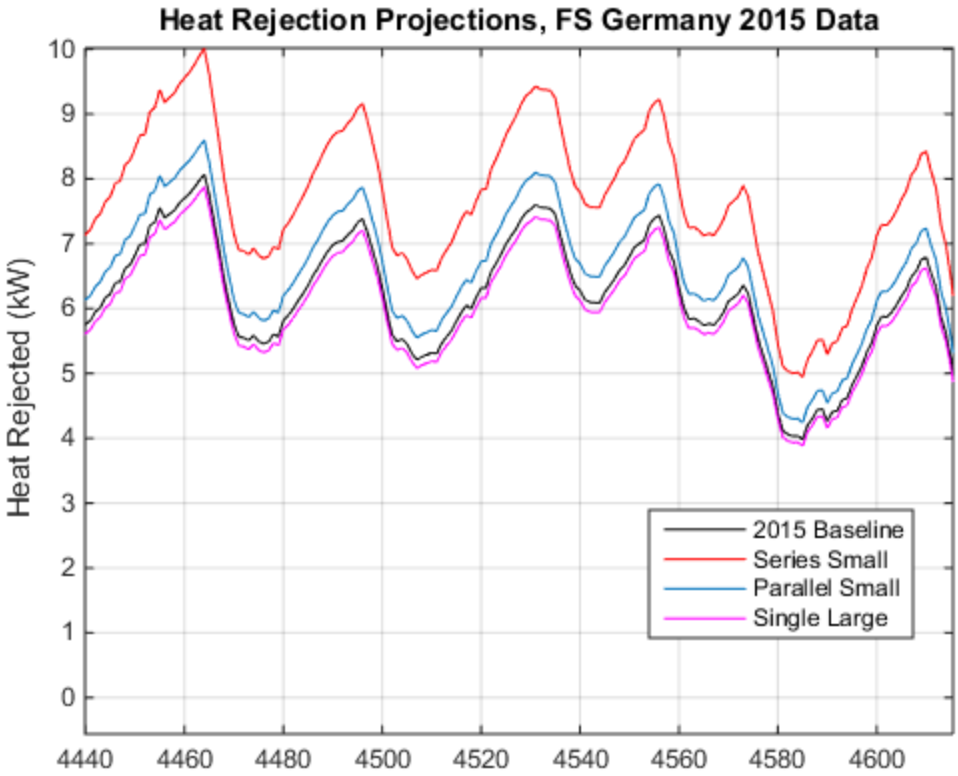

Figure 4.1: A copy of Figure 3.8 which shows the estimated heat rejection of different radiator configurations using data from FS Germany 2015.

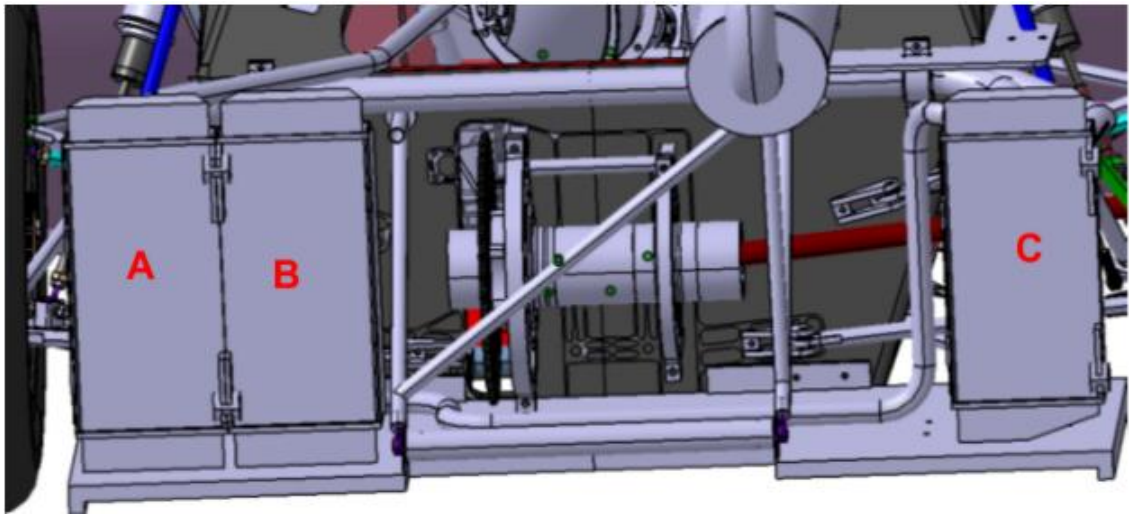

Figure 4.2: Radiator position as seen from rear of 2016 cCar model.

In the above image, the three radiators are labeled A, B, and C. A is the left water radiator, which the water passes through first. The water travels through a line along the diffuser to C, the right water radiator, before reentering the right side of the chassis. B is the oil radiator, packaged next to A within the same ducting system (hidden in the above image). Radiator C is modeled after the "right side" radiator from 2005-2008 CRF 450 bike models, as indicated by the different reservoir shape at the bottom and the slightly shorter

core area. Both radiator designs were made by using calipers and a ruler to measure the various features of the radiator, resulting in models that are approximations of the physical parts.

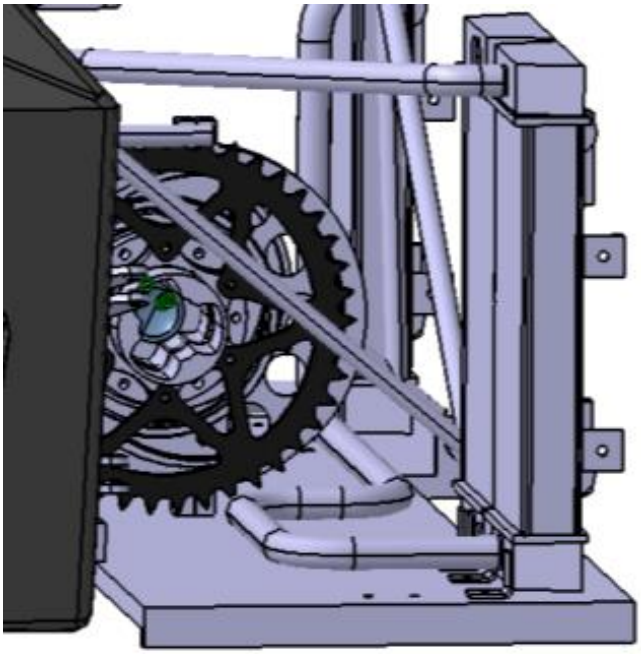

Figure 4.3: Side view of diffuser with radiators, showing proximity to chassis.

4.1.2 Diffuser

The diffuser design was selected based on the core criteria of being simple and only as large as necessary to reduce weight. The radiators were moved as far forward as possible before interference with other parts became problematic, such as the anti-roll bar. That became the constraint around which the diffuser was designed. The distance rearward was limited to only extend as far as absolutely necessary; the part was no longer treated as an aerodynamic element but a part to merely provide a mounting location for the coolers. Additionally, the design was changed from 2015 to be flat. The 2015 diffuser had mounting on the sides of the chassis, as shown below in Figure 4.4. Due to packaging and access issues, this bolt was investigated for potential removal. With Phil Arscott's assistance, the bolt here was removed and the car was jacked with no noticeable deflection in this area. Thus, the 2016 diffuser was designed without this mounting solution.

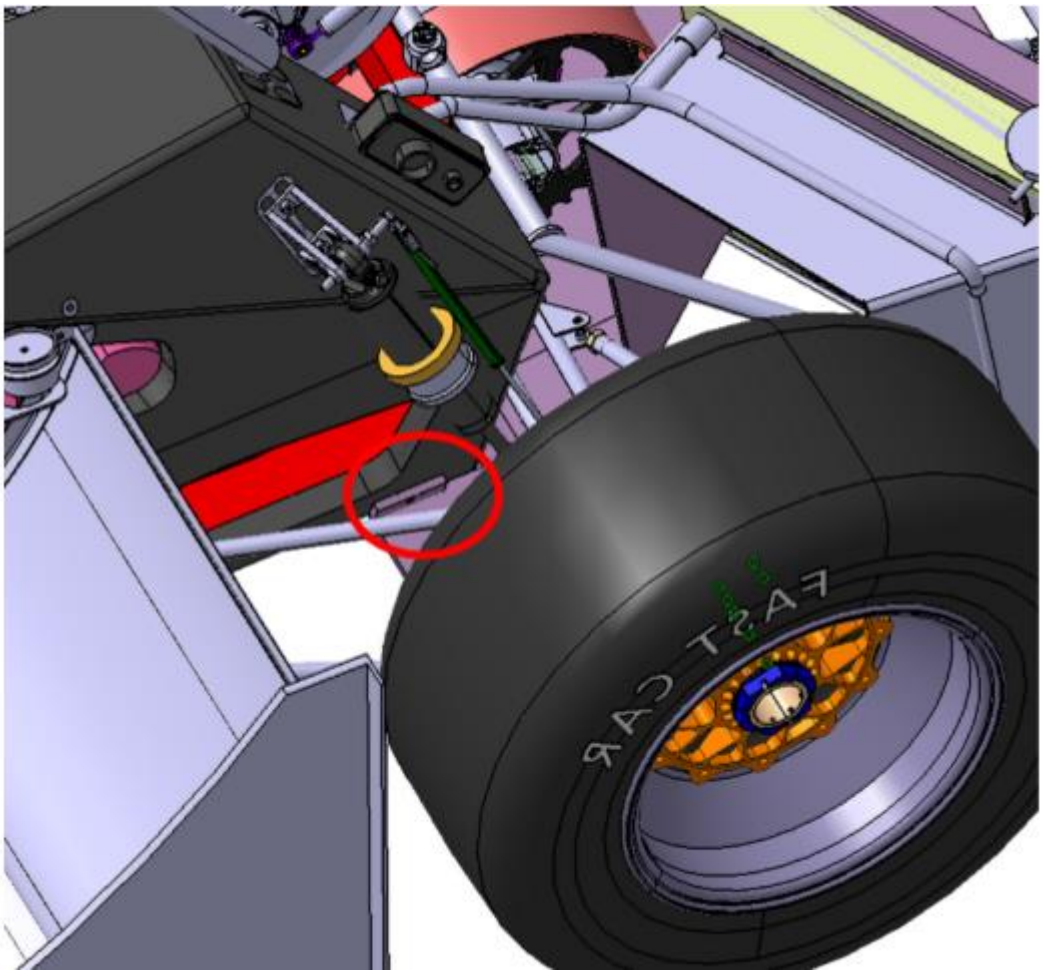

Figure 4.4: Diffuser side mounting on 2015 car chassis.

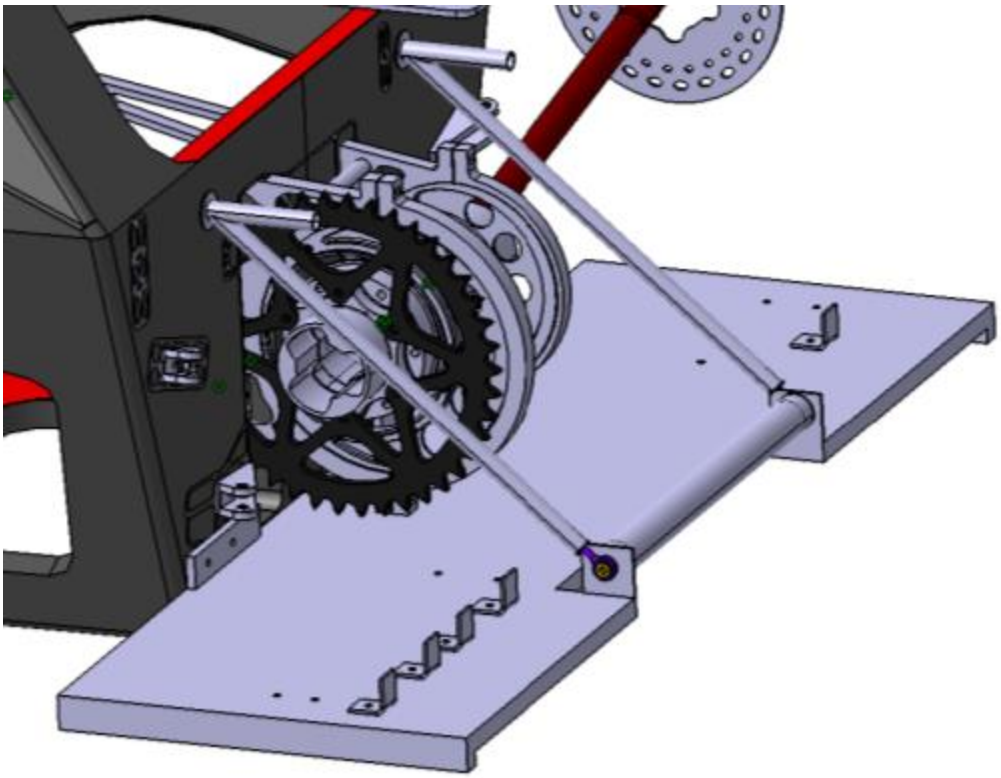

Figure 4.5: 2016 diffuser design.

Phil Arscott brought up some design issues that plagued the 2015 diffuser and were addressed with this design. First, there were problems with the diffuser striking the ground during races, especially while cornering. This was alleviated by having the bottom of the diffuser about 60mm above the XY plane of the CAD model. The 2015 diffuser was flush with the bottom of the chassis; in the 2016 design case, the diffuser was moved so the bottom surface is around 28mm higher than the bottom of the chassis. Second, mounting of various elements such as radiators and ducts needed to be more secure as the 2015 car had some issues with loose mounting (according to several technical leads). To mitigate this, simple hardpoints were placed inside the diffuser during layup. A third issue was the jack bar - diffuser linkage interface. The 2015 car used clevises welded to the jack bar, but this required a specific positioning of the bar; if it rotated, the angle and distance for the linkage system would be thrown off. The diffuser linkage system is discussed below, following the jack bar discussion.

The jack bar was designed to fit within the parameters of the rules while being as light as possible. Thus aluminum tube of 1” outer diameter and just under 12” length was used, with inserts welded in the ends to bolt into the diffuser making up the remaining distance to hit 12”. The following figures show how the diffuser connects to the upper mounting of the chassis.

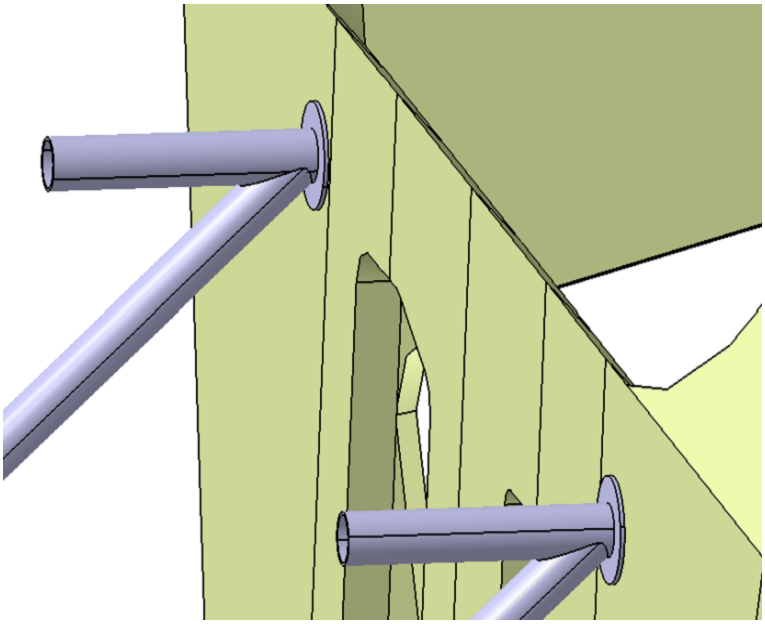

Figure 4.6: Linkage mounting points on the chassis. Plate is bolted to chassis. The horizontal tube welds to the plate. The diagonal tube is welded to the chassis and interfaces with the jack bar bolts via an M5 rod end.

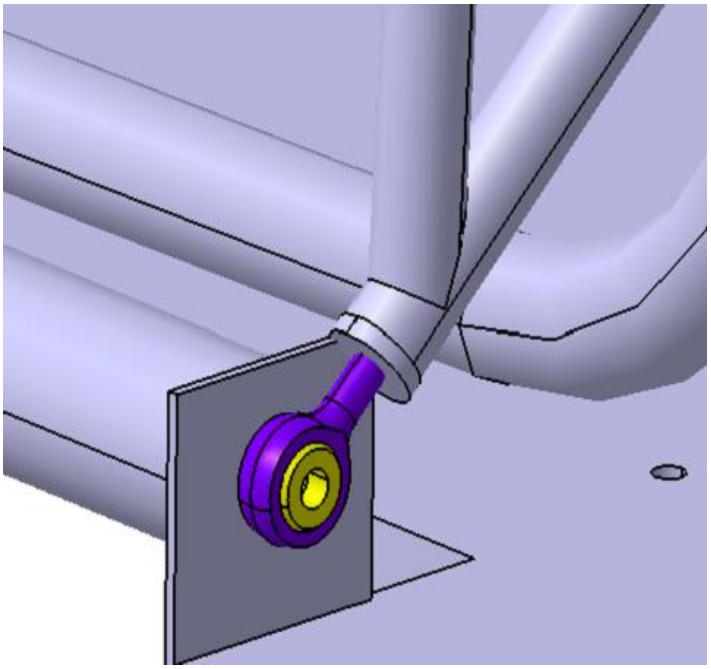

Figure 4.7: Linkage tube with rod end. Vertical tube is part of the exhaust mounting system.

The diffuser linkage system is fairly similar to the 2015 car. A plate was welded to a tube for mounting to the chassis, with a second tube being coped and welded to the first tube, extending down to the jack bar location, as pictured in the two images above. To fix the mounting issue, rod ends were used. This allows the linkage to be mounted to the same bolt as the jack bar, but does not require the jack bar to be in a specific position about its axis, decreasing the required precision of machining and mounting.

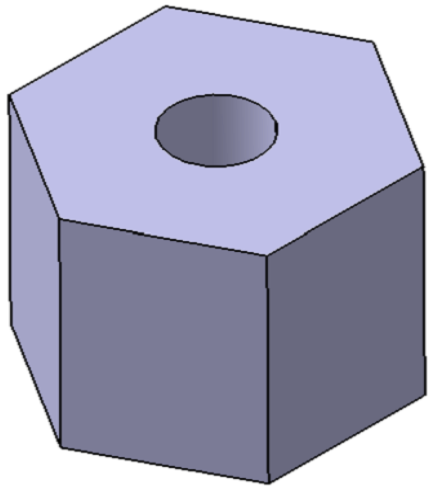

Figure 4.8: The diffuser hardpoint design. The hardpoint is 0.5” tall to match the thickness of the core and 0.5” wide, measured side to side.

The diffuser contains 13 hardpoints for bolting the ducts and radiators (4 for each front duct, 2 for each radiator on left, and one for radiator on right side). The cross section of the hardpoints was selected based on the reasoning used by Connor Torris in the 2015 Sidewing report [20]. To summarize, it was found that a round cross section would only give small benefits to mass of the car, while a hexagonal cross section gave an extra layer of security in case adhesive tape failed in the core; the edges would help resist rotation as a torque is applied to the bolts.

4.1.3 Jack Bar

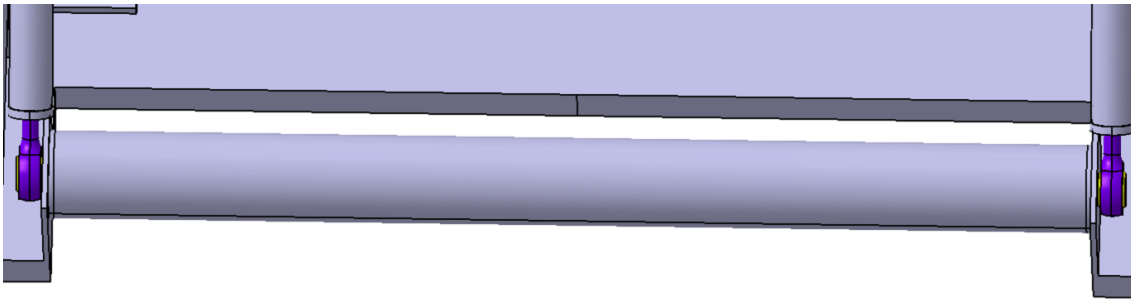

Figure 4.9: Jack bar as installed in the diffuser.

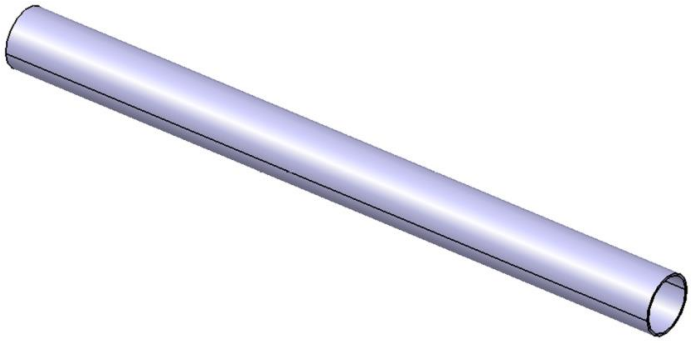

Figure 4.10: Jack bar tube without inserts.

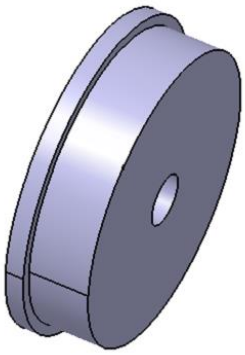

Figure 4.11: Jack bar inserts to be welded into tube. The hole is tapped for an M5 bolt.

The above images show the components of the jack bar. As a reminder, the jack bar needs to be roughly 12” long, per Rule T6.6.2 [2]. This length was achieved by cutting the tube just below 12” and filling the remaining length with the flange on the inserts. The bar is mounted between two tabs in the diffuser with M5 bolts. These bolts also connect to rod ends for the diffuser linkage.

4.1.4 Ducts

As was the case with the design of the diffuser, simplicity was key with the duct designs. Front ducts were made to come straight forward off the radiators, and making sure the outer walls did not extend further than the diffuser as rub against the tires was an issue with the 2015 cCar, as mentioned by Phil Arscott. The front ducts also require cutouts for the anti-roll bar to prevent interference issues.

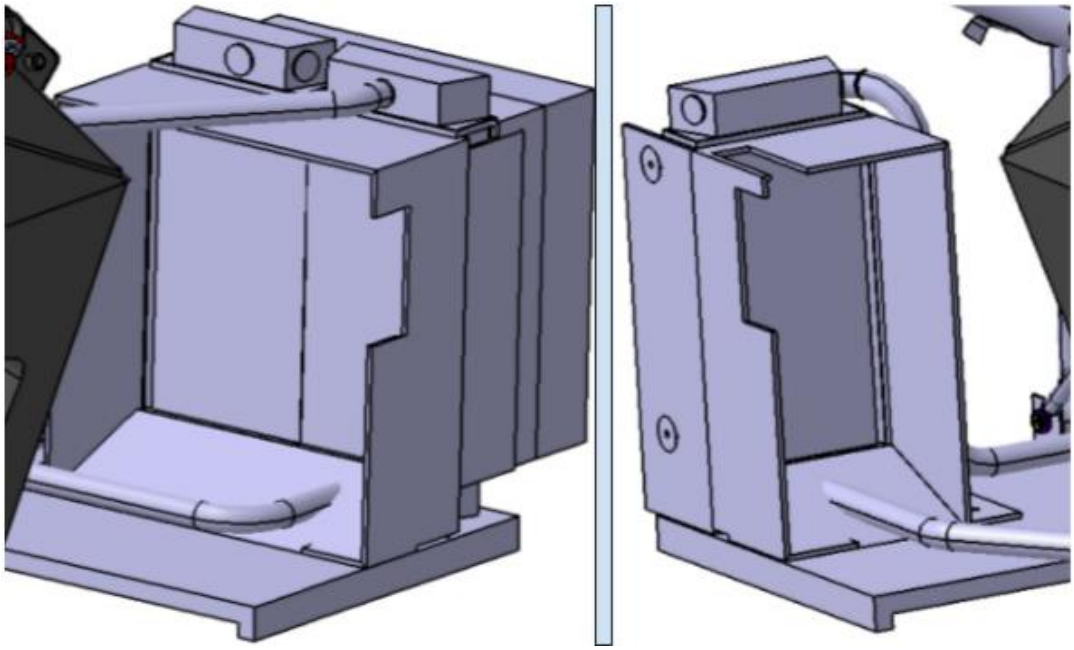

Figure 4.12: Left: Left front duct system, with the first water and oil coolers; Right: Right front duct with the second water cooler.

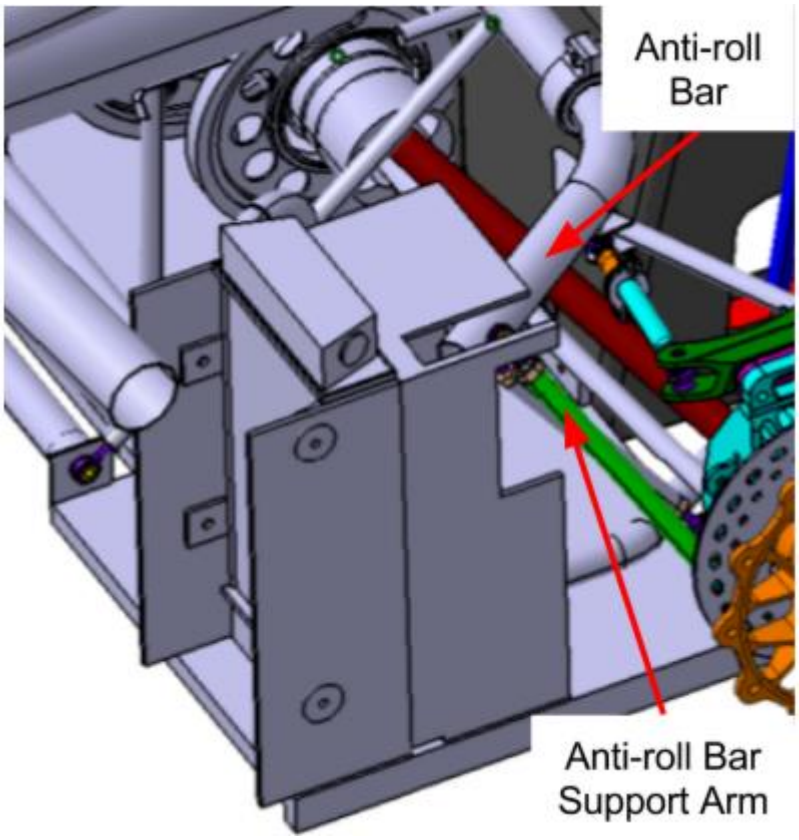

Figure 4.13: The anti-roll bar (ARB) and ARB support arm caused concern for potential interference with the front ducts (the cutouts are outdated in this image as they are based on a previous ARB design).

The right duct does not feature an exit duct piece as there is no need for a fan. The exit duct for the left side was designed to contain the air and have it pass through a circular opening, acting as a fan shroud, with a fan to be mounted on the exterior rear of the duct, covering the hole. The size of the opening was selected based upon available space. Even having the duct come straight out (as opposed to converging) at the exit, there was still not enough room for a 10” fan, such as the one used in 2015. Instead, a 9” fan from SPAL was selected. Based on hole locations for mounting the fan, the final hole for the duct was given a diameter of 8.5”.

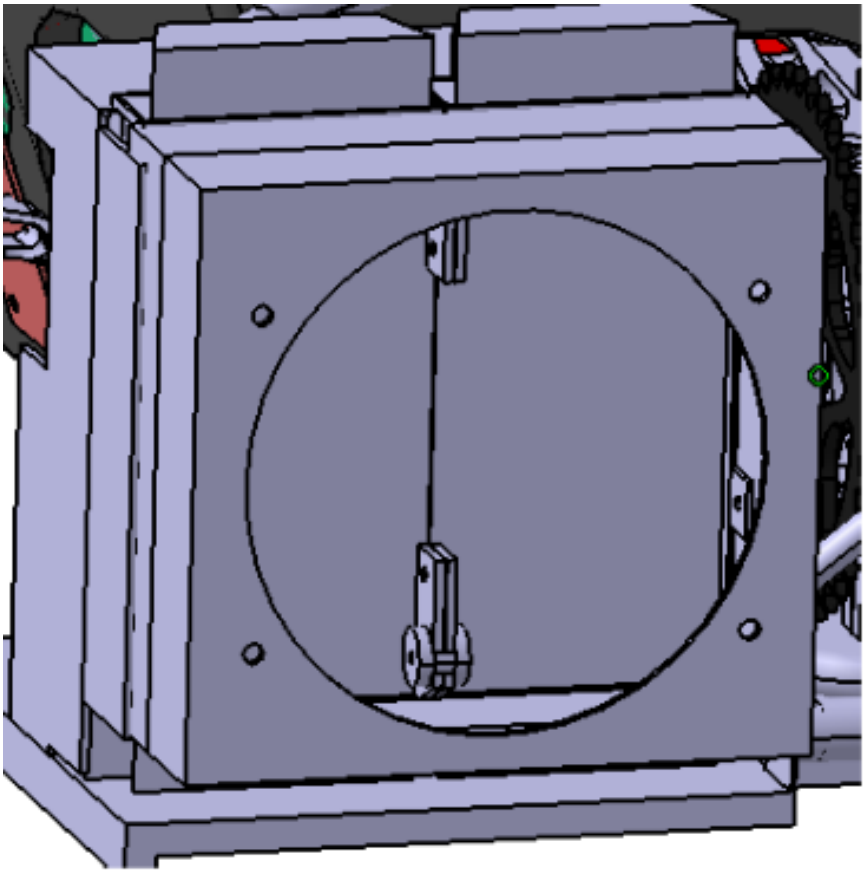

Figure 4.14: Exit duct as mounted on the left side in the model, showing the 8.5” circular opening and four mounting holes for the fan.

The final components for the ducts are the “bottom duct” pieces, small ramps that lead up to the bottom edge of the cooling area for the radiators. These are extremely simple parts made to simply keep the air from diverting around and under the coolers. The ramp was designed to be an L shape for ease of manufacturing.

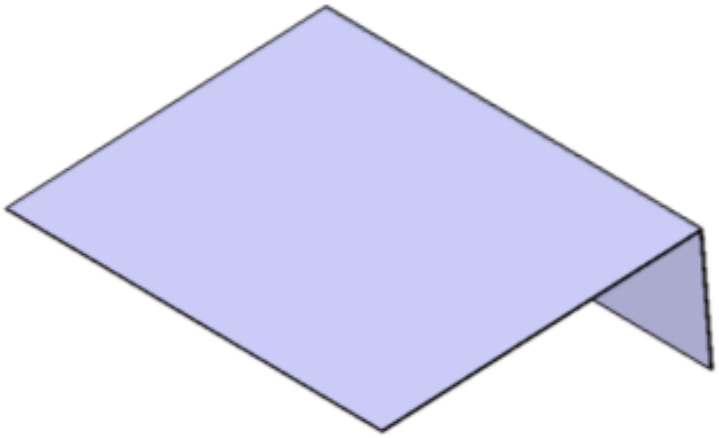

Figure 4.15: Bottom ducting for the left ducts; the right side is the same shape but slightly shorter as the front duct is not as wide for a single cooler; not modeled are holes for plumbing to pass through to the bottom reservoirs. This design could be improved with horizontal flanges to mount the piece to the diffuser easily with Velcro.

Flanges were built into the ducts to allow them to mount to the diffuser. The holes were reinforced with washers to prevent the foam core from crushing when bolting onto the car. For more information, see Appendix A.

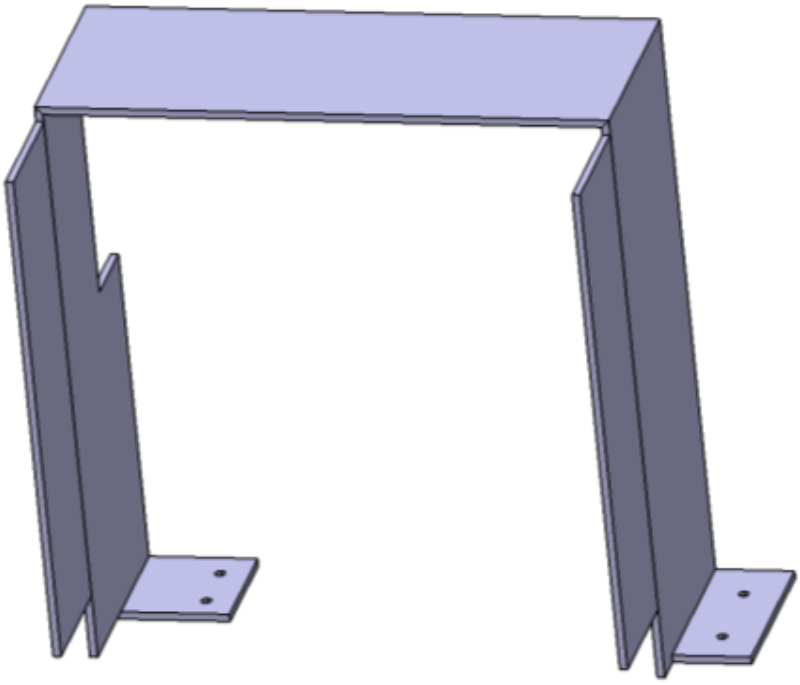

Figure 4.16: The left front duct, isolated to show the flanges and holes for M5 bolts to secure the front ducts directly to hardpoints in the diffuser.

4.1.5 Plumbing

In line with the major change in radiator selection, the plumbing was modified greatly from the 2015 car. Because the 2015 cCar had a single radiator located on the right side of the car, the water line exited and reentered on the right side of the chassis. However, due to position and orientation of the engine in the engine bay, the water outlet is slightly closer to the left side of the chassis. The 2016 design calls for the line to come out the rear chassis hole, as shown below in Figure 4.17.

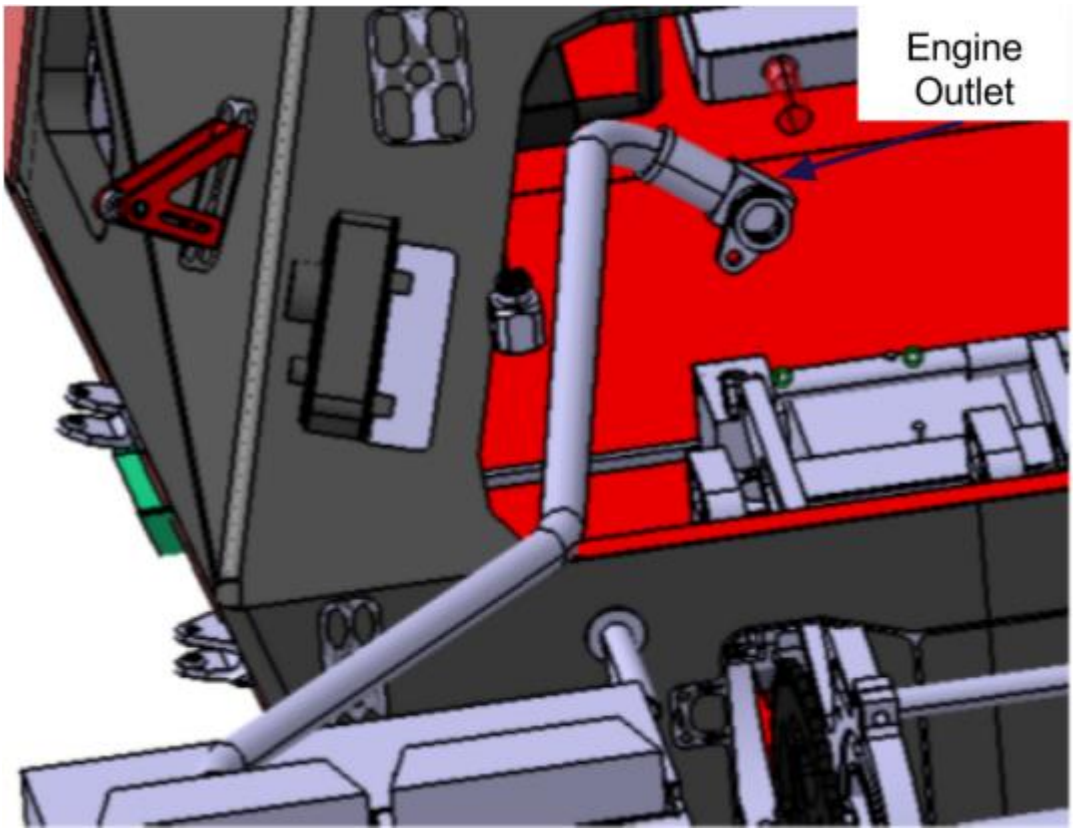

Figure 4.17: “Engine Outlet” line: the plumbing connecting the engine outlet to the first water radiator (engine not shown).

The line connecting the two water radiators proved to be far more troublesome to nail down. Early on, the design called for an excessive number of bends. After reworking, the line was changed to what can be seen in Figure 4.20. The first design can be seen in Figure 4.18 and 4.19. The pipe was thought to need to move past the ducts, then move back to the rear of the diffuser to get past the drivetrain parts, before finally making its way to the second radiator on the right side. However, this was changed so that the pipe comes through the left duct, requiring another hole to be made just above the right flange.

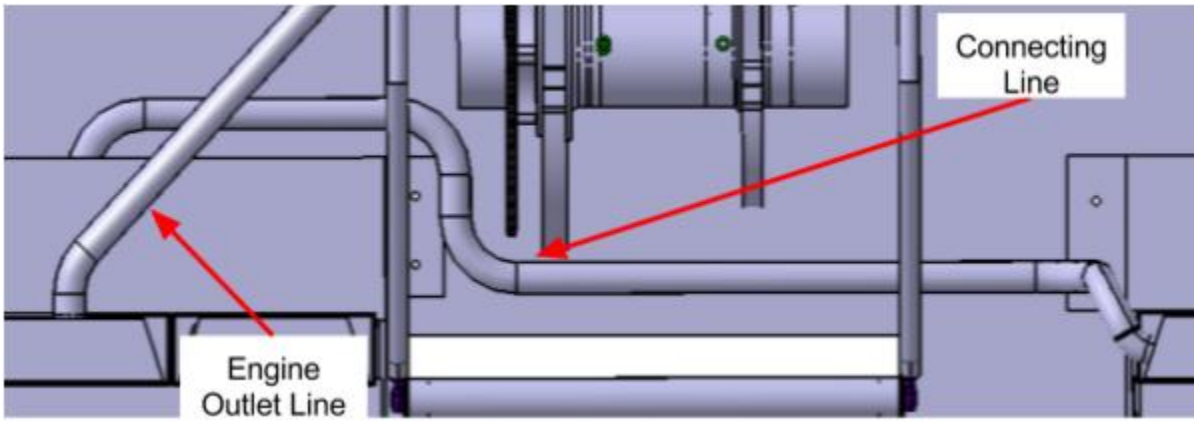

Figure 4.18: Top view of the diffuser showing the connecting line and its bends as it approaches the right radiator (initial design).

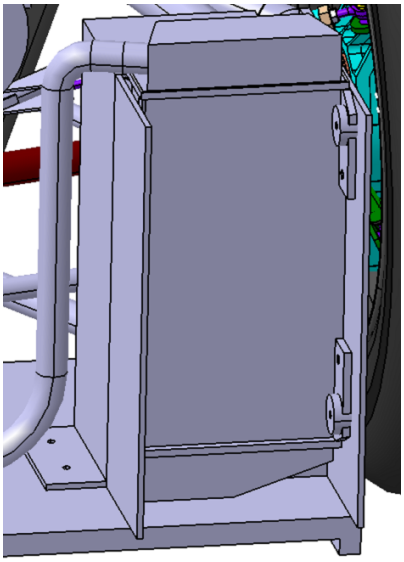

Figure 4.19: The connecting line as it interfaces with the right radiator.

Figure 4.20: Final connecting line, as installed, coming out of left duct.

Finally, the line connecting the second radiator to the engine inlet currently interfaces at an inlet piece similar to the 2015 cCar's port. However, Gabe Gray and Eric Bramlett have discussed the possibility of modifying the water pump cover (which is right below the inlet piece, but is not pictured in Figure 4.21). This would require welding in a bung and modifying the cover but would get rid of a 90 degree change in flow direction if successful. This project does not cover that modification, but later iterations of the cooling system may incorporate it.

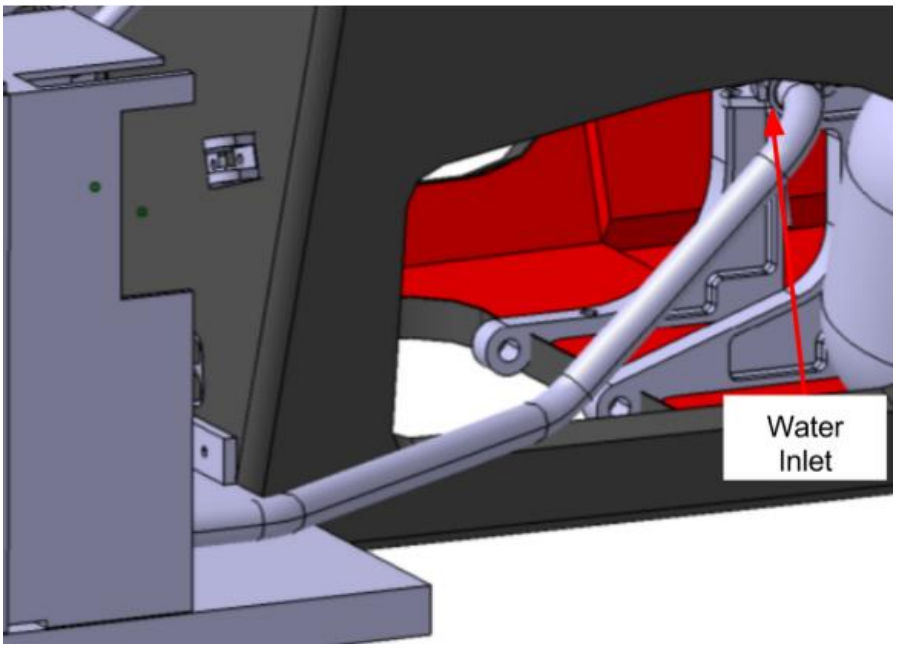

Figure 4.21: “Engine Inlet” line: the water line connecting the second cooler to the inlet of the engine near the water pump cover (not pictured).

Note on above images for plumbing: These images came from a somewhat early CAD model, prior to silicone being modeled. Once made, silicone was used only at radiator and engine ports. All bends in the middle of the lines were made into the aluminum tubing by Elliott Bending.

4.1.6 Other Parts

Initially, the catch cans to be used were based on the 2014 design. Designed to be approximately 1 liter in capacity, the design is more than sufficient for the amount of fluid in the system [21]. Based on both physical measurements of the new radiators and measurements of the plumbing in CAD, as well as information found in the CRF 450 engine manual, I found that the system should have no more than 4 liters of water flowing through it (and that is an estimate on the high side - it should be closer to 3 liters). Recall Rule T8.2.2, which states that the catch can capacity must be the greater of 0.9 liters or 10% of the fluid in the system [2]. Since the fluid is well below 9 liters, the 0.9 liters is the target minimum, validating the selection of the 2014 catch can design.

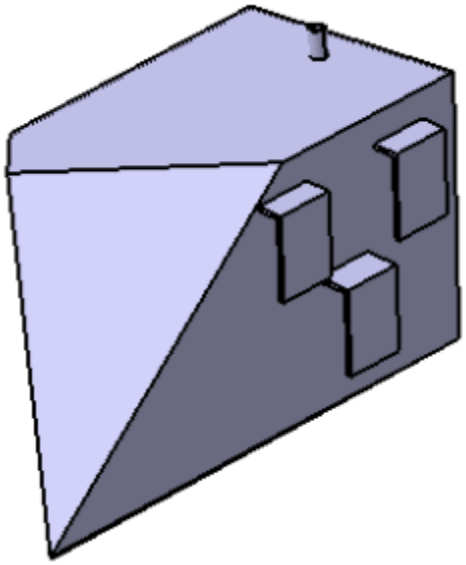

Figure 4.22: The catch can design from the 2014 CAD model, with simplified geometry (i.e., no rounded corners).

However, a large cylinder (over 4” in diameter) made of aluminum was found and used to make a basic, cylindrical catch can for both the oil and water loops. Details can be found in Appendix A3.4.2.

The components not discussed previously include several of the fittings, such as those found on the catch cans and the oil lines, as well as the oil lines themselves. Many of the fittings can be purchased, in the case of T-fittings and other AN-style parts for the oil loop.

4.2 Technical Specification

Cooling Capabilities

This has already been discussed at length in previous sections. See Section 2.2.1 for calculation methodology and Section 3.1 for results. To reiterate the findings, the expected cooling capabilities of the system is to be about 24% improved over the 2015 cCar at any given point in the competition; as cooling is dependent on car speed and other factors, a specific heat rejection value cannot be given.

Weight

The 2016 cCar’s weight was influenced most heavily by the following components: water plumbing, radiator selection, and aerodynamic elements. Many of the fittings and other cPowertrain-related items, such as catch cans, were largely unchanged from last year. As stated previously, the radiator selection resulted result in around 450 grams of weight savings for a total of 1650 grams between the two water and single oil coolers. The aerodynamic elements are tabulated below.

Table 4.1: Weights of the aerodynamic components for the system.

Partnumber	Description	Estimated Weight [g]	Quantity	Total Part Weight [g]
GFR_16_10_41_211_PRT_A	Diffuser Plate	505	1	505
GFR_16_10_41_212_PRT_A	Jack Bar	55.983	1	55.983

GFR_16_10_41_213_PRT_A	Jack Bar Insert	7.73	2	15.46	
GFR_16_10_41_214_PRT_A	Diffuser Hardpoint	4.327	13	56.251	
GFR_16_10_41_216_PRT_A	L Bracket	5.59	5	27.95	**LEGEND**
GFR_16_10_41_221_PRT_A	Right Duct, Front	121	1	121	Composites
GFR_16_10_41_225_PRT_A	Right Duct, Bottom	5	1	5	Steel
GFR_16_10_41_231_PRT_A	Left Duct, Front	118	1	118	Aluminum
GFR_16_10_41_232_PRT_A	Left Duct, Exit	132	1	132	
GFR_16_10_41_235_PRT_A	Left Duct, Bottom	11	1	11	
GFR_16_10_41_241_PRT_A	Left Linkage Tube	82.318	1	82.318	(323mm long)
GFR_16_10_41_242_PRT_A	Left Chassis Mount, Tube	19.421	1	19.421	(75mm long)
GFR_16_10_41_243_PRT_A	Left Chassis Mount, Plate	4.759	1	4.759	
GFR_16_10_41_244_PRT_A	Right Linkage Tube	82.318	1	82.318	(323mm long)
GFR_16_10_41_245_PRT_A	Right Chassis Mount, Tube	19.421	1	19.421	(75mm long)
GFR_16_10_41_246_PRT_A	Right Chassis Mount, Plate	4.759	1	4.759	
GFR_16_10_41_248_PRT_A	Linkage Insert	8.793	2	17.586	
			TOTAL	**1278.226**	

The weights for the composites elements were determined from the Composite Weight Calculator [7]. The steel and aluminum part weights were determined from applying materials to the parts in CATIA and using the program to estimate the weight based on part volume and material density. The linkage tube dimensions are noted below further in Section 4.2. The total weight estimated for aerodynamic elements was about 1280 grams. Note that this is only an estimate of the weights, especially with regard to composite parts that use rough approximations of area to determine weights. Not shown above is the fan, which weighs about 1000g [22], similar to the measured weight of the fan used in 2015.

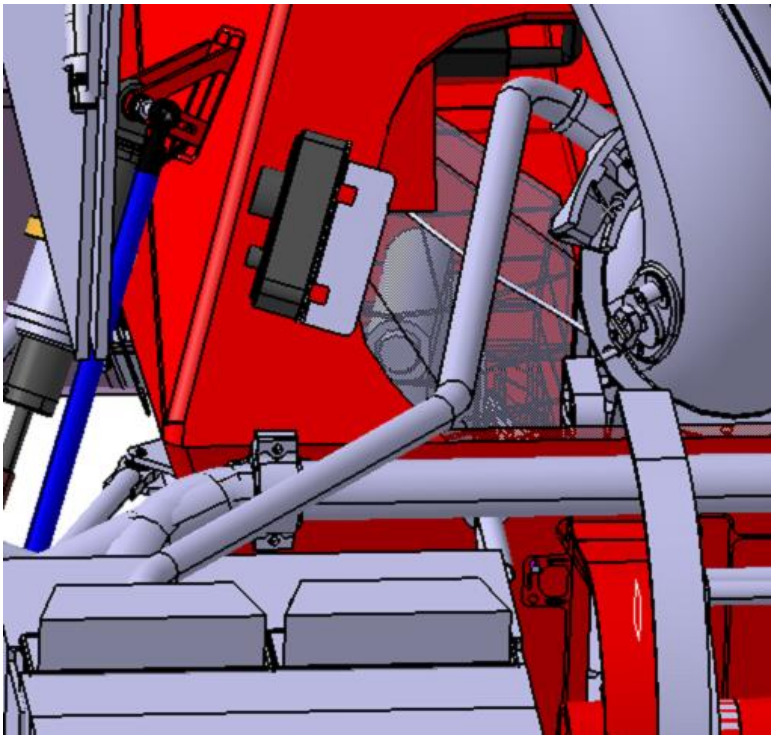

Figure 4.23: Aluminum line, engine outlet to first radiator.

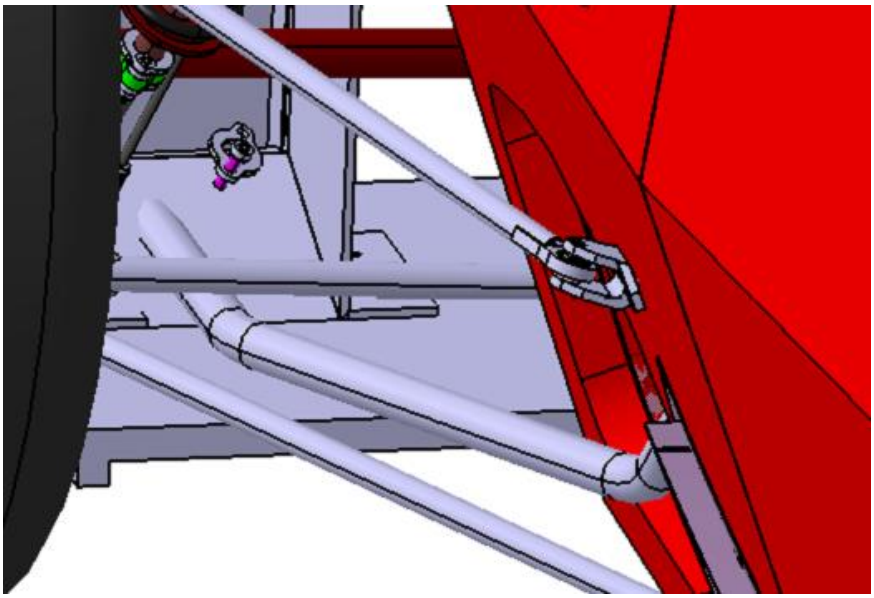

Figure 4.24: Aluminum water line, second radiator to engine inlet, view of radiator.

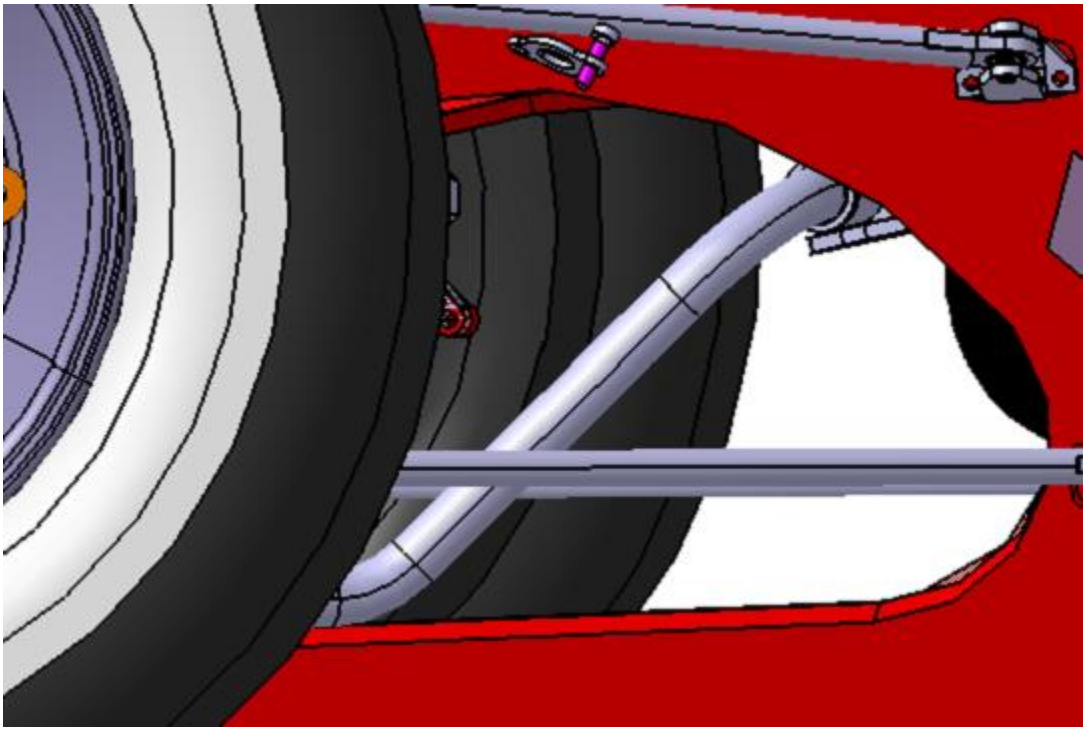

Figure 4.25: Aluminum water line, second radiator to engine inlet, view of engine inlet.

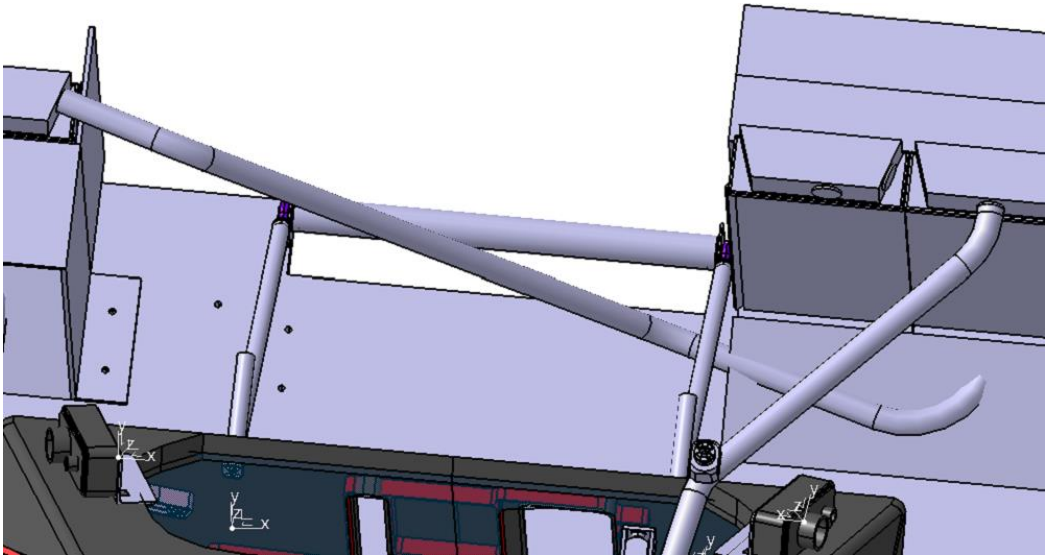

Figure 4.26: Aluminum water line, first radiator to second radiator (updated design).

Table 4.2: Weight estimates for water lines.

Line	Length of Aluminum [mm]	Length of Silicone [mm]	# Hose Clamps	Weight [g]
Engine Outlet	570	180	4	197
Radiator Connecting Line	443	180	4	181
Engine Inlet	628	180	4	204
			TOTAL	**582**

Table 4.2 was compiled based on estimations using the lines as seen in Figure 4.23 through Figure 4.26, with a resulting total of 582 grams for empty (no water in system) lines. These weights use the same measured weight for the materials from Section 3 (0.127 g/mm for aluminum, 0.380 g/mm for silicone, and 14 g per hose clamp). These distances were found estimating around 90mm long sections of silicone tube at each joint, with each joint being an inlet or outlet from engine or radiator. The aluminum length was found by designing the pipe as a single piece, then subtracting the length of silicone from the total length. These estimates were made prior to incorporating the thermostat into the system, which added two hose clamps and some silicone hose to the line.

Aerodynamics

According to the Aero Run/Ran results for GFR16_HB_ALv6_CL_1 (which was summarized as part of Table 3.1 and corresponds to a small cooler behind the tire), around 2.6 N of lift and 0.3 N of drag were to be expected for the right side cooler. The cooler selection was based heavily on this design. As the design progressed, a simulation was run by Hannes which looks into the airflow through each radiator in the left duct system as well as an updated simulation of the right duct and radiator. These simulations take into account the updated design at the rear of the vehicle, including the new diffuser and anti-roll bar. The total downforce and drag, as a result of the cooling ducts, are a bit higher than initially anticipated, at 4.62 N of lift and 2.36 N of drag.

Table 4.3: 2016 cCar radiator airflow (data from Hannes's Radiator CFD Analysis [23]).

Sim condition	Total Downforce [N]	Total Drag [N]	Mass flow, left outside radiator [kg/s]	Mass flow, left inside radiator [kg/s]	Mass flow, right radiator [kg/s]	Cooling DF [N]	Cooling DR [N]
Straight	832.03	317.77	.14	.15	.25	-4.62	2.36

Strength Requirements and Material Selection

For the components in the diffuser system (linkage and jack bar), the 2015 material selection acted as a baseline and some calculations were performed to double check numbers.

Jack Bar:

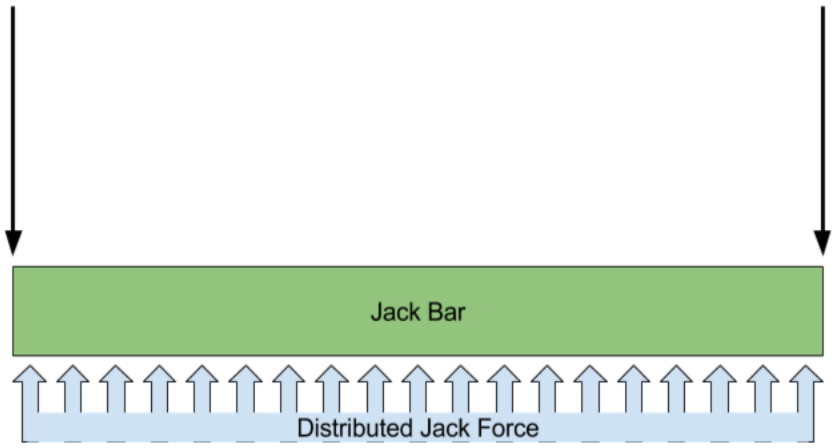

Figure 4.27: Free-body diagram for the jack bar, with a distributed load while jacking and two reaction forces at the ends where the bar bolts to the diffuser.

The equation used was:

$$\sigma = \frac{My}{I}$$

which becomes:

$$\sigma = \frac{PLr_o}{8I}$$

for a round beam, pinned at each end, with a distributed load, for which the maximum stress due to bending is the middle of the beam (lengthwise). P is the force applied to the jack bar, L is the length of the bar, r_o is the outer radius of the jack bar, and I is the area moment of inertia for the bar. P was approximated at 1556N, based on roughly 500 pounds for a car with rider inside (estimated 350 pound car weight and 150 pound rider weight, summed and converted to 2224N). The weight of the vehicle and rider is supported both by the front wheels and the jack bar; Alex LaFranchi recommended approximating the CG as 58% rearward. Summing moments at the location of the front wheels then results in an estimated load of 1556N on the jack bar. Radius is 0.5"and length is 12". This gave a stress of approximately 146 MPa, assuming 0.035" wall thickness when calculating I. As aluminum 6061-T6 has a yield strength of 276 MPa, the safety factor is just under 2 for the jack bar [18]. This validates the use of a 1" OD / 0.035" wall thickness aluminum 6061-T6 tube for the jack bar.

For a tube of the same material but with 1"OD / 0.028" wall thickness, the calculations provide a stress of 179 MPa. This still provides a factor of safety just above 1.5. Finding such material was difficult, as it seems to be a special order item, not directly off the shelf. 0.035" wall thickness was used for the 2016 components but can be replaced if material is found later.

Linkage System

The point of analysis for this piece is where the linkage tubes are welded to the chassis plate/tube mounts. Welding weakens the material and the bars are subject to some high loads, so care was used to approximate the stresses in these components. The geometry of the tubing was assumed to be 0.5" outer diameter, 0.035" wall thickness, with additional considerations for 0.028" wall thickness tubing.

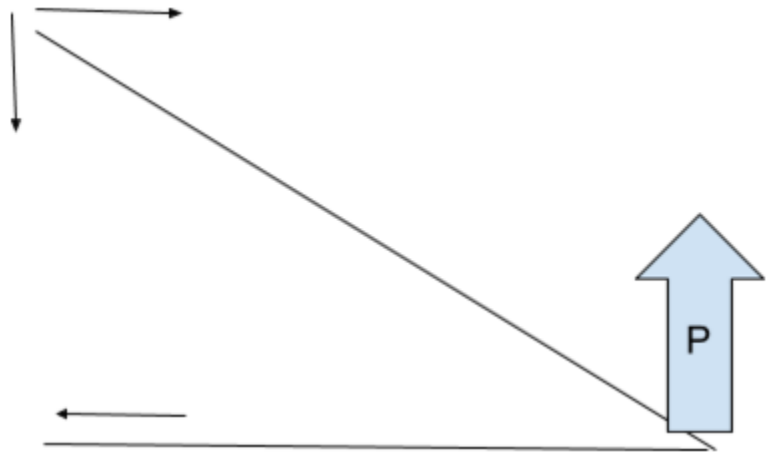

Figure 4.28: FBD of the diffuser system, seen from side; horizontal line is the diffuser plate as a two-force member, and the linkage arms approximated as a two-force member extend up and left; P is the applied jacking force and the smaller arrows are reactions at the chassis mounts.

The analysis was simplified by assuming two-force members and each linkage arm supports half the resulting load. Thus, P was assumed to be 1100 N for each linkage arm system. First, the system was analyzed for buckling, using:

$$E = \frac{F(KL)^2}{\pi^2 I}$$

where K is 0.699 for a beam with one fixed end and one pinned end, L is approximately 322mm (length of the linkage arm), F is the load that would cause buckling ($\frac{P}{sin(\theta)}$ was used as the minimum force that needed to be supported, where theta is the angle between the tube and diffuser) and I is the moment of inertia for the beam. The result of this calculation gave a required modulus of elasticity of 14.5 GPa, one of the requirements for material selection.

As the system was approximated as a two-force member, there was no analysis to be done for a moment at the chassis point. Rather, there is axial tension and compression to be considered. For compression, the condition of the jack in use is still considered, such that:

$$\sigma_c = \frac{F}{A} = \frac{P}{sin(\theta)\pi({r_o}^2 - {r_i}^2)}$$

In the above equation, theta is angle between the linkage tube and the diffuser, r_o is the outer radius, and r_i is the inner radius. Solving with a P of 1112N (the maximum force in the system, considering the weight of the vehicle and ignoring any support of the front tires still resting on the ground for conservative estimates) and it is found that the compressive stress is around 50 MPa.

A final consideration to make is the tensile stress that the tubes may see. During a competition, according to Gabe Gray, the tubes may experience 2g vertically as the car travels over small bumps in the road, as well as high forces laterally during cornering. At the time of design, the weight of the exhaust system was unknown, so an overestimate of 15kg of load was assumed to be supported by the system. So, for 15kg on Earth at 2g, the expected force exerted downward on the diffuser is around 294N. To simplify the calculations, this force was assumed to act at the end of the diffuser, at the jack bar. This allows the above analysis to be used, with a P of 294 N / 2 to be used (147N in each tube system, down). The resulting tensile stress is then around 4.5MPa, based on the same equation used for compression.

Rerunning the calculations for a tube with wall thickness of 0.028", the results for critical force of steel in buckling was found to be 19.3 kN, well over ten times the load expected in the linkage, and a maximum stress of 60.9 MPa (compression) and 5.5 MPa in tension.

The material selected to meet these criteria is steel 4130, with a tensile strength of 435 MPa and modulus of elasticity of 205 GPa [24]. For 0.5" outer diameter/0.028" wall thickness steel, this gives a factor of safety of around 80 in tension (though this member will primarily experience compression). Again, welding weakens the material, but Eric Bramlett was confident this selection would be satisfactory. It may seem overkill to use this material for the loads experienced by the diffuser, but the above analysis is massively simplified. In reality, the diffuser mounts act somewhat like fixed supports. However, because this would make the analysis statically indeterminate and the bolts do not generate a significant moment, this fact was neglected. Either way, the loads are likely more strenuous than these calculations convey, so it is better to remain on the safe side.

5. Testing

5.1 Tests Completed to Date

5.1.1 Forces

Because jacking the car exerts a large load on the car, specifically the rear, the system was tested (and later put to use) by using a jack on the jack bar. With the exception of scraped paint, there is no damage and there has not been any noticeable issue with the diffuser supporting the load.

5.1.2 Cooling

The following section will have plots from MoTeC collected thus far. The graphs below show two portions of data collected. The top half shows engine temperature (blue line) and oil temperature (green line) over the course of the tests. The bottom plot shows the load from the fan. If there is a peak, the fan turned on. If it is flat at 0, then the fan is off.

The fully assembled water line (that is, including the thermostat) has been run through two endurance tests and a number of other runs, plus competition at FSAE Michigan. The two test endurance runs were both skewed by a failure in the left sidewing that resulted in it falling off the car, but the run from Michigan reflected a fully assembled vehicle. Without the sidewing, the airflow to the left side radiators was much higher, resulting in better (but uncharacteristic of a final vehicle) cooling. The first test, seen below, never required the fan to run, although this may have been due to the sidewing issue.

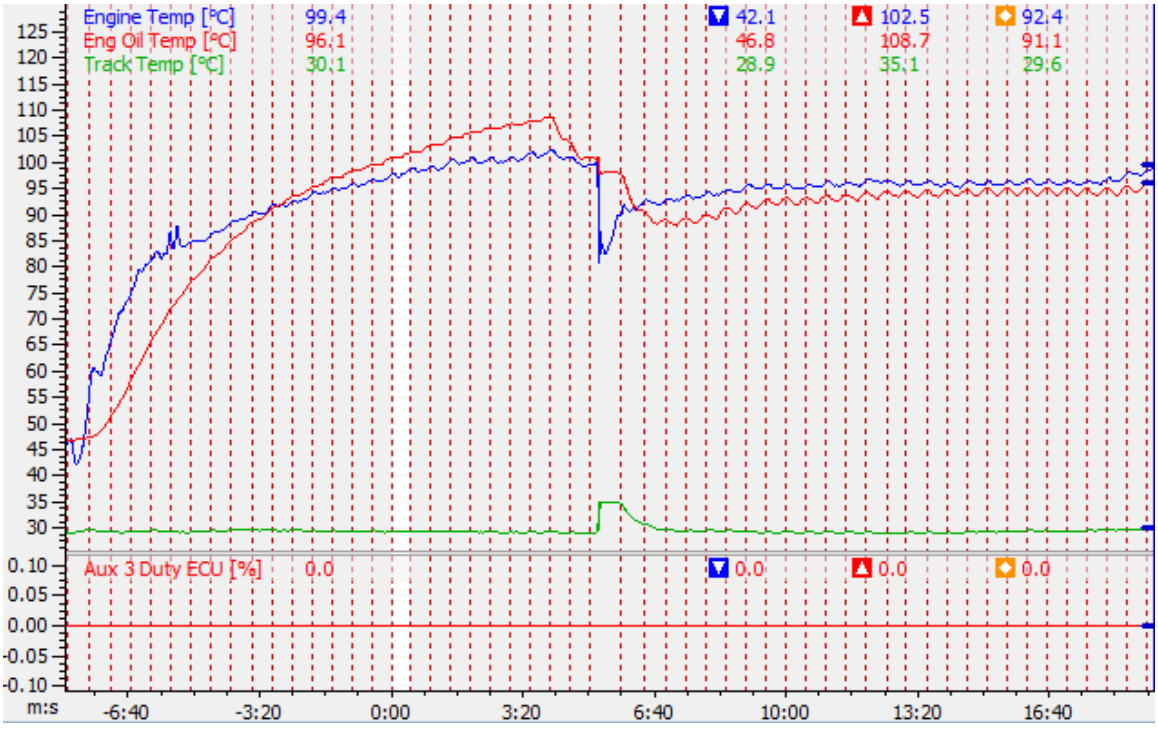

Figure 5.1: Data from May 1's first endurance test. Water temperature never went over 103°C. Oil never went over 109°C. Sidewing ailed right before driver change; driver change can be seen where the blue line plummets halfway through the plot.

Again, during the second endurance test, the fan was never actuated. However, this data is faulty as the

sidewing was still off the car. The temperatures for the engine oscillate around 90 degrees Celsius, far lower than the first endurance test. This is most likely due to the increased airflow to the radiators rather than a direct result of the cooling system design.

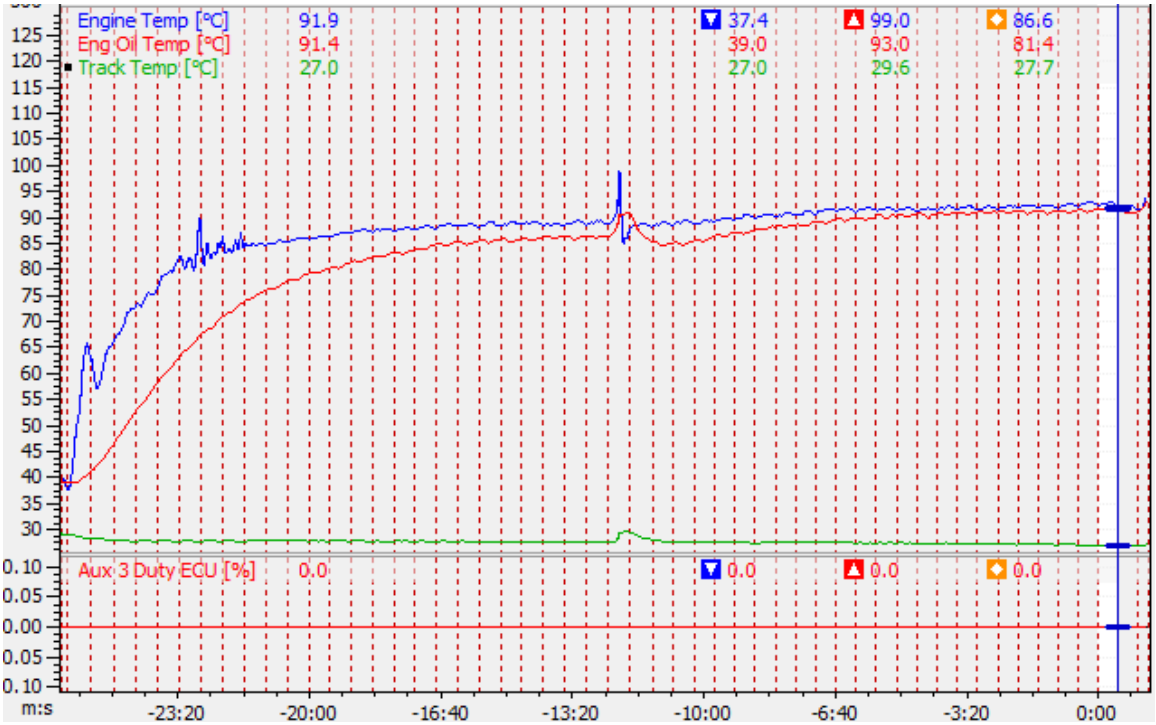

Figure 5.2: May 1's second endurance test. Water temperature peaked at 99°C, while oil stayed at or below 93°C. Note the location of peak water temperature; this is likely an outlier during driver change.

Unfortunately, it cannot be said that the fan had yet to be turned on. An example of this can be seen below; during April 30's skidpad testing, the fan actuated twice during the final run as water temperatures hit 110°C. The fan was enough to help the system stabilize.

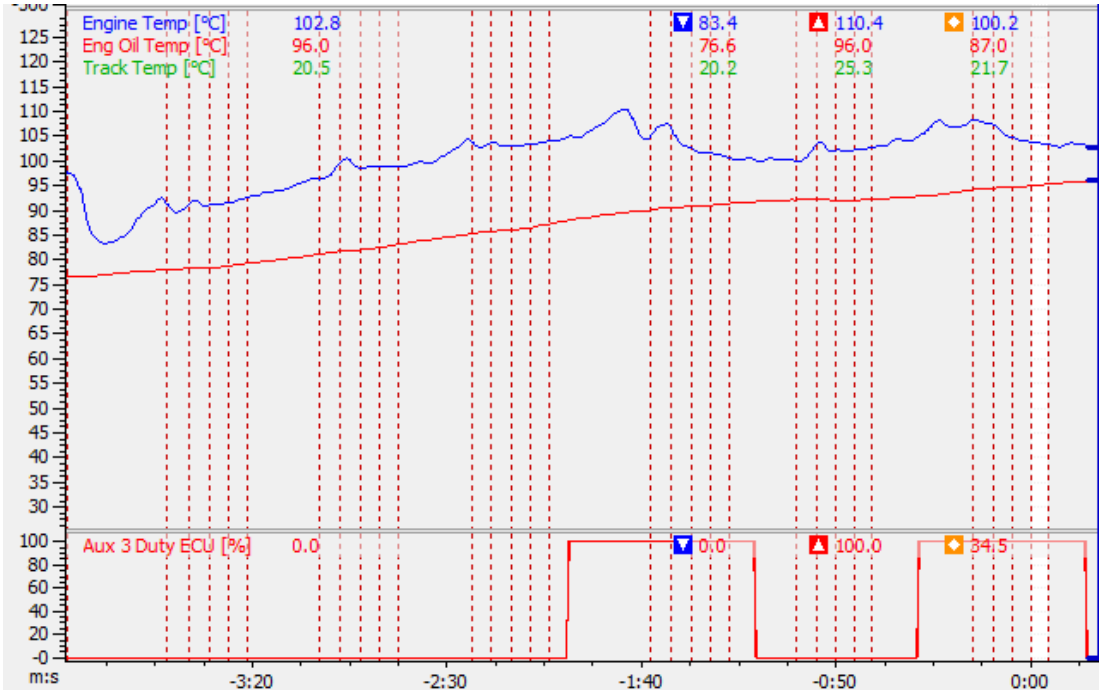

Figure 5.3: April 30's final skidpad test data. Fan turned on twice during this run. Water temperature peaked at 110°C.

While not ideal, the below plot shows the endurance data from April 30. This does not include the final cooling loop design, but does show cooling trends at operating temperature and is included for completeness. The engine temperature never broke 100°C, and oil stayed at or below 107°C.

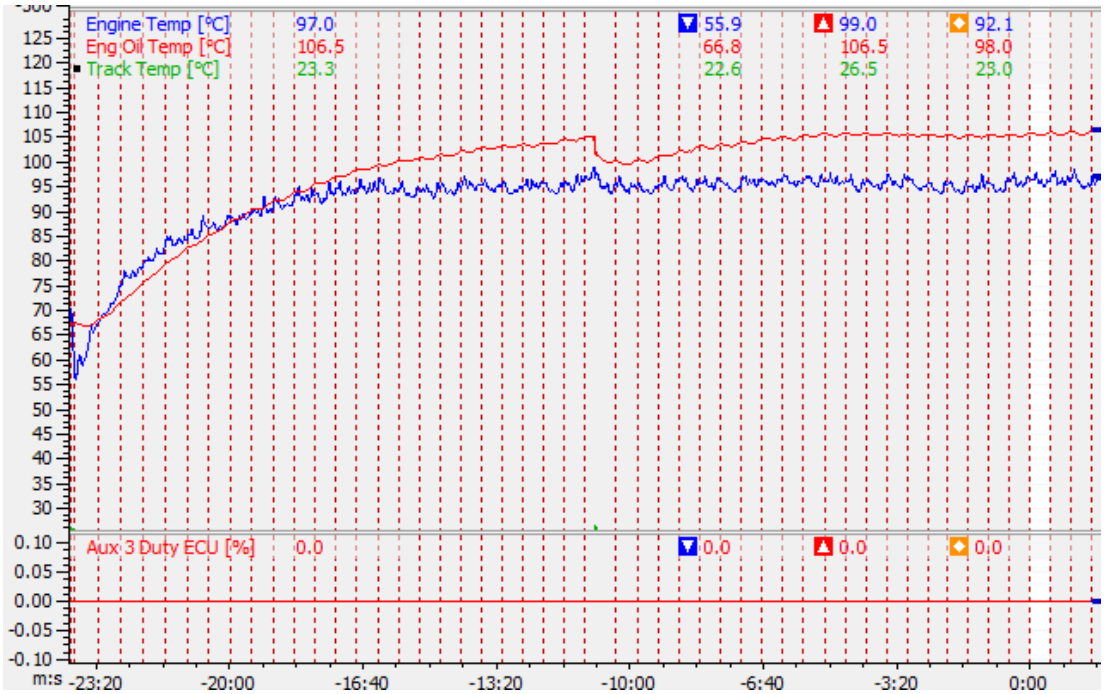

Figure 5.4: April 30's endurance run (no thermostat).

At Formula SAE Michigan in mid-May, the cooling system continued to have no issues with remaining at a moderate operating temperature, even with the sidewings installed.

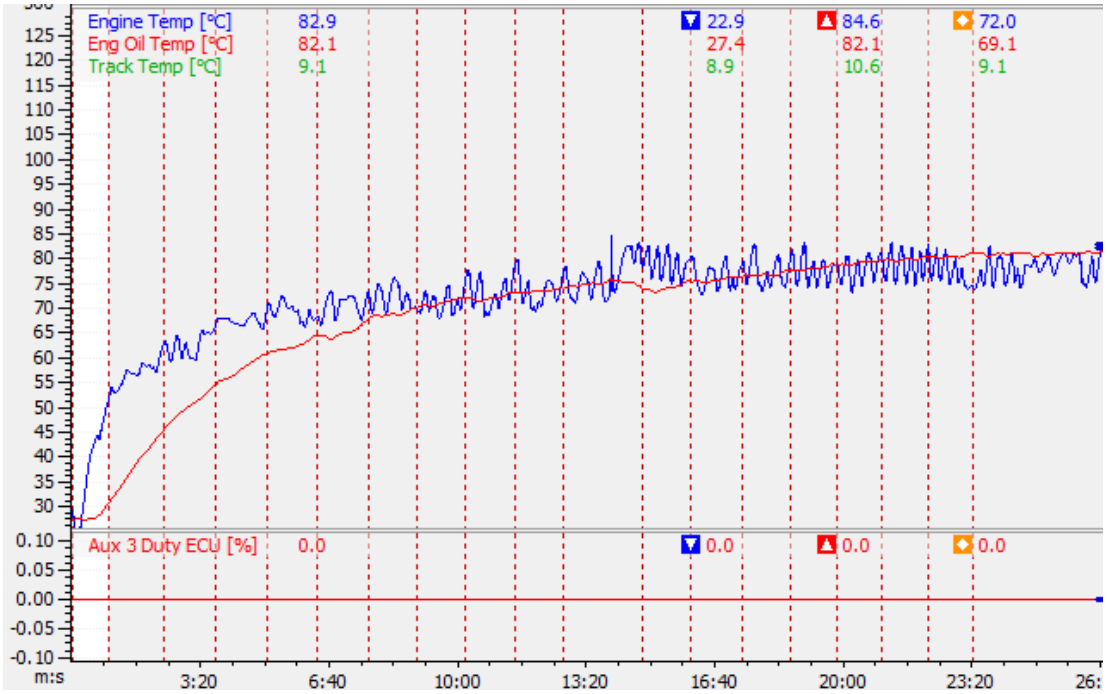

Figure 5.5: Michigan competition Endurance temperature data. The fan was not needed. Water temperature did not go above 85°C and oil remained at or below 82.1°C.

Even during the skidpad event, the car had no problem keeping cool in the Michigan climate.

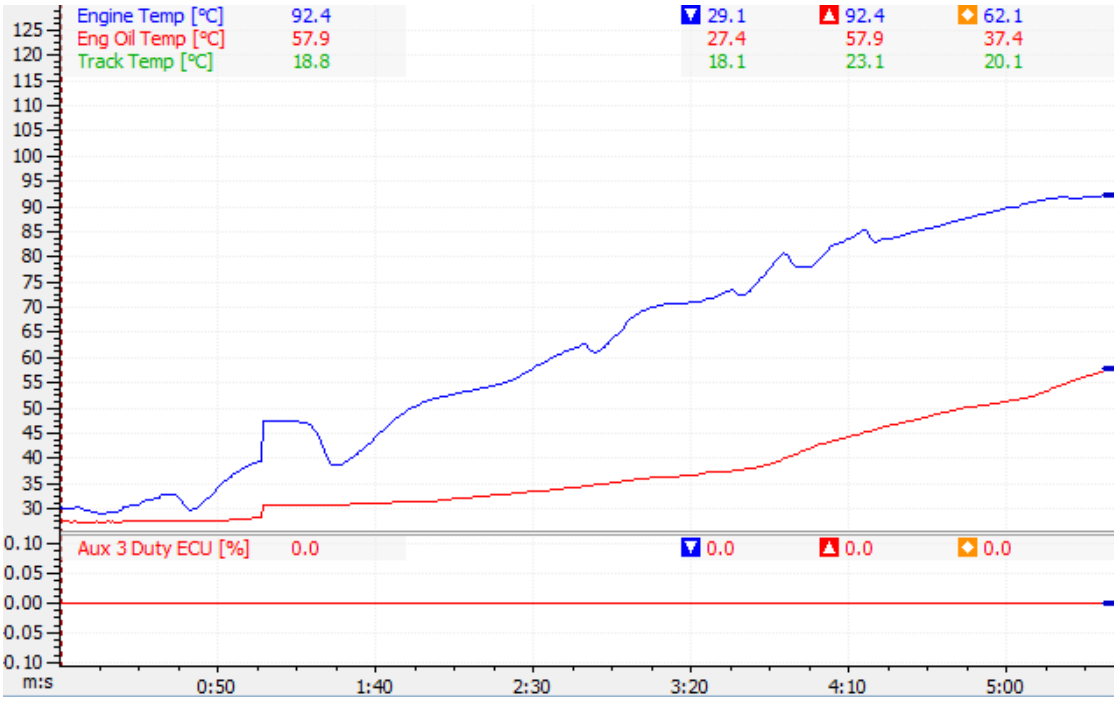

Figure 5.6: Michigan competition Skidpad temperature data. The oil temperature remained very low, peaking at 58°C. Water remained below 100°C during the run. The fan was not needed in this run.

Thus far, the cooling system seems to be working well. Engine temperatures are staying below 100°C typically, and fan is rarely engaged. With a repaired sidewing, more accurate data will be acquired and a better understanding of the cooling system's capabilities can be ascertained.

5.2 Tests to Complete

Further Engine Temperature Testing

While the data collected thus far suggests the cooling system is running very well, the real test is to come in the summer when ambient temperatures rise. This will make it tougher to reject heat to the surrounding air. Testing in hotter weather will be extremely useful for determining the quality of the cooling system.

Dyno Setup and Flow

One concern over this system is the pressure drop going across two smaller radiators. Calculations were never performed and are likely fairly high, especially compared to 2015's design. A flowmeter should help glean some information regarding pumping water through a system such as this one. If possible, it should be installed on the car for the most accurate representation of the flow conditions. However, installing the flowmeter on the dynamometer may be all that can be done.

6. Conclusion

6.1 Project Reflection

This project is a huge undertaking. In previous years, it was split up at least in two, with one student working on the aerodynamic elements and another working on the cooling loop related designs. While logical to combine the two, with little background in methods used in GFR and only modest machining experience, it can be a difficult task to tackle. Despite its difficulties, it was also an extremely rewarding experience. There are many lessons to learn on the path to designing a part of a car, both as an engineer and a group worker.

Winter term's manufacturing depends greatly upon how well fall term's design went. If things were designed well, winter can go by fairly smoothly. If things are left for later, though, they likely will not be finished until the car needs to be running, which could threaten to slow things down for everyone else. Additionally, there are many things that can be done fall term to get an early start on manufacturing, most critically being securing material. Most of this project was not begun until the third week of winter term due to orders being placed late and material not arriving until then. Future students are recommended to do as much as they can early to avoid such problems.

Working as a member of a group is also extremely important, especially on this project. Because the parts interact with many other subsystems, especially drivetrain and exhaust, communication is critical. Additionally, the aerodynamics subteam worked together often to manufacture difficult parts together. Getting to know each other as people goes a long way in establishing a healthy work relationship that makes what you are doing much more enjoyable. Finally, the TAs are students, too; getting to know them makes them more approachable when assistance is necessary.

While this was not the smoothest execution of a project, things worked out fairly well. To date, nothing in the system has been destroyed (save for a hole being made by a failed drivetrain; however, the structure of the diffuser is still sound). The preliminary cooling data suggests that overheating should not be a concern for the coming competitions unless something goes awry with the system in place. Overall, the design hit its targets and should continue to perform at a world class level.

6.2 Key Areas of System Improvement

Jawad et al. investigated implementation of a separate pump for a vehicle and found that it could help alleviate overheating issues when a car idles [25]. This could be helpful for driver changes during the endurance events when temperatures seem to spike, or everyday testing of the car. The additional weight and cost would need to be evaluated to decide if it is worth pursuing.

Simulation tools can assist with predicting cooling abilities for new thermal systems. As Simic et al. found, tools such as the SmartCooling library are able to achieve reasonable results for high level systems [26]. This could be useful for investigating improved cooling loops for the eCar especially, where there is a higher level of complexity in the thermal system.

There is potential to develop the system into a partially air cooled engine. Gokan et al. found that by combining oil cooling and air cooling, it is possible to achieve very similar levels of engine cooling to traditional water cooled motorcycle engines [27]. Weight savings could easily be over a kilogram from removing the necessity of water radiators alone. Factoring in the fluid weight, plumbing, and ducting, and the thermal management system for future cars could be far lighter than even the 2016 iteration.

The use of a “heat accumulator” can assist the system in remaining at a roughly constant temperature. Based on Vetrovec’s work investigating the use of phase change materials to store heat energy [28], this could be a viable solution to keeping the engine at a warm temperature between engine starts. The accumulator stores energy during operation by warming up a material with a high heat capacity. When the engine is turned off and the water in the system begins to cool, the heat dissipates out of the material and back into the water, helping keep the water temperature from excessively cooling [28]. If implemented, such a device could help the engine start faster.

The ducts could stand to be improved upon as well. Currently, the inlet on both sides acts as a nozzle, increasing airflow. However, when the air reaches the radiator, there is a chance that the pressure is too low to effectively push air through the fins, possibly resulting in air recirculation. Using a diverging duct could help with this by increasing the static pressure at the radiator [29, 39]. This would also free up mounting locations, as the exit of the ducts needs to be relatively low pressure to help drive the airflow through the radiators. The higher the pressure at the front of the radiator, the more freedom one has to locate the exit.

An additional project improvement that I feel is absolutely critical to this project would be to better characterize the pump head available, rather than just assuming mass flow rate is equivalent across all concepts. This is a huge assumption that was made for convenience and time savings, and before further work is done, I would suggest some research is done in this area.

7. Acknowledgments

I would like to extend my thanks to all of the past GFR students whose documentation was instrumental in getting me up to speed on all things GFR related. I would also like to specifically mention Phil Arscott and Hannes Mandler for providing CFD simulations relating to my project and Caleb Cluster and Dallas Sessions for their data collection methods to obtain my results.

I would especially like to thank Dr. Paasch for all of his assistance throughout this project and the guidance he provided for the thesis process. In addition, I would like to thank Dr. Squires for all of her advice regarding the thesis defense and being on my committee, as well as Dr. Fronk for his expertise on the subjects involved.

8. Works Cited

[1] Vandenbrink, A., "GFR14 Cooling Analysis, Heat Transfer Report," Global Formula Racing Report, 2014.

[2] SAE International, "2016 Formula SAE Rules," SAE International, 2015.

[3] Takaro, T., "Equating Design Parameters to Points," Global Formula Racing Private Home, accessed Oct. 2015.

[4] Volk, A., "GFR14 Side-Pod Report," Global Formula Racing Report, 2014.

[5] Al Baloushi, A. and Alqattan, E.., "GFR15 Sidepod Report," Global Formula Racing Report, 2015.

[6] AliExpress, http://www.aliexpress.com/item/ATV-parts-accessories-aluminum-radiator-For-Honda-ATV-TRX450R-TRX-450-2004-2009-motorcycle-engine-cooling/32464471928.html, accessed Oct. 2015.

[7] Global Formula Racing, "Composite Weight Calculator," 2015-2016.

[8] SPAL Automotive, "VA11 – AP8/C – 29A/S," 10" Fan Spec Sheet.

[9] Schaller, M., "GFR15e Cooling System," Global Formula Racing Report, 2015.

[10] Bergman, T., Lavine, A., Incropera, F., and Dewitt, D., "Fundamentals of Heat and Mass Transfer, Seventh Edition," (John Wiley & Sons, Inc, 2011), ISBN: 978-0470-50197-9.

[11] Carl, M., Guy, D., Leyendecker, B., Miller, A., and Fan, X., "The Theoretical Investigation of the Heat Transfer Process of an Automobile Radiator," presented at ASEE Gulf Southwest Annual Conference 2012, USA, April 4-6, 2012.

[12] Dube, P., Natarajan, S., Mulemane, A., and Damodaran, V., "A Numerical Approach to Develop the Front End Cooling Package in a Vehicle Using Predicted Engine Fan Performance Data and Vehicle System Resistances," SAE Technical Paper 2007-01-0542, 2007, doi:10.4271/2007-01-0542.

[13] Hansen, B., "GFR15 Oil & Cooling System Design Report," Global Formula Racing Report, 2015.

[14] AliExpress, http://www.aliexpress.com/item/Motorcycle-Radiator-For-Honda-CRF250R-CRF450R-CRF450-CRF-450-250-R-05-08-Aluminium-Radiator-Left/2053461237.html, accessed Nov. 2015.

[15] eBay, http://www.ebay.com/sch/sis.html?_nkw=Radiators+for+TaG+Racing+Go+Karts+IAME+Leopard+X30+PRD+125cc&_itemId=191600772530&_trksid=p2047675.m4096, accessed Nov. 2015.

[16] Arscott, P., "2016 Aero Pre-Development Concepts," Global Formula Racing, 2015.

[17] Global Formula Racing, "Aero Run/Ran," 2015-2016.

[18] Make It From, "6061-T6 Aluminum Material Properties," http://www.makeitfrom.com/material-properties/6061-T6-Aluminum/, accessed Dec. 2015.

[19] National Aeronautics and Space Administration, "Bernoulli's Equation," https://www.grc.nasa.gov/www/k-12/airplane/bern.html, accessed Dec. 2015.

[20] Torris, C., "GFR15 Sidewing Assembly," Global Formula Racing Report, 2015.

[21] Williams, N., "GFR14 Fluid System and Mechanical Design Report," Global Formula Racing Report, 2014.

[22] SPAL Automotive, "VA07 – AP12/C – 58A/S," 9" Fan Spec Sheet.

[23] Mandler, H., "GFR16 Radiator CFD Analysis," Global Formula Racing, 2016.

[24] Aerospace Specification Metals Inc., "AISI 4130 Steel," http://asm.matweb.com/search/SpecificMaterial.asp?bassnum=m4130r, accessed Dec. 2015.

[25] Jawad, B., Zellner, K., and Riedel, C., "Small Engine Cooling and the Electric Water Pump," SAE Technical Paper 2004-32-0084, 2004, doi:10.4271/2004-32-0084.

[26] Simic, D., Lacher, H., Kral, C., and Pirker, F., "Evaluation of the SmartCooling (SC) Library for the Simulation of the Thermal Management of an Internal Combustion Engine," SAE Technical Paper 2007-01-0541, 2007, doi:10.4271/2007-01-0541.

[27] Gokan, Y., Takahashi, Y., Inayoshi, M., Ishima, T. et al., "Development of Air/Oil-Cooled Motorcycle Engine Using Thermal and Fluid Analyses," SAE Technical Paper 2007-01-0538, 2007, doi:10.4271/2007-01-0538.

[28] Vetrovec, J., "Engine Cooling System with a Heat Load Averaging Capability," SAE Technical Paper 2008-01-1168, 2008, doi:10.4271/2008-01-1168.

[29] Toet, W., "Air Ducts – a down to earth guide to motorsport applications," https://www.linkedin.com/pulse/air-ducts-down-earth-guide-motorsport-applications-willem-toet, accessed March 2016.

[30] Katz, J., "Race Car Aerodynamics," (Bentley Publishers, 1995), 214-215, ISBN: 0-8376-0142-8.

[31] Clinton Aluminum, “Which Aluminum Alloy Bends Best?” http://www.clintonaluminum.com/which-aluminum-alloy-bends-best/, accessed Dec. 2015.

Appendix A: Manufacturing

A.1 Part Drawings

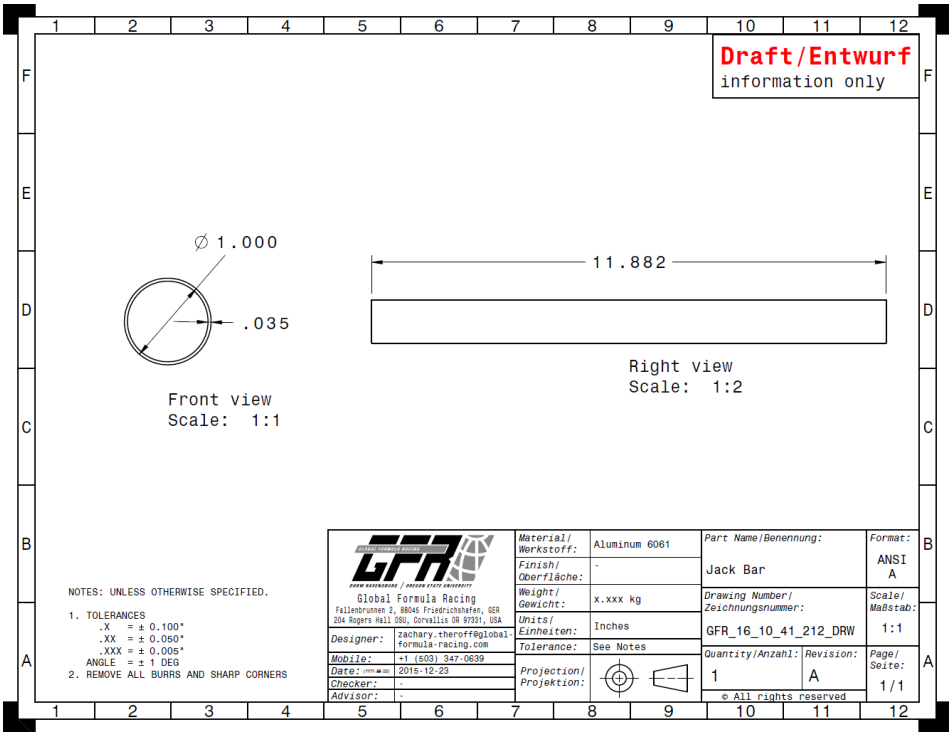

Figure A.1: Jack bar, just under 12” in length as the jack bar inserts will fill in the rest of the required length.

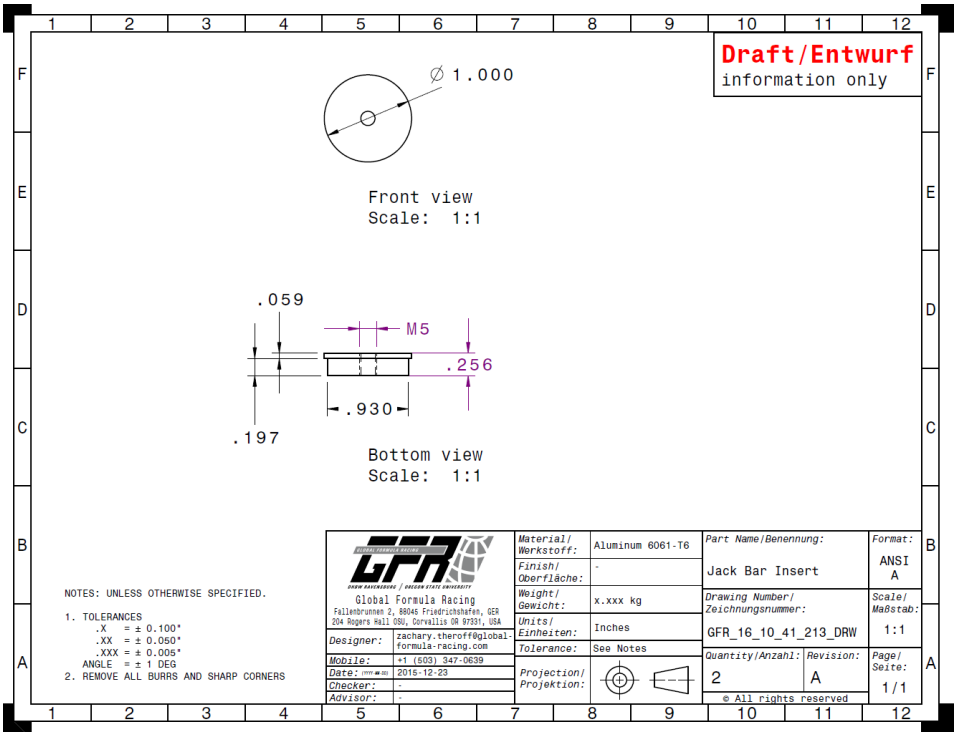

Figure A.2: Jack bar inserts, with threaded holes for M5 bolts, to be welded into the jack bar tube.

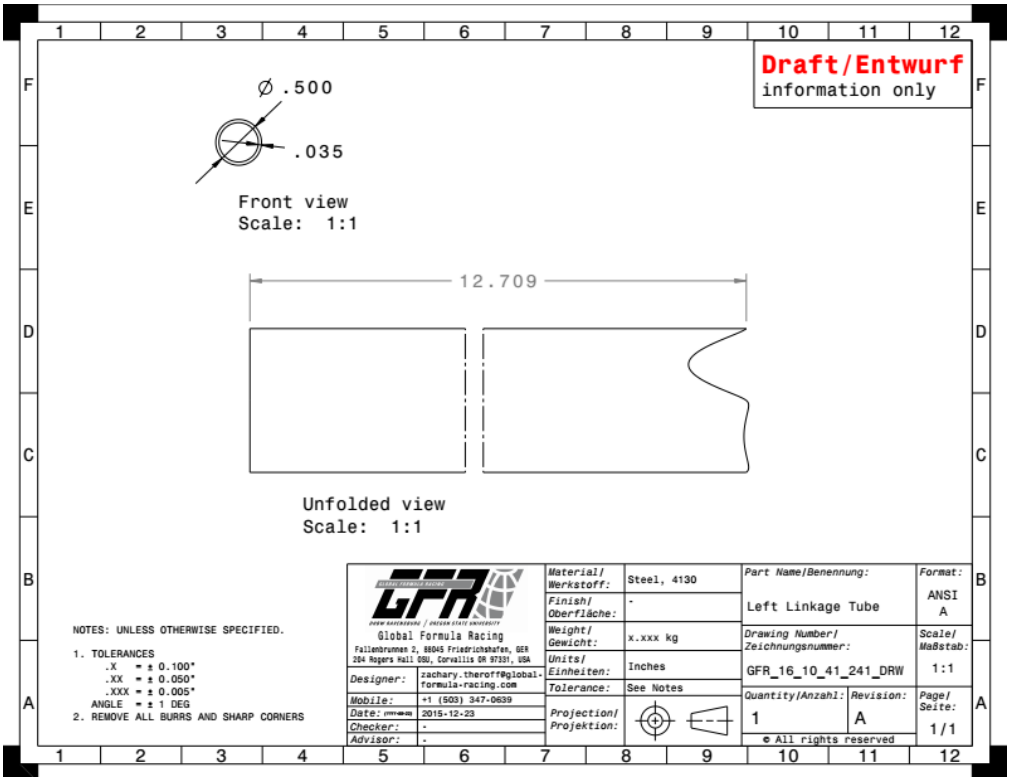

Figure A.3: Drawing for linkage tube connecting jack bar to chassis, with coping shown at the right edge of the "Unfolded View".

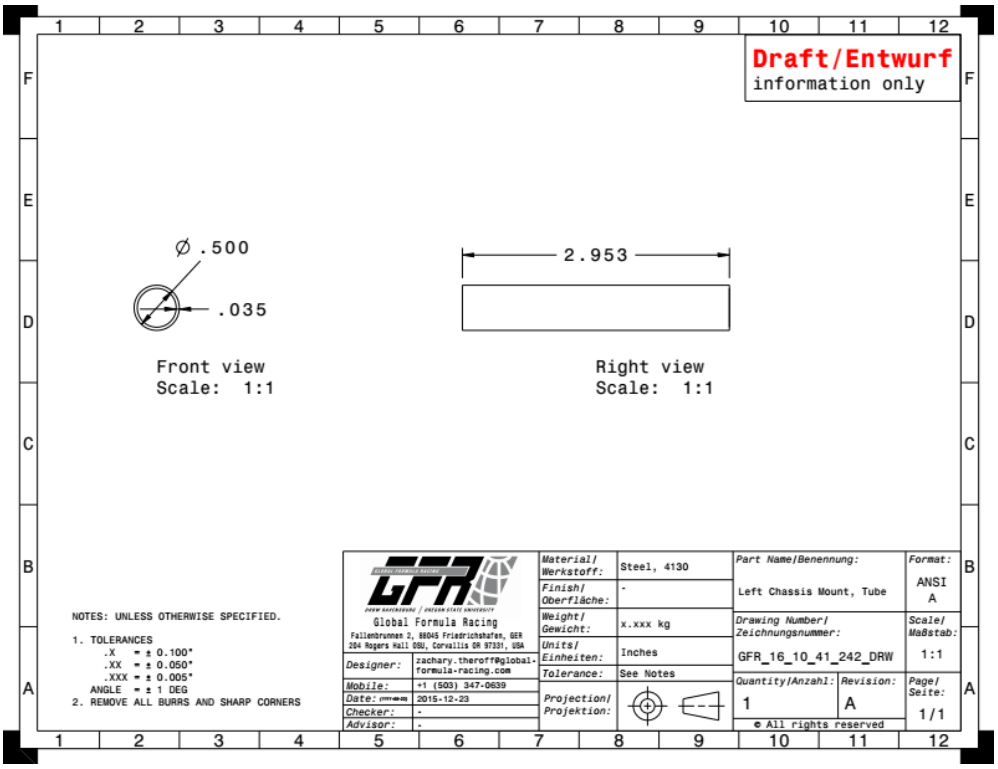

Figure A.4: Chassis mount tube that extends rearward from the chassis, where the linkage tube is welded.

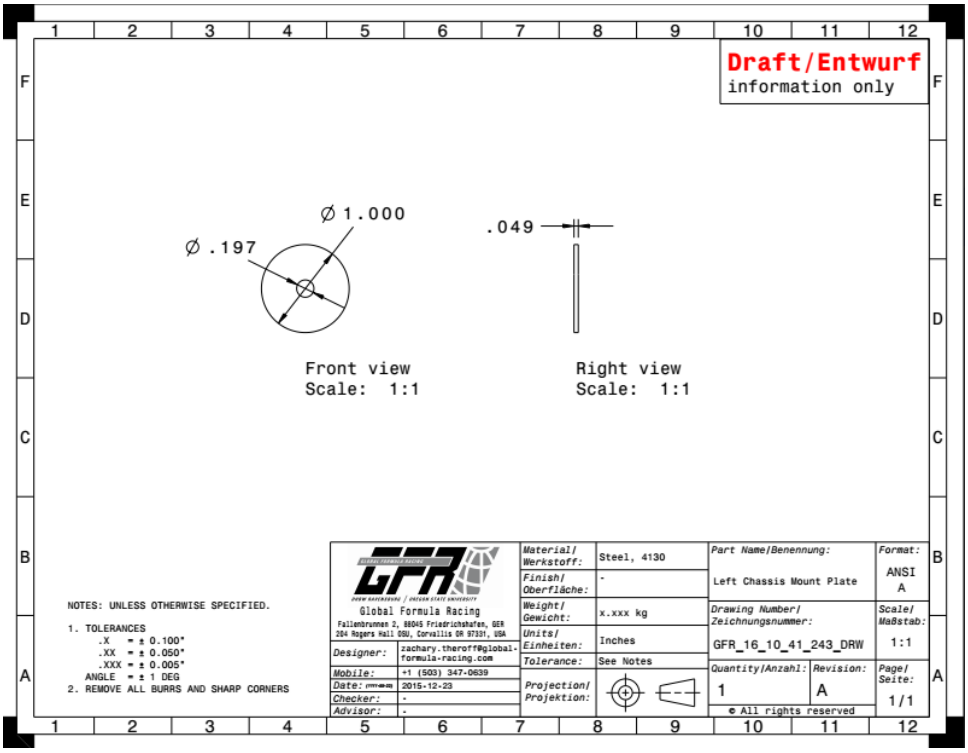

Figure A.5: Plate that is welded to the end of the chassis mount tube and bolts to the chassis.

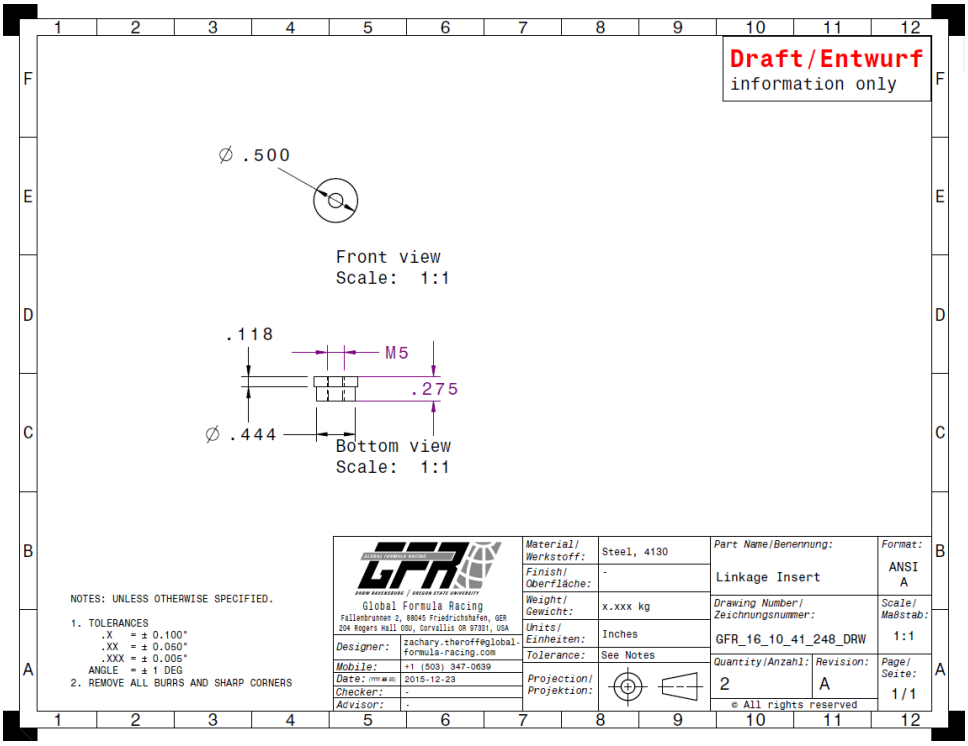

Figure A.6: Insert that is welded to end of linkage tube with a threaded hole for an M5 rod end.

A.2 Manufacturing Plan

Composite Parts

All parts made using composites (diffuser and ducts) were made using sheet metal molds from GK Machine and carbon supplies from Toray. The molds were all made of A36 steel, 12 gauge. Due to limitations in GK's capabilities, especially with respect to the length of the flanges of the front duct mold, the molds were split into two pieces for both the front left and front right duct molds. These pieces were to be cut and bent separately, then welded together when they arrive at Oregon State University. However, the single piece versions were also sent to GK Machine, just in case they were actually able to make them. In the case of the left front duct, the two piece variation was unnecessary.

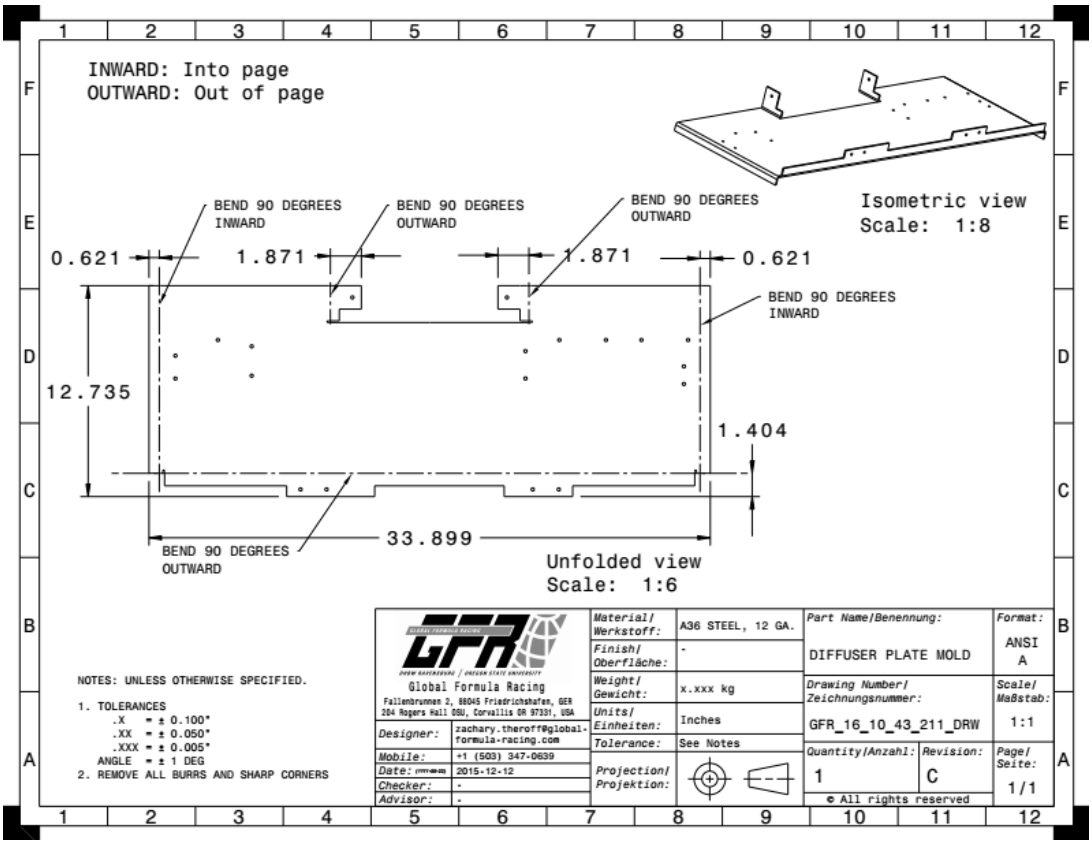

Figure A.7: Mold for the diffuser plate.

Diffuser:

- Layup was done using the mold pictured in the above drawing
    - The mold is A36 steel, 12 gauge
    - Laser cut and bent at GK Machine
- Carbon: T700
- Core: 0.5" Kevlar honeycomb
- Layup:
    - Main plate/side strakes: One layer of carbon, glue sheet, one layer of core, glue sheet, one layer of carbon
    - Mounting tabs (jack bar/chassis): 10 layers of carbon (no core)

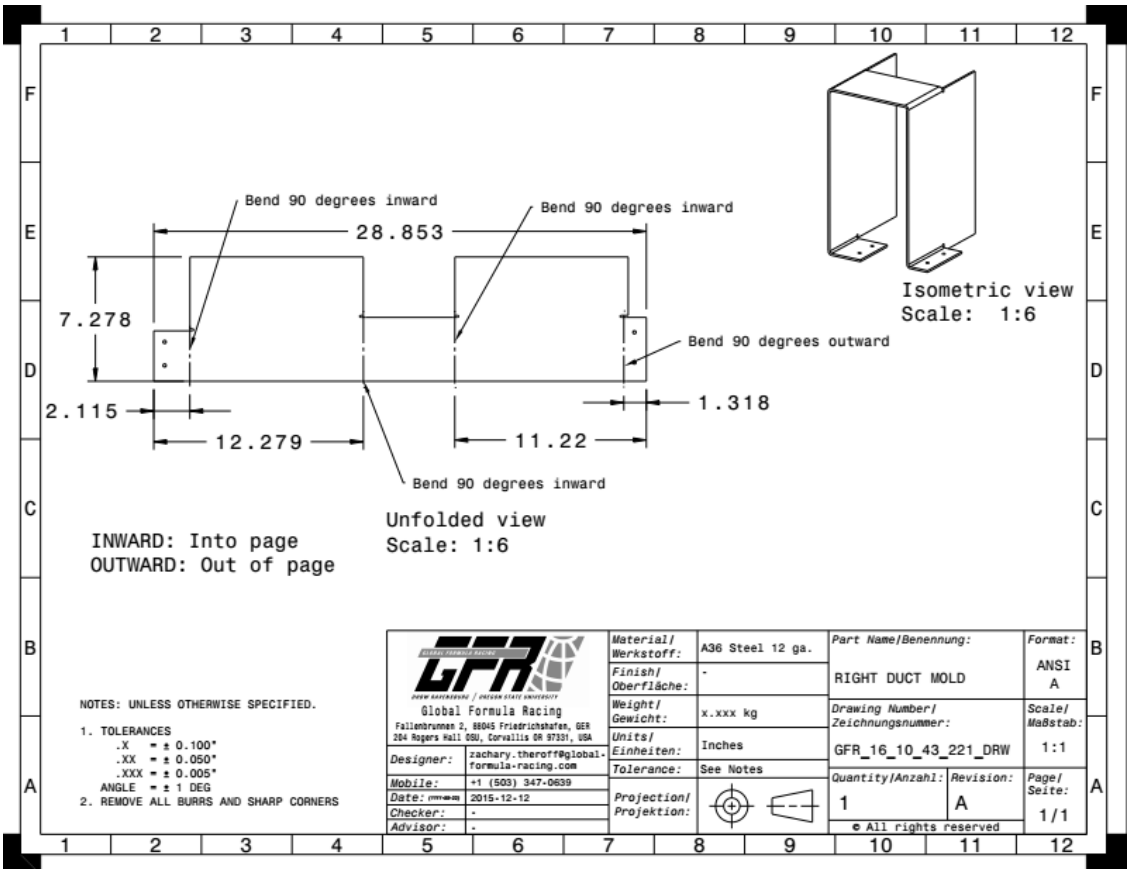

Figure A.8: Mold for the right front duct, single piece version; sent to GK Machine but was not deemed manufacturable. Two piece version welded together instead.

<u>Front Right Duct:</u>

- Layup was done using the two piece mold variant, below (welded to appear like the above mold)
    - The mold is A36 steel, 12 gauge
    - Laser cut and bent at GK Machine
- Carbon: T700
- Core: Divinycell 0.125” (foam)
- Layup: One layer of carbon, one layer of core, one layer of carbon

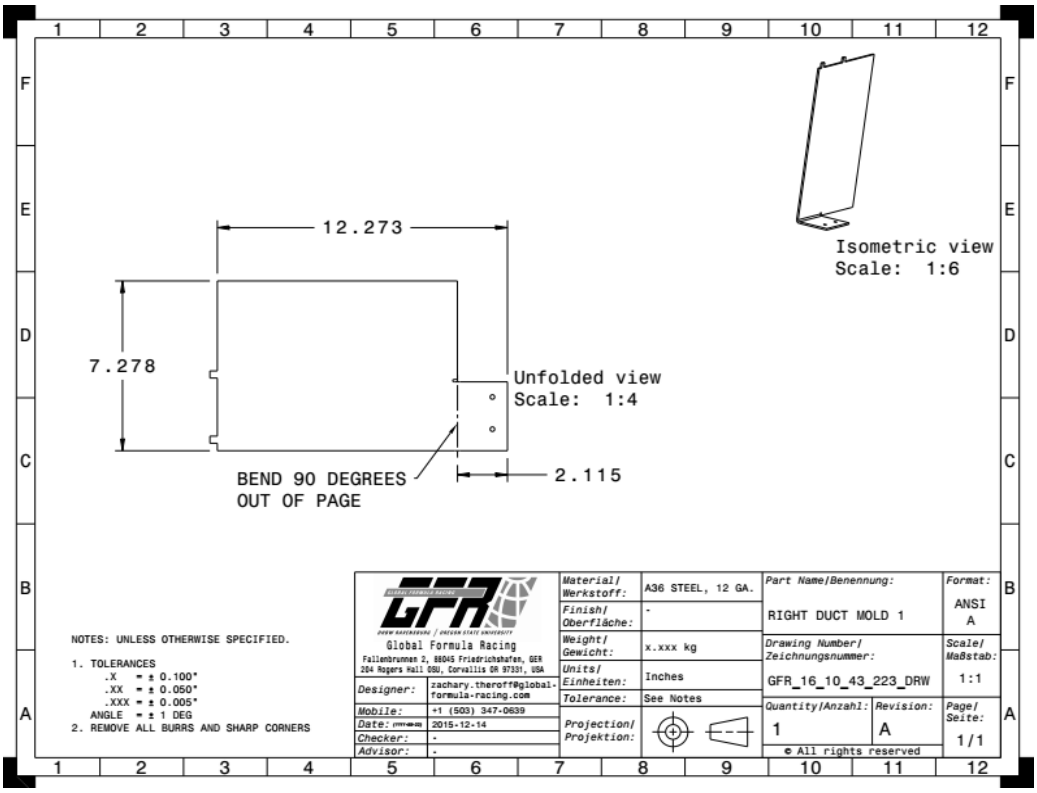

Figure A.9: Right front duct mold, double piece version, piece 1.

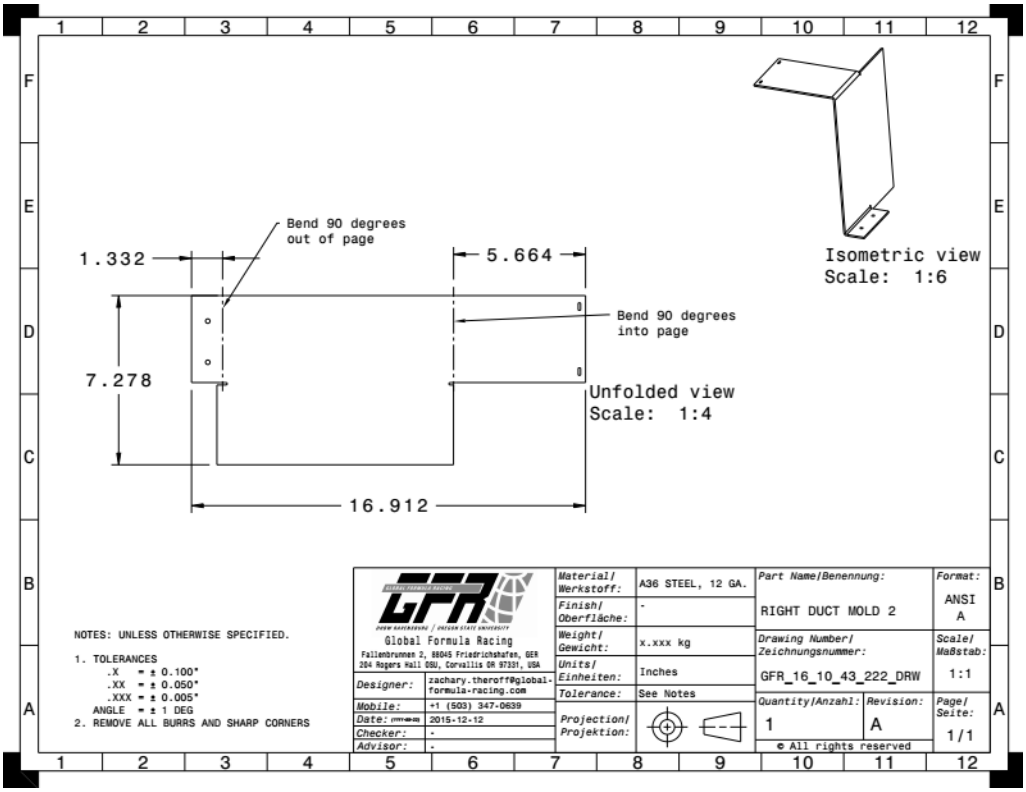

Figure A.10: Right front duct mold, double piece version, piece 2.

For the double piece version of the right front duct mold, the long flange in piece 1 has two extended pieces that interface with holes found in piece 2. These help locate the pieces relative to each other and provide a way to weld the molds together.

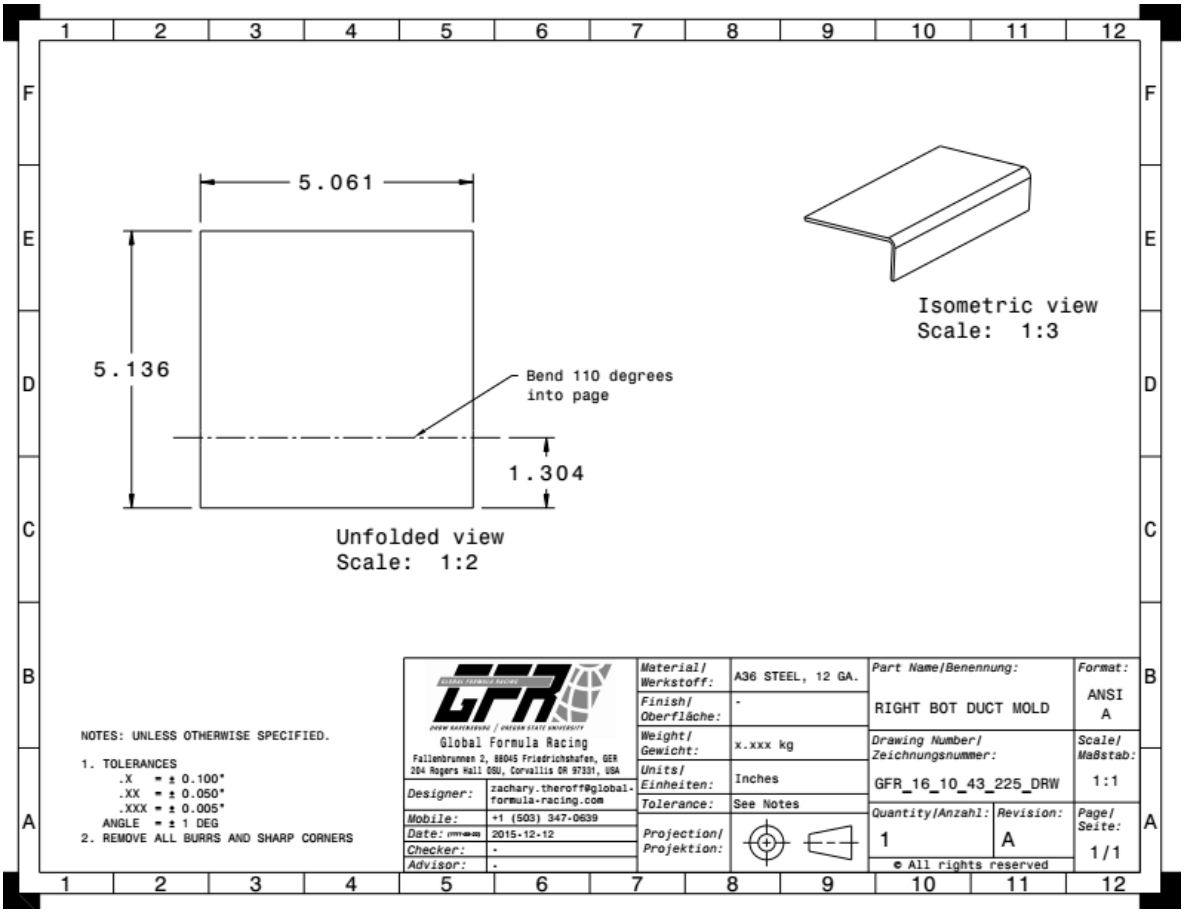

Figure A.11: Right bottom duct mold.

<u>Right Bottom Duct:</u>

- Layup was done using the mold pictured in the above drawing
    - The mold is A36 steel, 12 gauge
    - Laser cut and bent at GK Machine
- Carbon: T700
- Core: None
- Layup: Single layer of carbon

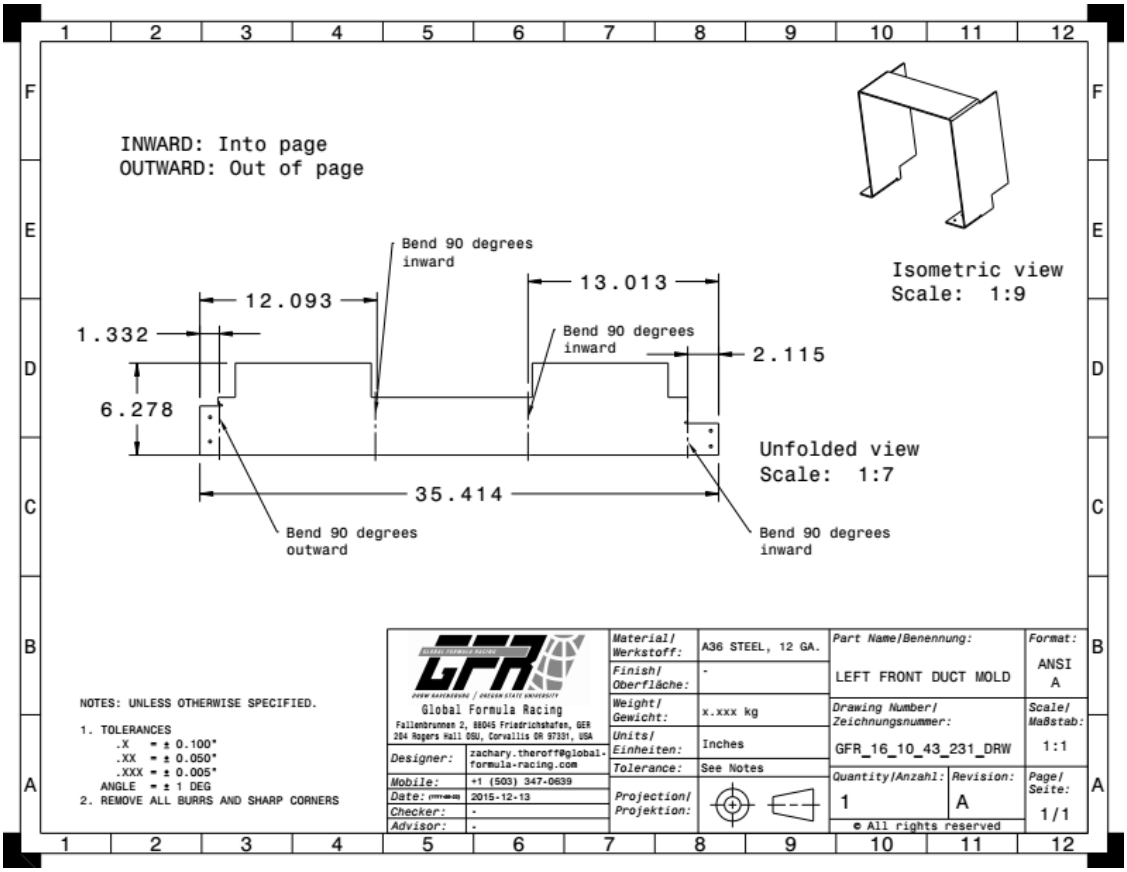

Figure A.12: Left front duct mold.

Front Left Duct:

- Layup was done using the mold pictured in the above drawing
    - The mold is A36 steel, 12 gauge
    - Laser cut and bent at GK Machine
- Carbon: T700
- Core: Divinycell 0.125” (foam)
- Layup: One layer of carbon, one layer of core, one layer of carbon

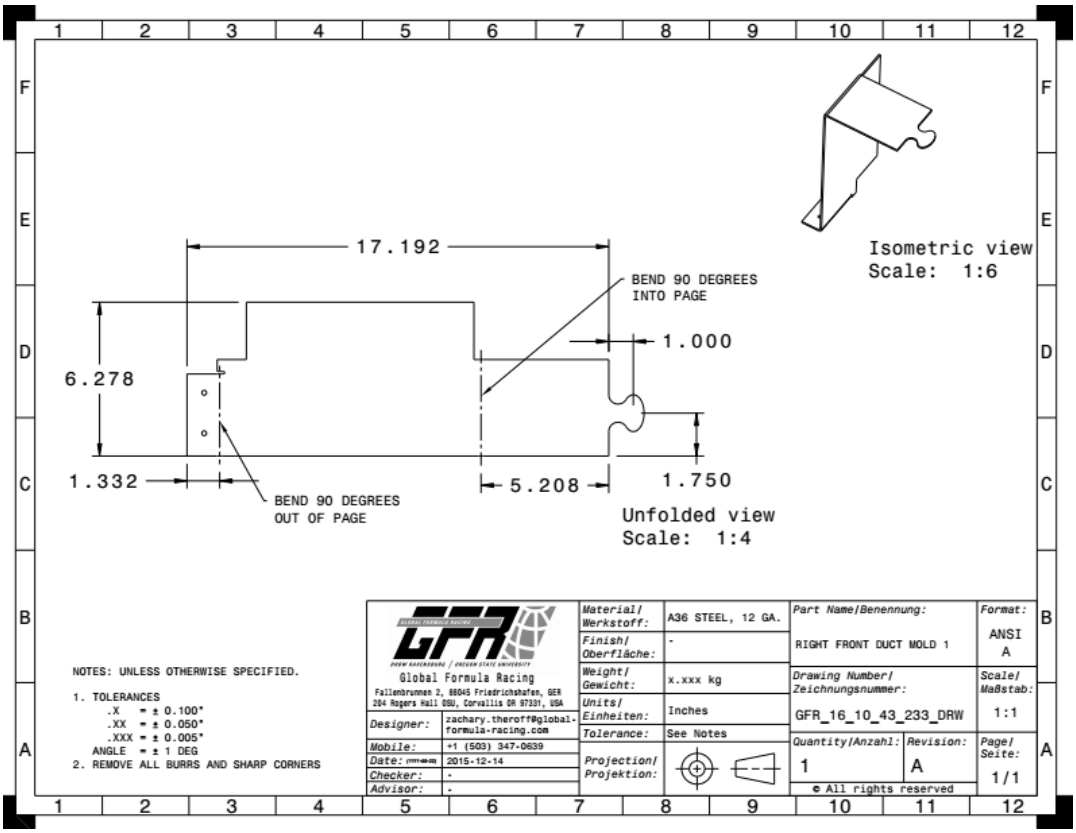

Figure A.13: Left front duct mold, double piece version, piece 1.

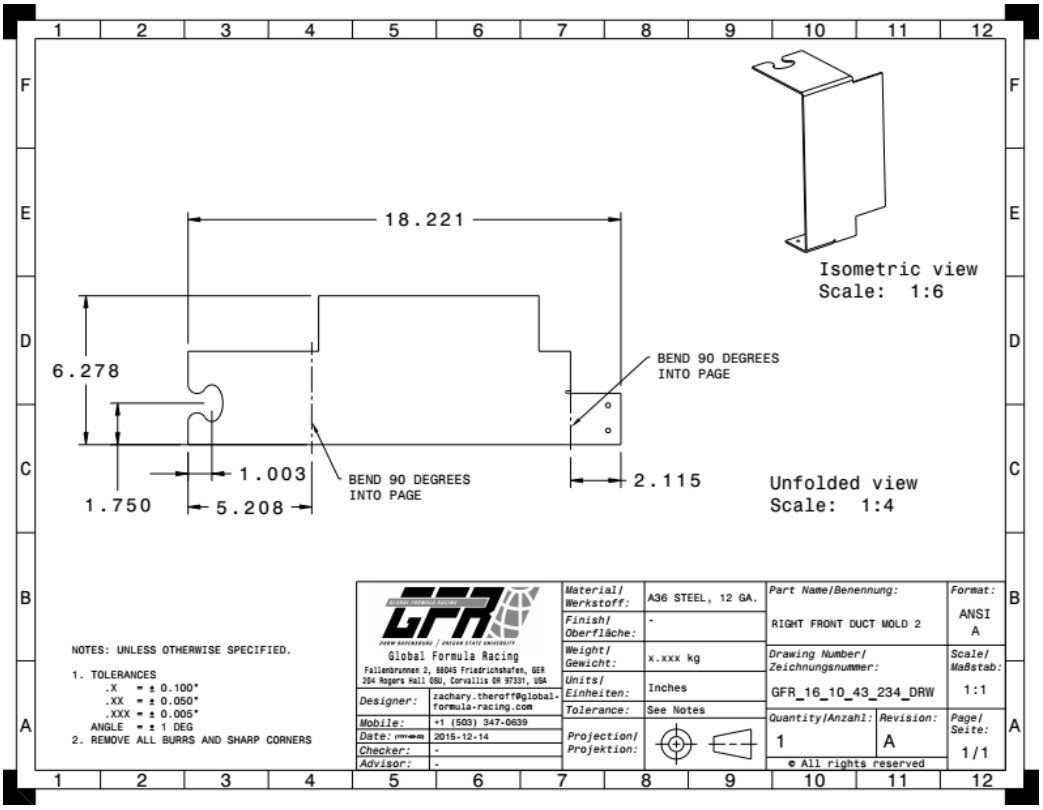

Figure A.14: Left front duct mold, double piece version, piece 2.

For the two piece version of the left front duct, a puzzle piece-like tab was designed to interface the two pieces. Piece 1 has the male part, while piece 2 has the female portion. This allows the molds to lock together and be welded along the tab, creating a smooth weld that will only minimally interfere with layup. Because GK Machine was able to make the single piece version, the split version was not necessary, but included here for historical completeness.

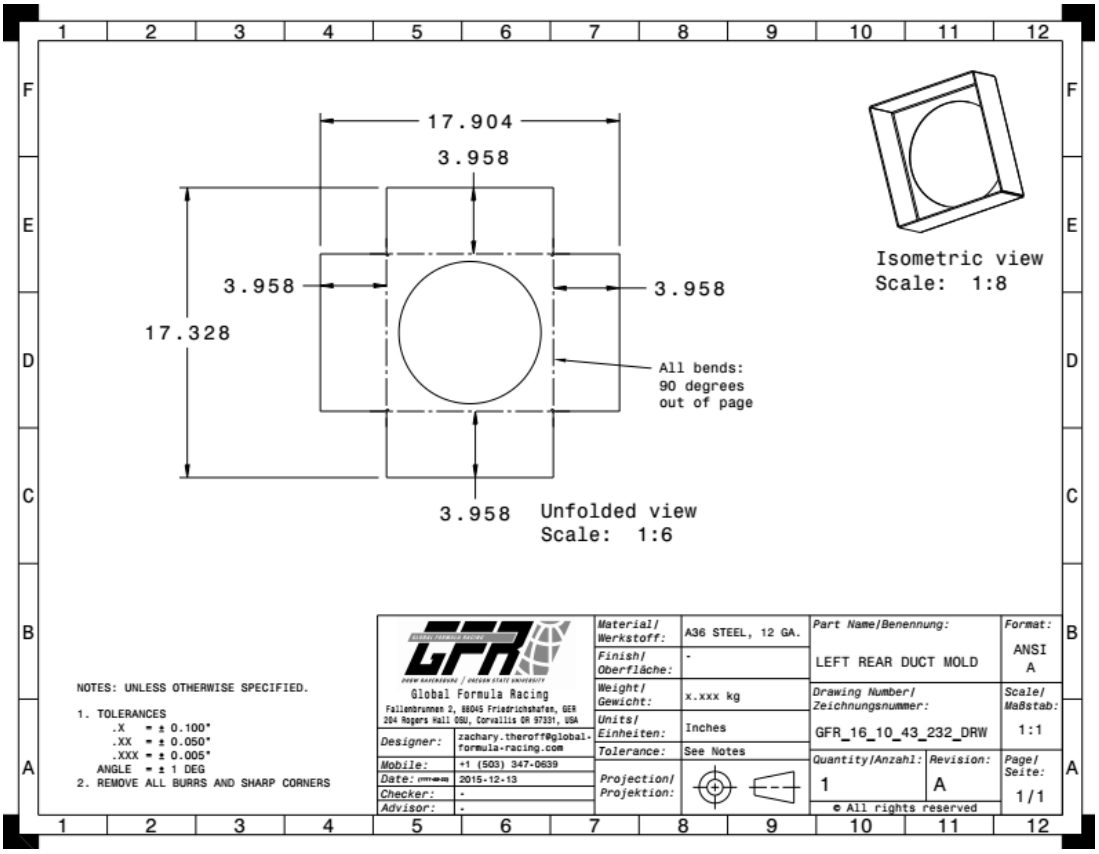

Figure A.15: Left exit duct mold.

Left Exit Duct:

- Layup was done using the mold pictured in the above drawing
    - The mold is A36 steel, 12 gauge
    - Laser cut and bent at GK Machine
- Carbon: T700
- Core: Divinycell 0.125”
- Layup: One layer of carbon, one layer of core, one layer of carbon

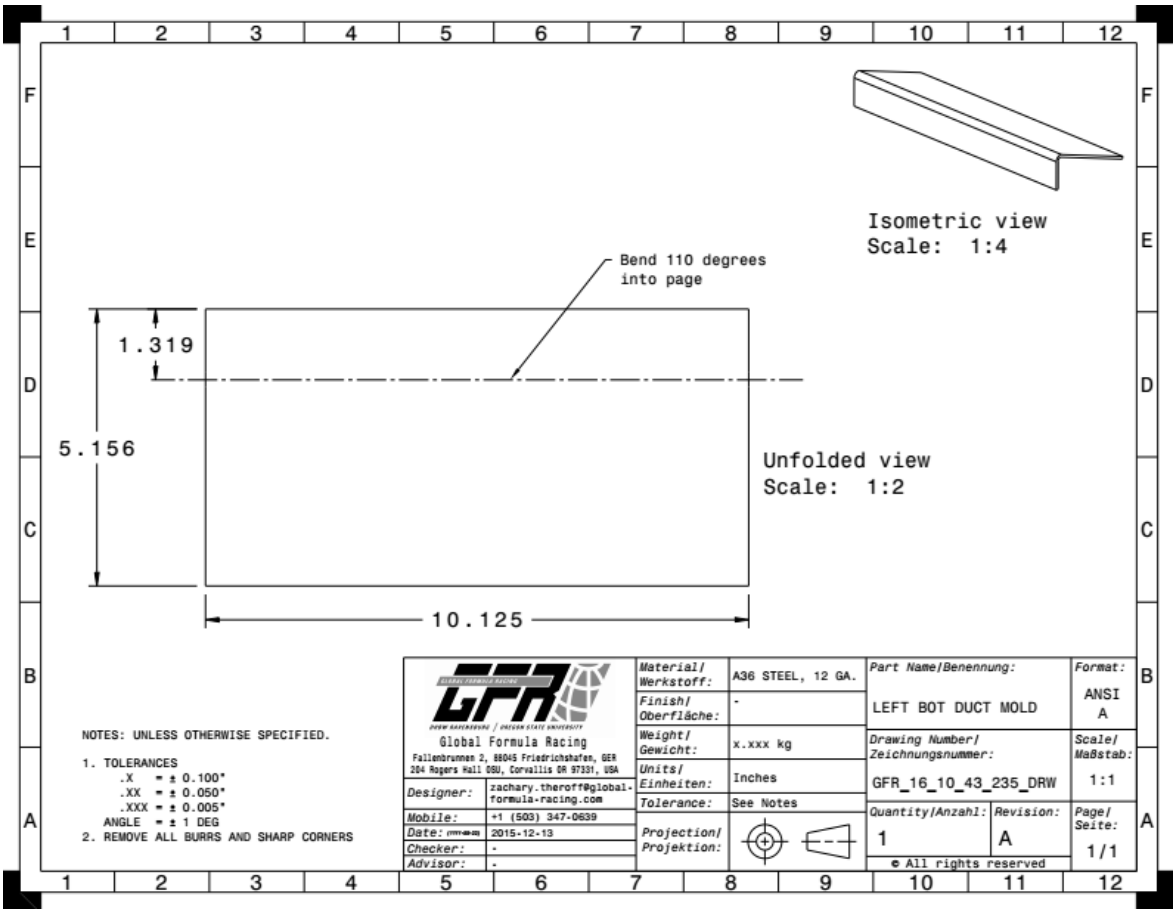

Figure A.17: Left bottom duct mold; longer version of the right bottom duct mold.

Left Bottom Duct:

- Layup was done using the mold pictured in the above drawing
    - The mold is A36 steel, 12 gauge
    - Laser cut and bent at GK Machine
- Carbon: T700
- Core: None
- Layup: Single layer of carbon

Diffuser Components - Metal Parts

The L-brackets for mounting coolers were made of aluminum 5052, for easier bending compared to 6061 [31]. These brackets were laser cut and bent by GK Machine.

The jack bar and jack bar inserts were made of aluminum 6061-T6, which can be purchased at a variety of retailers, such as Online Metals.

Jack Bar

- Aluminum 6061-T6
- 1” OD / 0.035” wall thickness (0.028” wall thickness if possible)

Jack Bar Inserts

- Aluminum 6061-T651

- 1” diameter rod

The linkage system needed to be made of steel as it will be subject to some high loads. One choice was steel 4130.

Linkage Tubes and Chassis Mount Tubes
- Steel 4130
- 0.5” OD / 0.028” wall thickness

Chassis mount plates
- Steel 4130
- Sheet metal, 0.049” thick

Plumbing

Aluminum Tubing
- Aluminum 6061-T6
- 0.075” OD / 0.035” wall thickness

Silicone Hosing
- From Performance Silicone Hoses or Samco Sport
- 0.75” ID

Hose Clamps
- From Hose Clamp Kings
- 5/8 to 1-1/16” diameter range
- 9mm width
- 430 stainless steel

Oil Fittings
- From BMRS and Summit Racing
- BMRS supplies 90 degree and straight AN -6 fittings
- Summit Racing supplies bungs for radiators

A.3: Implementation

A3.1 Aerodynamic Cooling Elements

A major problem with the aerodynamic elements was the GK Machine order being delayed. Due to sloppy drawings and other similar issues, mold manufacturing did not begin until winter term was well underway. This is something to be mindful of; make sure there are other things that can be done so that there is no wasted time waiting for parts.

A3.1.1 Right Ducts

Right Front Duct

Before the right front duct could be made, the mold had to be welded together (recall the manufacturing limitations of GK Machine and the flanges being too long for their bending table). The mating points of the two pieces can be seen in Figure A.18 and Figure A.19 below. The pieces were loosely placed together and welded.

A.18: Half of the right front duct mold, prior to welding together.

Figure A.19: Other half of the mold that needs to be welded. These tabs insert into the holes seen in the previous image.

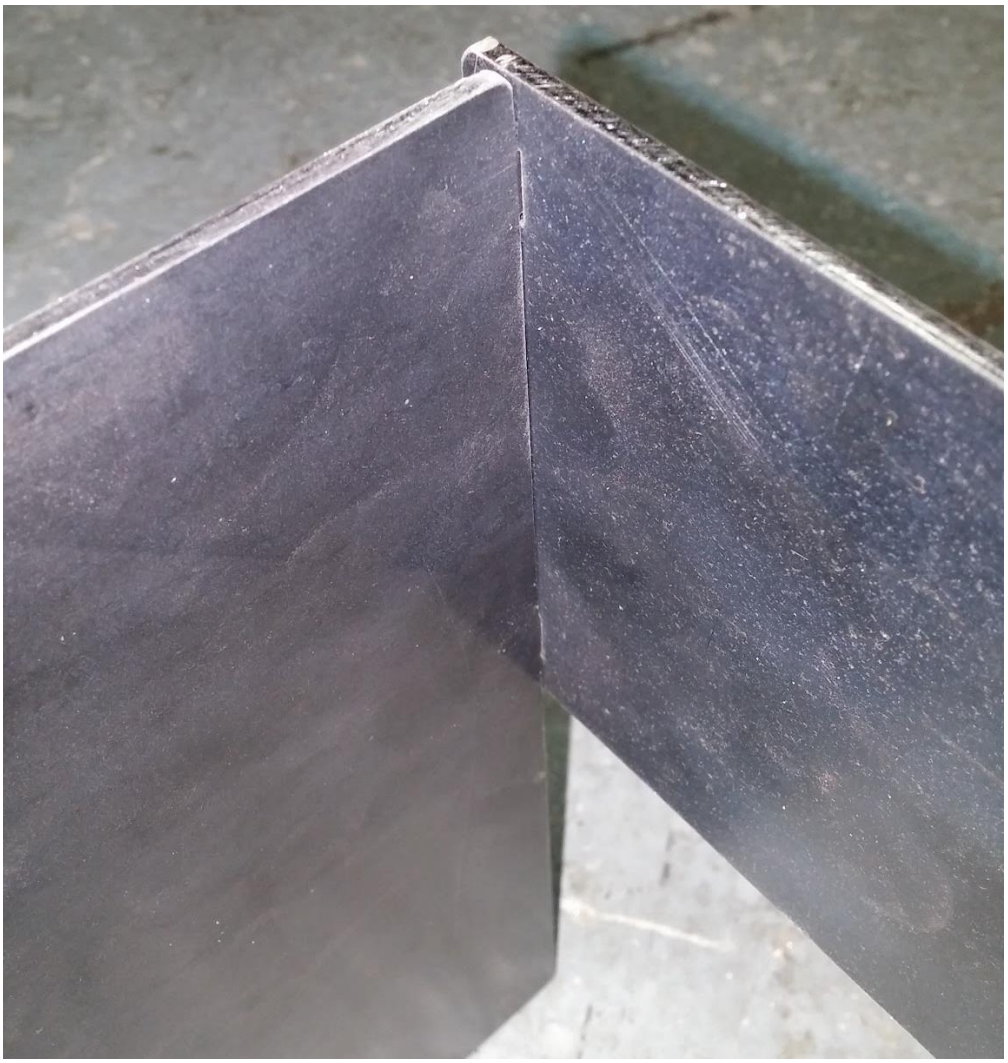

Figure A.20: Fitting the two pieces of the mold together for welding.

Core should be cut to the same dimensions as the sides of the mold. In order to prevent crushing of the core at the locations where the duct bolts into the diffuser, it is recommended to use a hardpoint of some sort. In this case, two washers were stacked together as the combined thickness was roughly that of the ⅛” foam core. They were wrapped in glue sheet in preparation for layup. One of the four hardpoints can be seen in Figure A.21. Holes wide enough for the washers should be cut into the foam of the mounting flanges of the duct.

Figure A.21: Wrapping washers in glue sheet to act as through-hole hardpoints.

The actual layup consists of one global layer of carbon, core and hardpoints, and a second global layer of carbon. For the first layer, the piece can be a single rectangle. Ensure it is long enough to go from one mounting flange, wrap around the mold, and reach the other mounting flange, and wide enough to span the widest part of the mold. It should extend past the edges of the mold at least 10mm on every edge. This will allow it to be trimmed down a bit and folded over the core to interface with the second layer of carbon. Figure A.22 and Figure A.23 show the first layer on the mold, after being trimmed down to follow the edges of the mold better. There are also relief cuts to allow it to fold on every edge of the core.

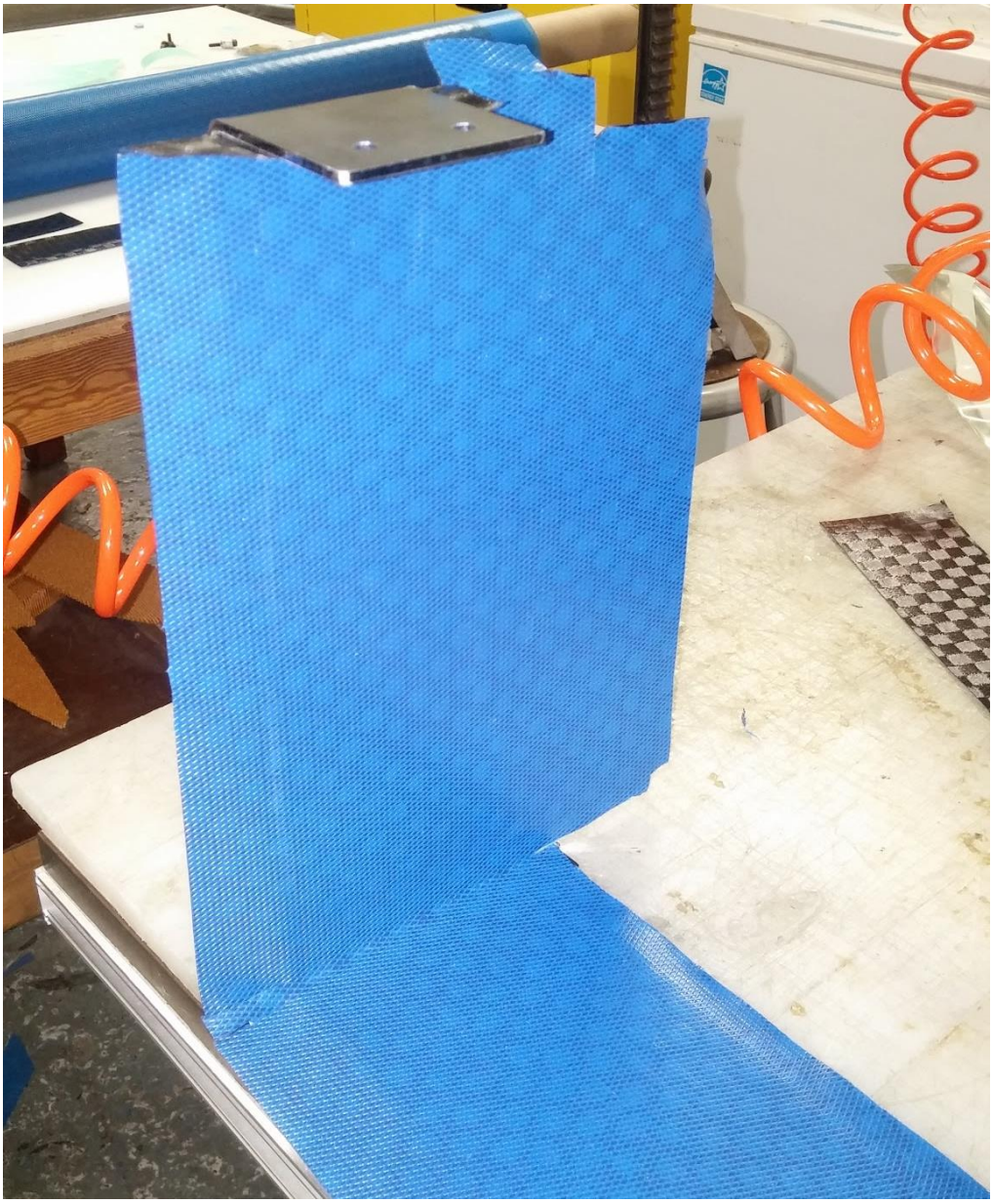

Figure A.22: Layer 1 of the duct: global with extra off the edges to fold over core.

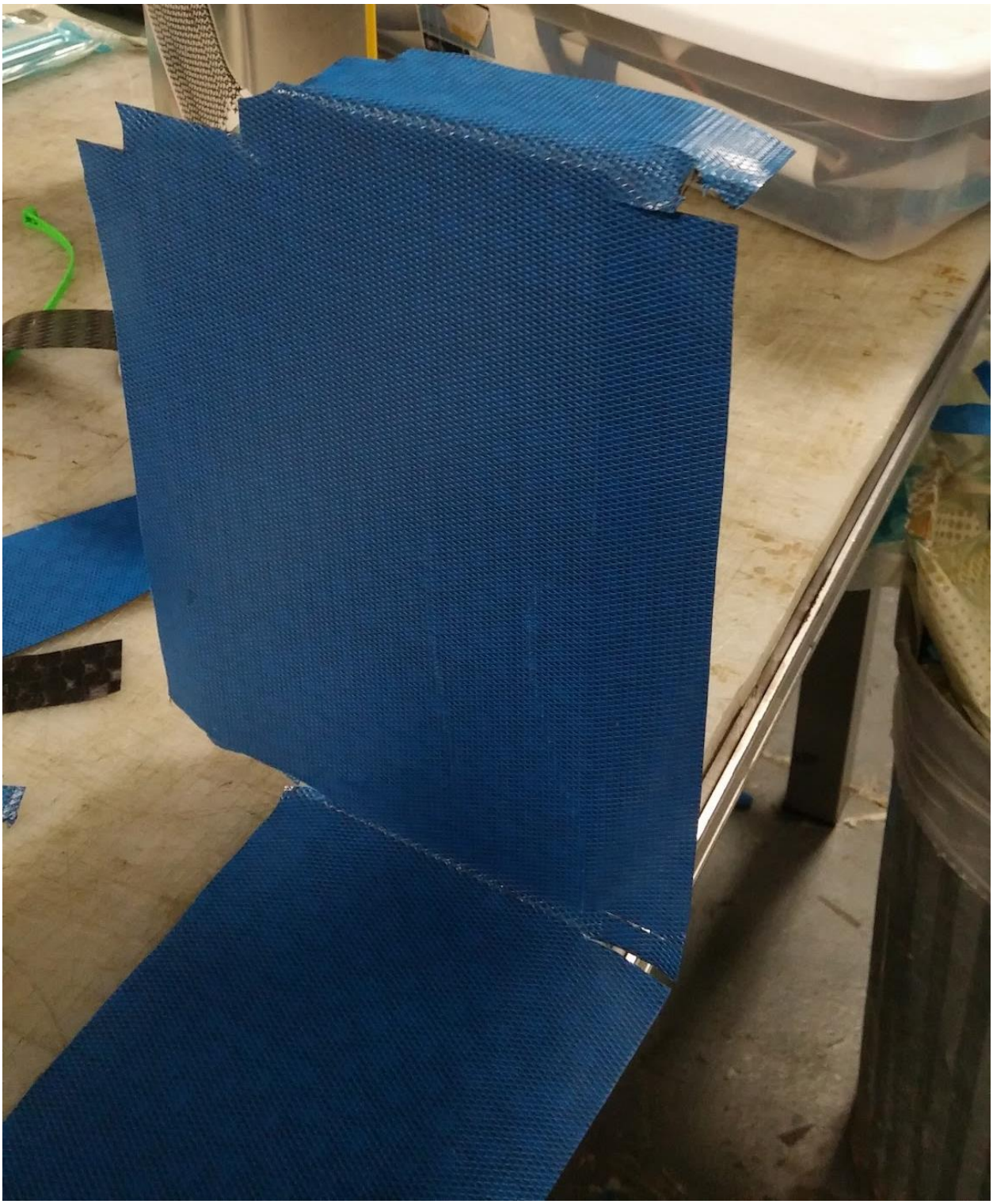

Figure A.23: More of the first layer of carbon. Note that it is trimmed off along edges and relief cuts are added to help for folding.

Once the carbon is trimmed down to extend only about 10mm off every edge of the mold and cuts are added to help with folding, the core is placed. Figure A.24 below shows the core for the side of the duct partially exposed, with carbon from the first layer folded over. On the flanges that bolt to the diffuser, short

bolts should be placed in the holes of the mold to help align the washer hardpoints. These bolts can also be seen in Figure A.24. The following image, Figure A.25, shows the last piece of carbon being placed on this section of core.

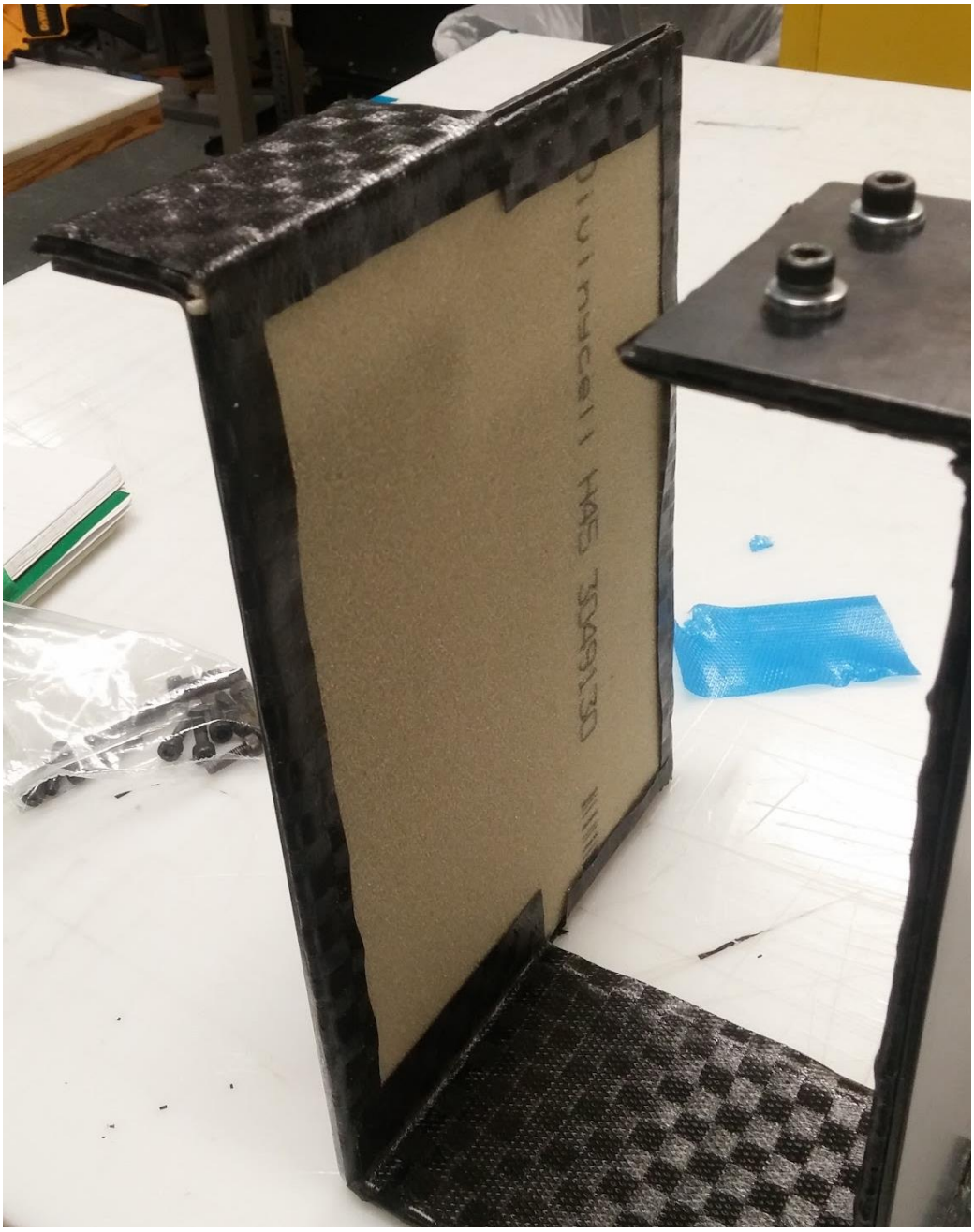

Figure A.24: Core placed on first layer of carbon and edges folded over the sides of the core.

Figure A.25: Placing the last layer of carbon over the core.

While the second piece of carbon could be done as a single piece, I found it much easier to manage smaller pieces on each face of the core. This will add a little weight, as there needs to be overlap in the carbon at each piece to keep the structure complete and strong, but it is fairly negligible and made layup very easy.

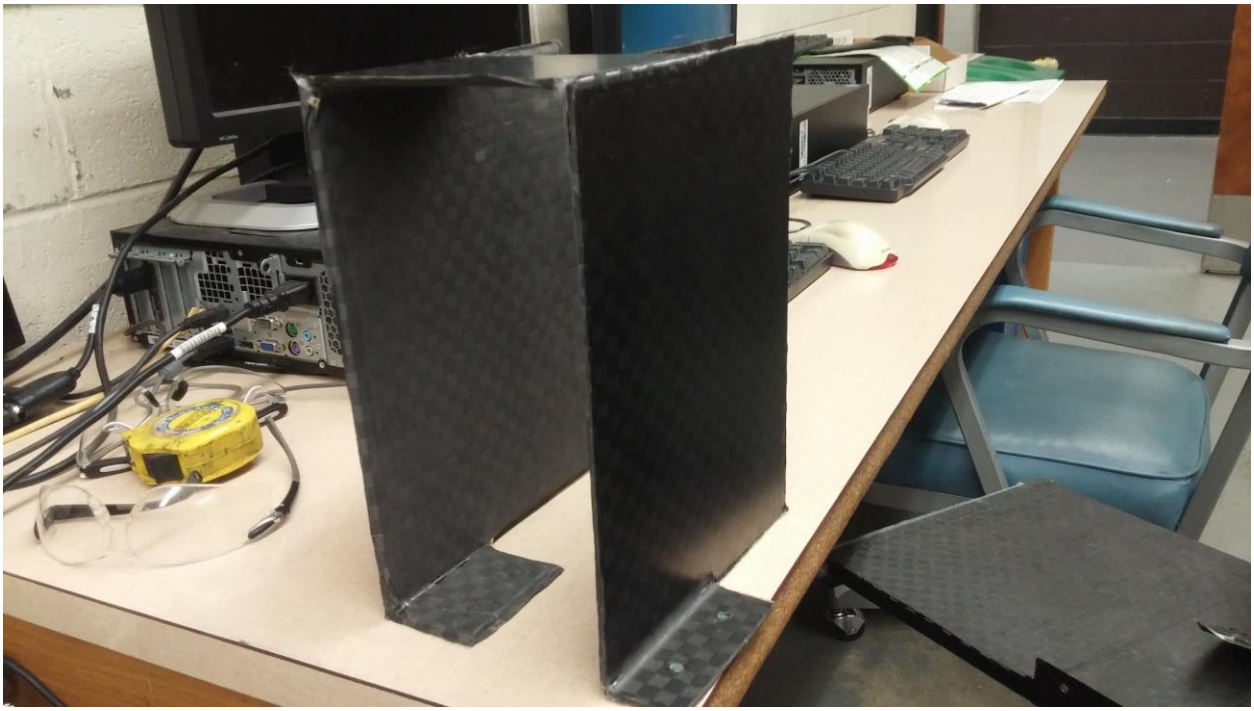

Figure A.26: Cured duct piece, prior to some post-processing.

To prevent damage to the radiators, rubber edging should be added on any edge that could rub the core.

Weight of right front duct: 108g.

Right Bottom Duct

The 2015 bottom duct mold was used as the dimensions were fairly close to the 2016 design, with the benefit of having the two flat edges to help with mounting to the diffuser.

The easiest way to make this part is to measure the distance between the walls of the right front duct once mounted on the diffuser. Measure the distance along the mold to determine how wide to make the carbon and oversize it by 20mm. Oversize the distance between the front duct by 10mm. Layup the single piece of carbon on the mold and trim off the extra material. Once cured, the piece can be trimmed down to fit into the duct and around any piping.

Weight of the right bottom duct: 6g.

A3.1.2 Left Ducts

Left Front Duct

For layup details, see the Right Front Duct section (A2.1.1), as it follows the exact same procedure. This piece took three attempts to make for the cCar. This is because the foam core was cut too small on the first attempt and the bag lost vacuum in the oven during the second attempt. The results of the first mistake can be seen in Figure A.28.

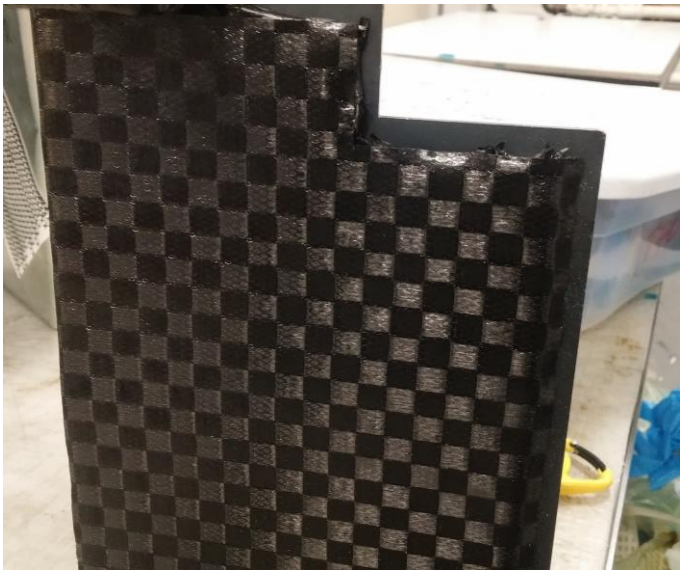

Figure A.27: Last layers of carbon added. NOTE: This is the first failed attempt. The core was cut too small, as seen by the carbon not extending all the way to the edges of the mold. The flanges were too short for the tabs of the radiator to bolt to.

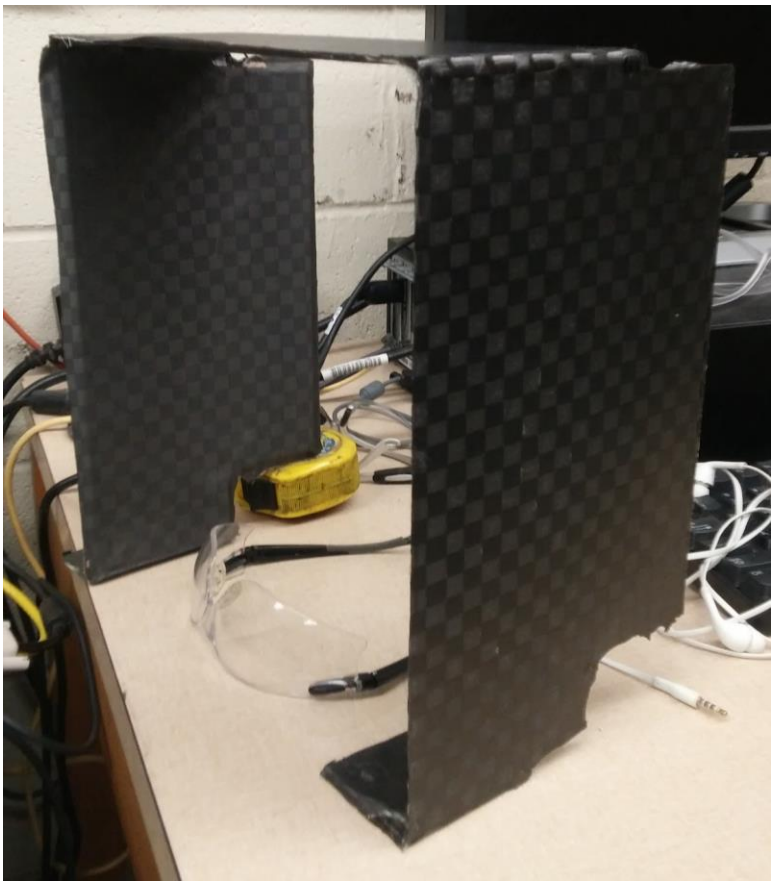

Figure A.28: A front left duct piece before being post processed. Note the rough edges that need to be sanded.

Weight of the left front duct: 108g.

Left Bottom Duct

For an explanation of the layup, see section A2.1.1: Right Bottom Duct.

Left bottom duct weight: 13g.

Left Exit Duct

Before laying up the exit duct, the cracks in the mold (where the sides of the bent flanges meet) needed to be filled in with brown tape to prevent carbon from going through the cracks. The tape can be seen in Figure A.29 and Figure A.30. Once placed, the mold was cleaned with acetone and thoroughly coated in mold release in order to ensure easy removal of the part.

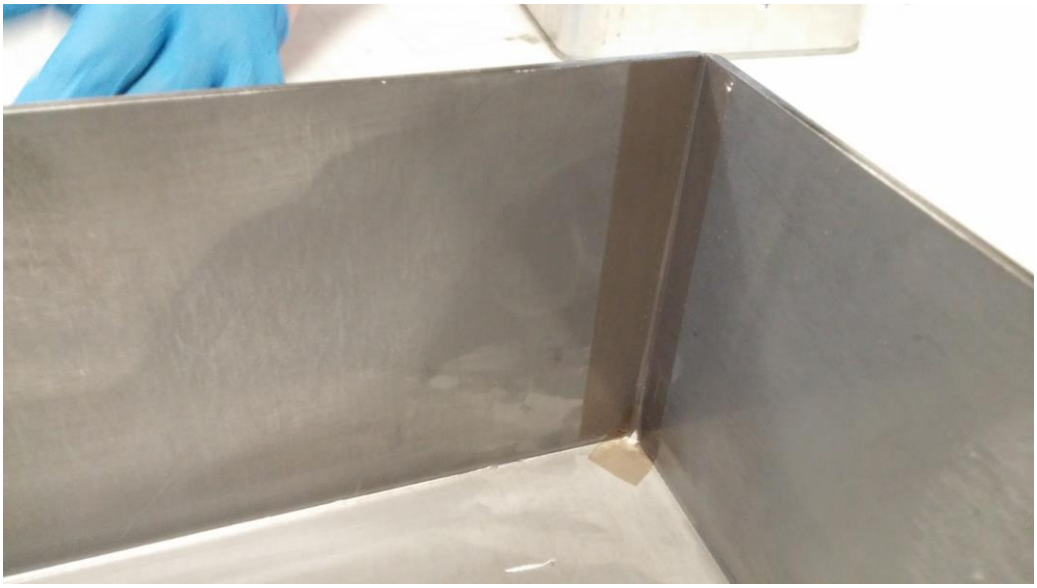

Figure A.29: Tape should be used at the corners where cracks are in the mold.

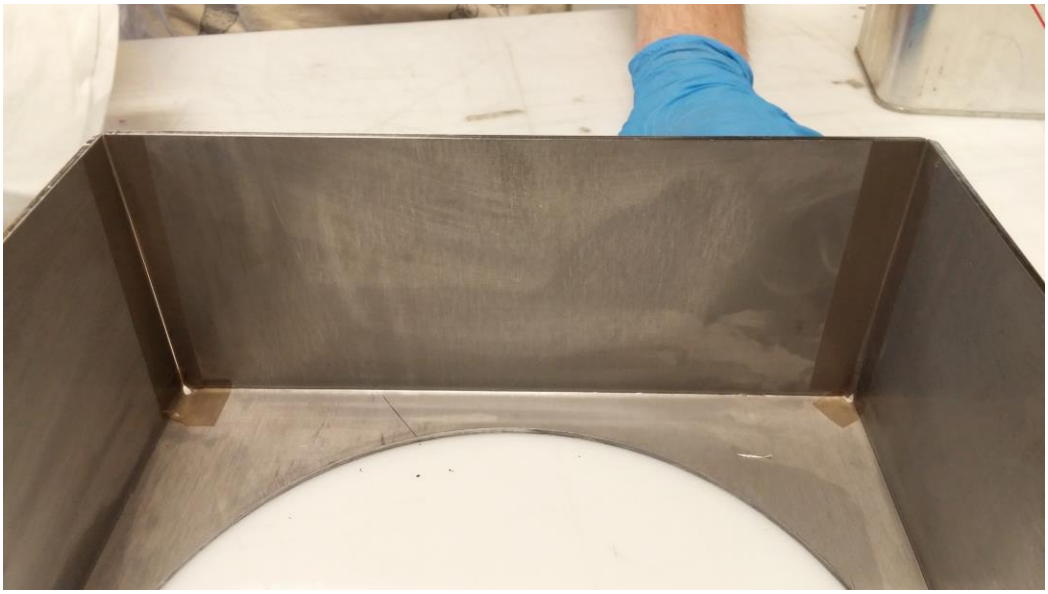

Figure A.30: Another image showing the tape at the corners of the mold.

The first layer of carbon was cut in a + shape, with about 10-15mm extra at each end to wrap around the foam core. Once placed in the mold, a circle was cut in the center for the hole of the mold. Again, this was offset to allow the carbon to fold over the core (see Figure A.30).

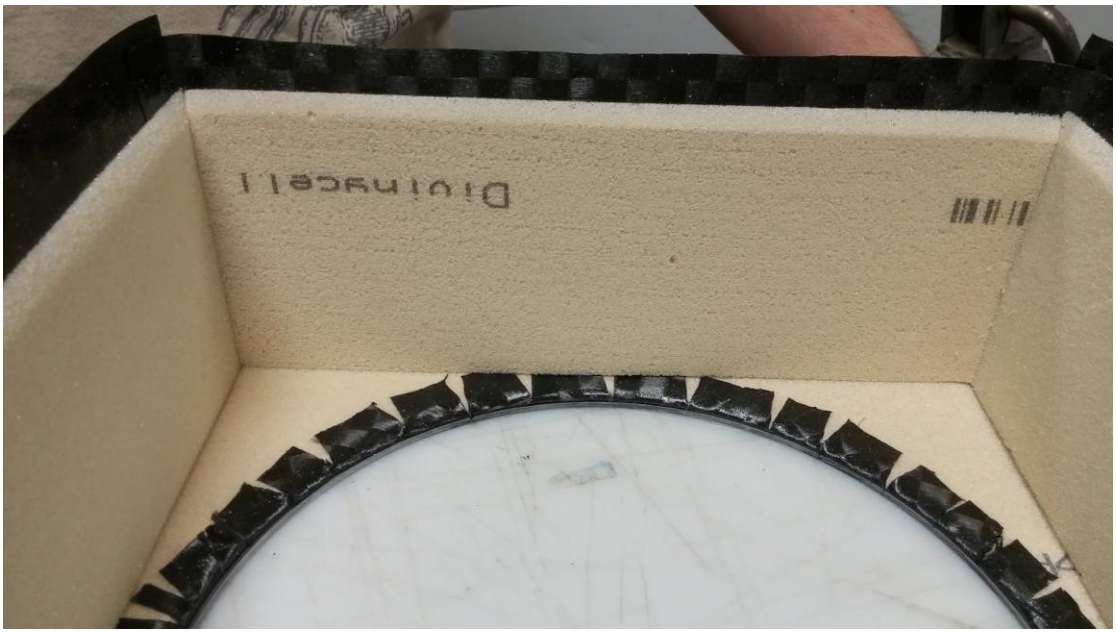

Figure A.30: Core placed on the first layer of carbon. Note the extra material for folding over the core.

Once the core is in place on all edges of the mold, the rest of the carbon can be placed. Two sides can be simple strips (Figure A.31), with extra material on the bottom and sides to overlap other plies.

Figure A.31: First piece of the second layer of carbon. Note the extra material on the left and right sides.

The other two sides need to be covered in carbon that also covers the face of the mold with the circular cut out (Figure A.32). Careful measuring ensures that all the core is covered by these pieces of carbon. Any remaining core must be covered before vacuum bagging the part.

Figure A.32: Second style piece of carbon for the second layer. Note the carbon extending to the face with the circular cutout.

Once the duct piece had finished curing, an issue with the mold was discovered. Two of the sides were bent up more than 90 degrees, meaning the mold gets slightly smaller opposite the circular cutout face. This made it extremely difficult to get the part out. Future mold designers should keep this flaw in mind.

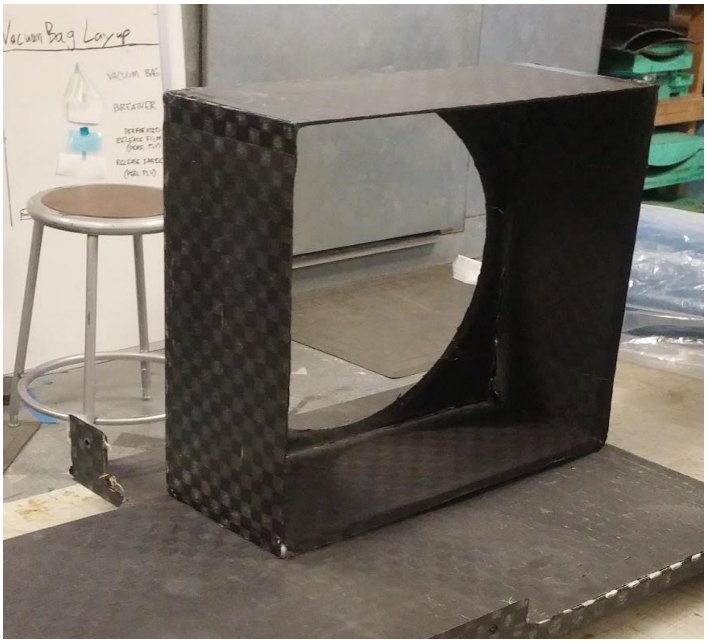

Figure A.33: Completed exit duct.

A change was made to the design after initial manufacturing. Because the duct does not converge or diverge, there is no need for it to be any longer than just large enough to mount the fan off the radiators. Therefore the exit duct was cut down until there was a length of 1” on the sides. This change both serves to reduce weight and reduce the moment arm of the fan (which weighs just over 1kg).

Figure A.34: Exit duct after being cut down.

Left exit duct weight, original: 106g.
Left exit duct weight, material removed: 51.7g.

A3.1.3 Diffuser

Before laying up the part, 13 threaded (M5) hardpoints are required. The stock used was 0.5” hex stock, by recommendation of Connor Torris. This made manufacturing the hardpoints very quick as they could be parted off to a rough length, faced to the final size, and then drilled in the lathe. Finally, the parts were removed and tapped at the tapping station.

Figure A.35: Parting off a piece of hex stock.

Figure A.36: Using a turning tool to reduce the length to 0.5” via facing.

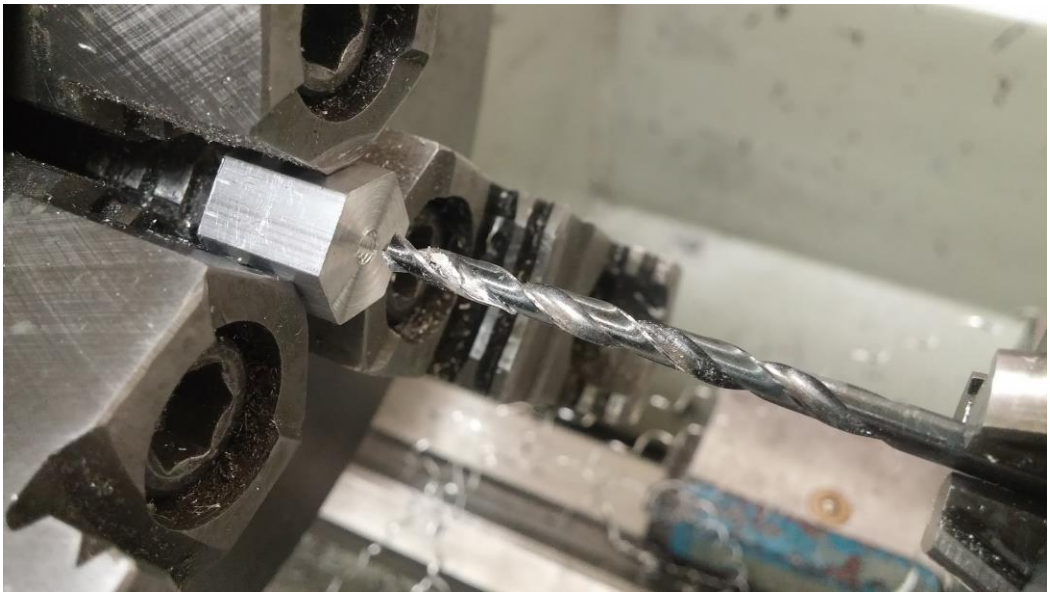

Figure A.37: Drilling hole through one of the hex hardpoints.

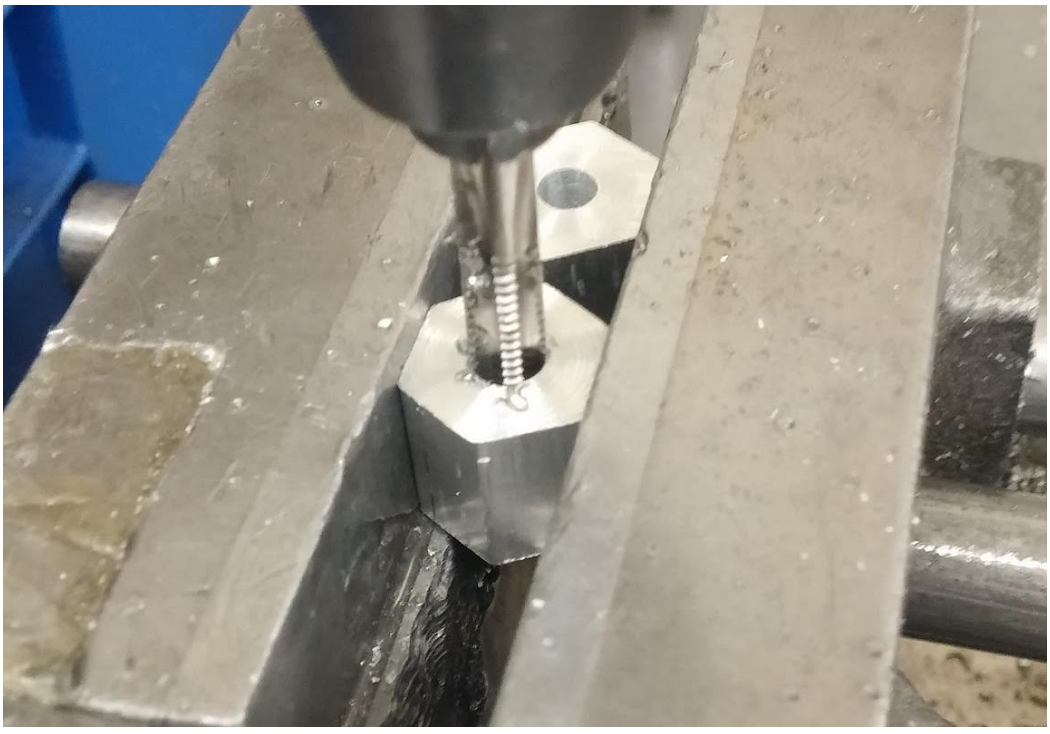

Figure A.38: Tapping holes with an M5x0.8 tap.

The general layup schedule is one global layer of carbon, core, and one global layer of carbon, with reinforcement at bolt tabs and hardpoint locations. To begin, the first global layer is placed.

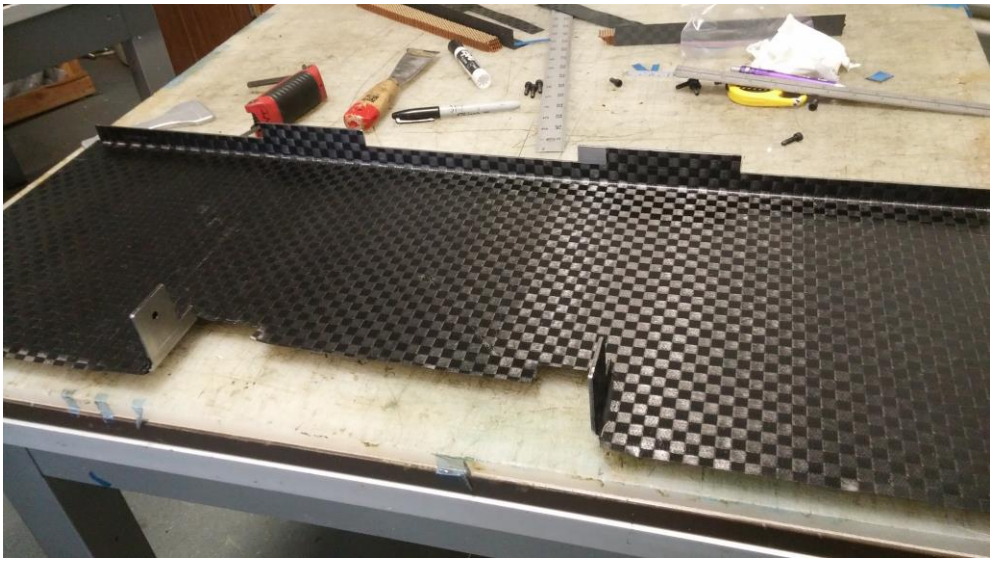

Figure A.39: First global layer of carbon.

To reinforce the mounting tabs, two layers of carbon were cut extending from the chassis mount to the jack bar mounts (Figure A.40). Each tab should have three layers of carbon (one global plus two reinforcement pieces).

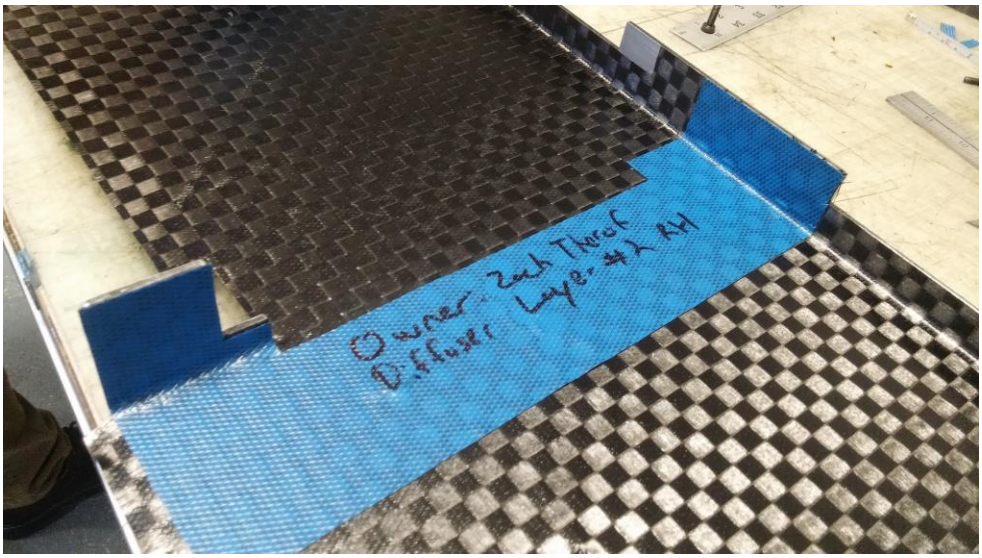

Figure A.40: Example of a tab-strip combination piece.

For further tab reinforcement, three more layers of carbon were used at the tabs, but without the strip extending along the diffuser. Each tab now has six layers of carbon.

Figure A.41: Example of basic tab reinforcement pieces (the first of three pieces photographed above).

Small squares were added at each hardpoint location, with the exception of any hardpoints where carbon from the tab reinforcement was added.

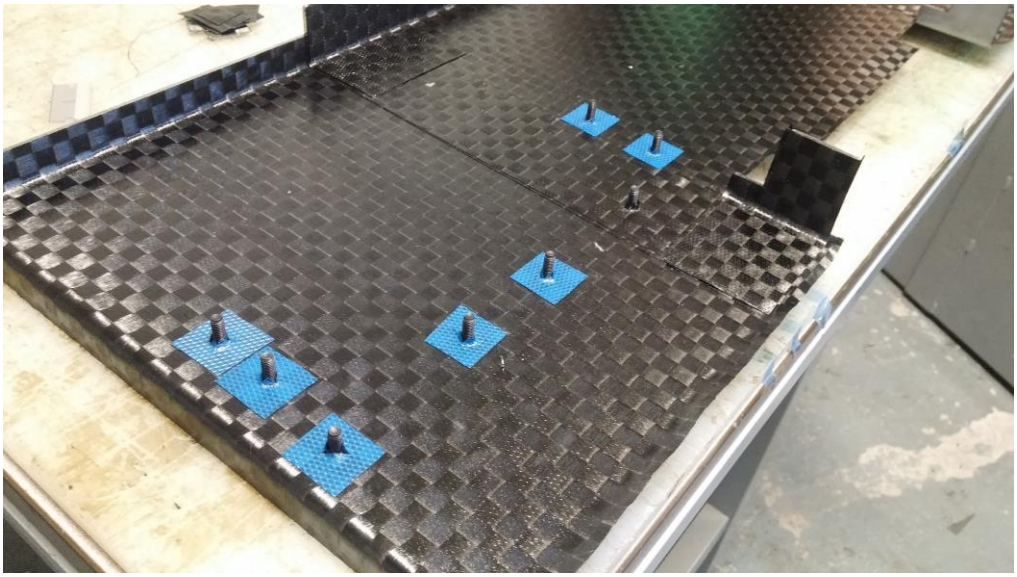
Figure A.42: Hardpoint reinforcement patches.

As we prepared to place the core, we noticed that there was not enough carbon along the edges to wrap around the core. To fix this, extra strips were added along many of these edges. An example is seen in Figure A.43.

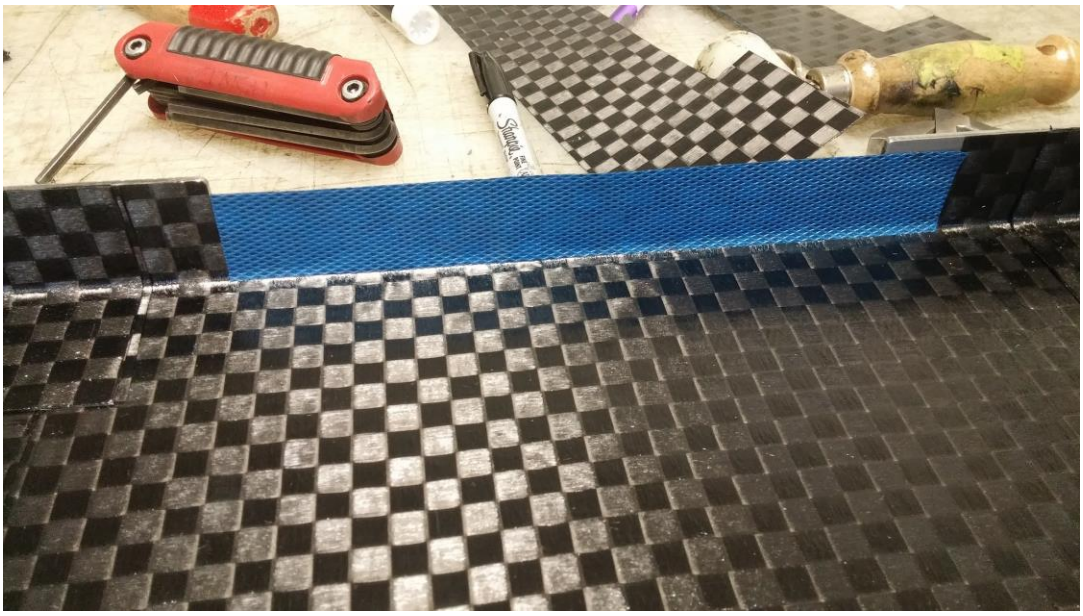

Figure A.43: One of several strips added to fold over the core.

Once the main piece of carbon was placed, the side strake core had to be placed. This required carbon L brackets to be made before layup. The L bracket was placed on the core and the resulting piece was placed on the mold along the edge of the main core piece, as seen in Figure A.45.

Figure A.44: Preparing the core and carbon L bracket for the sides of the diffuser.

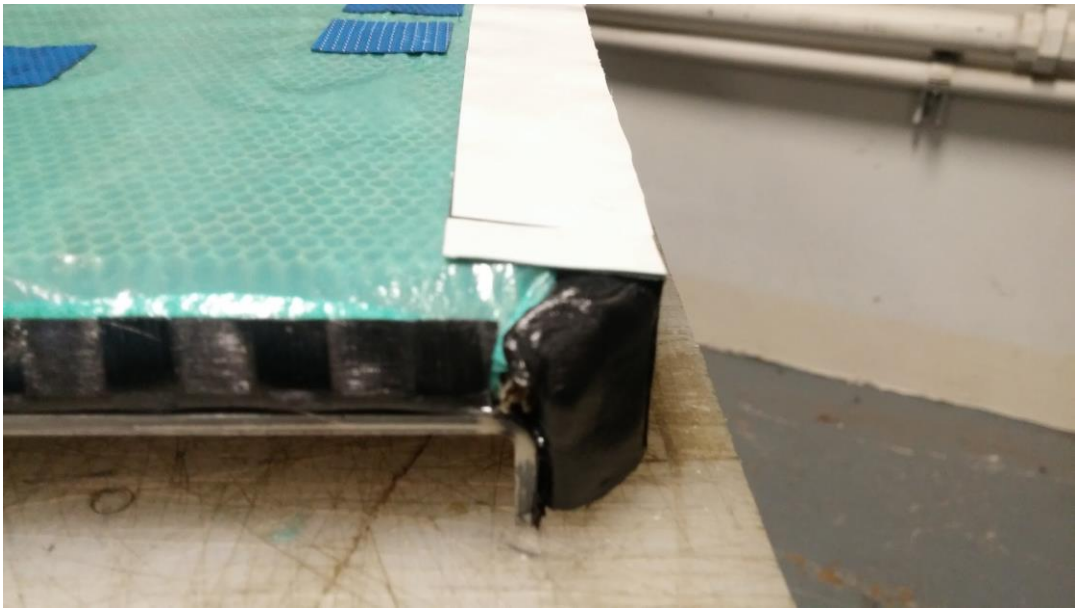

Figure A.45: Placing the core piece for the side strake.

The process of reinforcing the part continues with adding another square patch at each hard point location, small tab reinforcement pieces at each tab (three for each tab), and tab-strip combination pieces (two for each tab). Finally, a second global layer is placed over the core and mount flanges. If there is any core exposed on edges or corners, additional strips of carbon can be used.

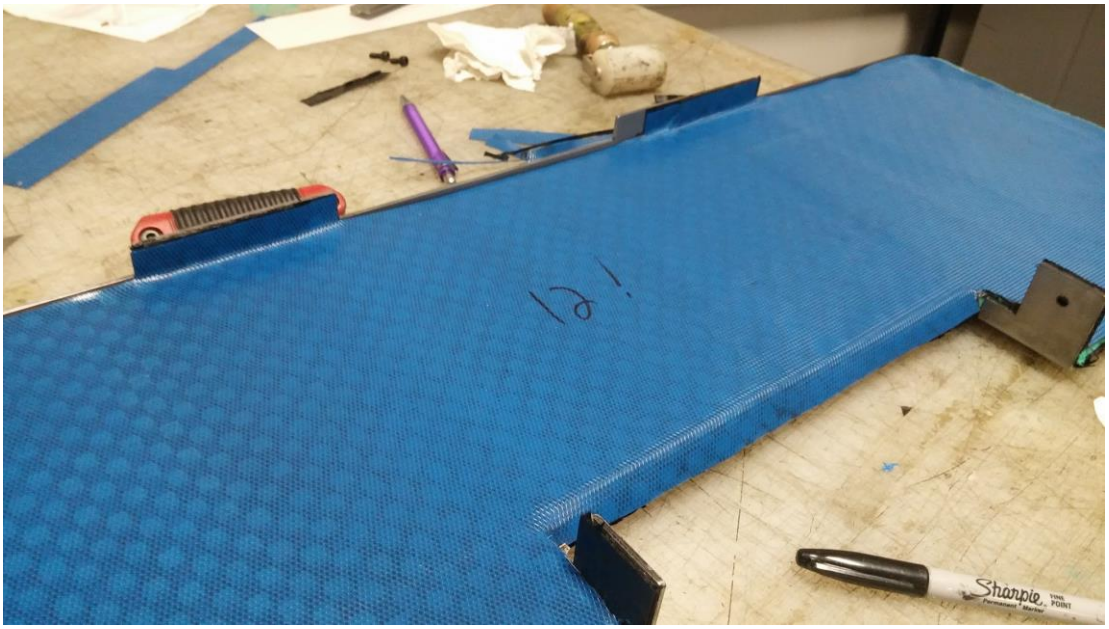

Figure A.46: Last global layer.

Diffuser plate weight: 535g.

Jack Bar

Jack Bar - Inserts

The inserts were made by turning 1” aluminum 6061 rod stock on a lathe. The end was cut with an initial facing pass, and the length of the rod was turned down to remove the outer layer of material. If desired, this cut can be used to reduce the stock to a measured 1”.

Once the material is prepared properly, turning passes can be made to reduce the diameter of the tip to the same inner diameter of the tube being used. In this case, with a 1” OD / 0.035” wall thickness tube stock, the target was 0.93”. The fit can be checked with a piece of the tube. Make sure the fit is not loose or even easy to get on. If the insert needs to be forced into the tube by pressing hard or even with a hammer, this will help the welder by preventing motion during welding. This was not done for the first two jack tubes for the cCar, but was done properly for the eCar parts.

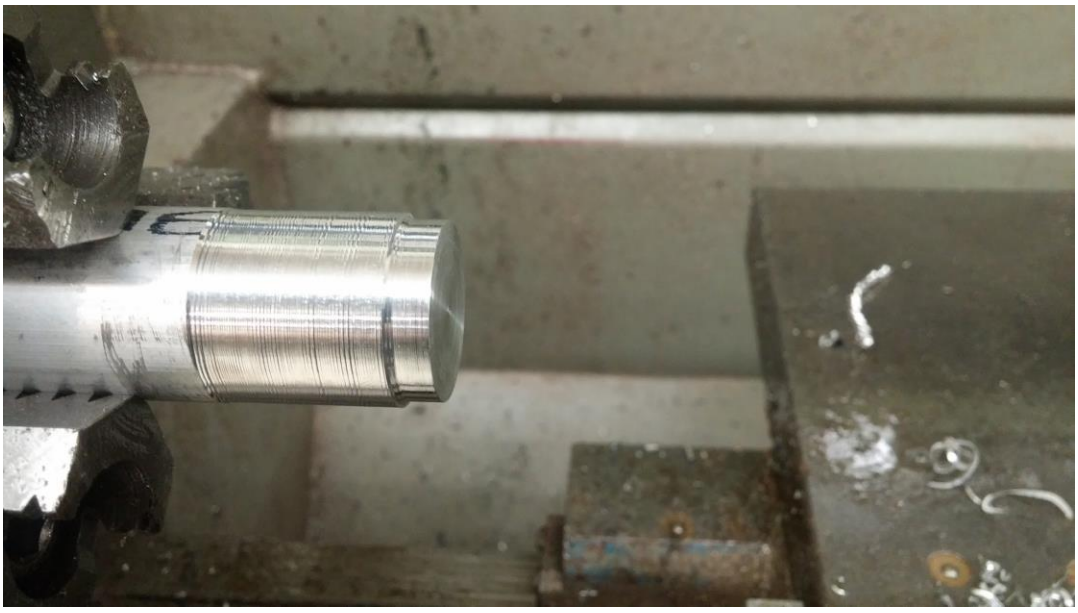

Figure A.47: Turning down the end to the desired diameter to fit the inside of the tube.

Once the inner face of the insert is finished, the insert can be parted from the stock. While making the inserts, 0.1” of length was the target for the flange thickness (Figure A.48). If there is excessive material, there may be enough material to carefully clamp the smaller diameter portion in a jaw chuck or even a collet. If so, the parted face can be cut down to the desired thickness with a turning tool (Figure A.49).

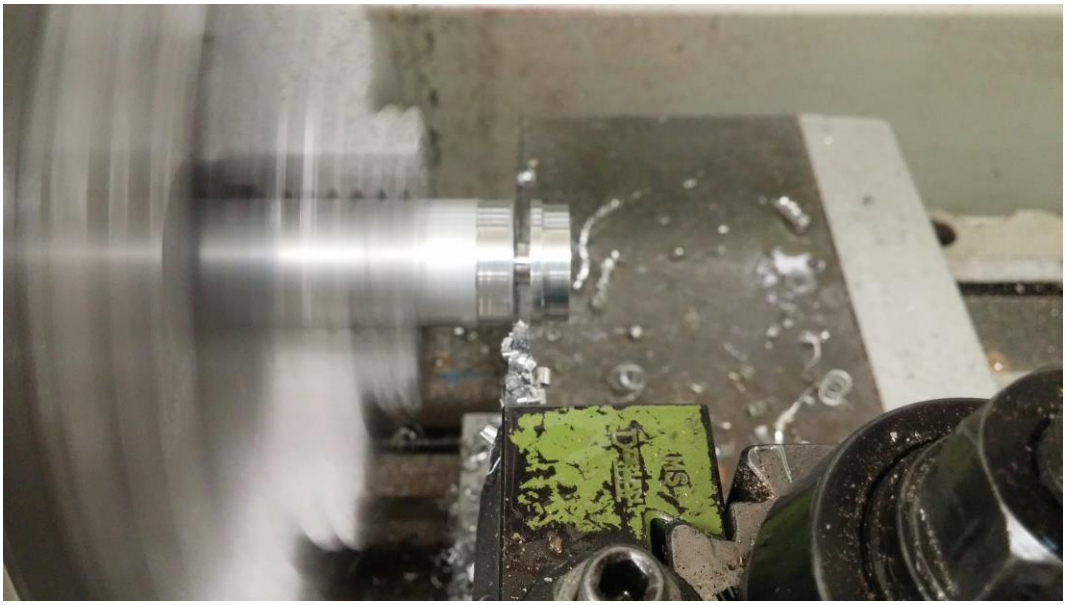

Figure A.48: Parting the insert off the stock.

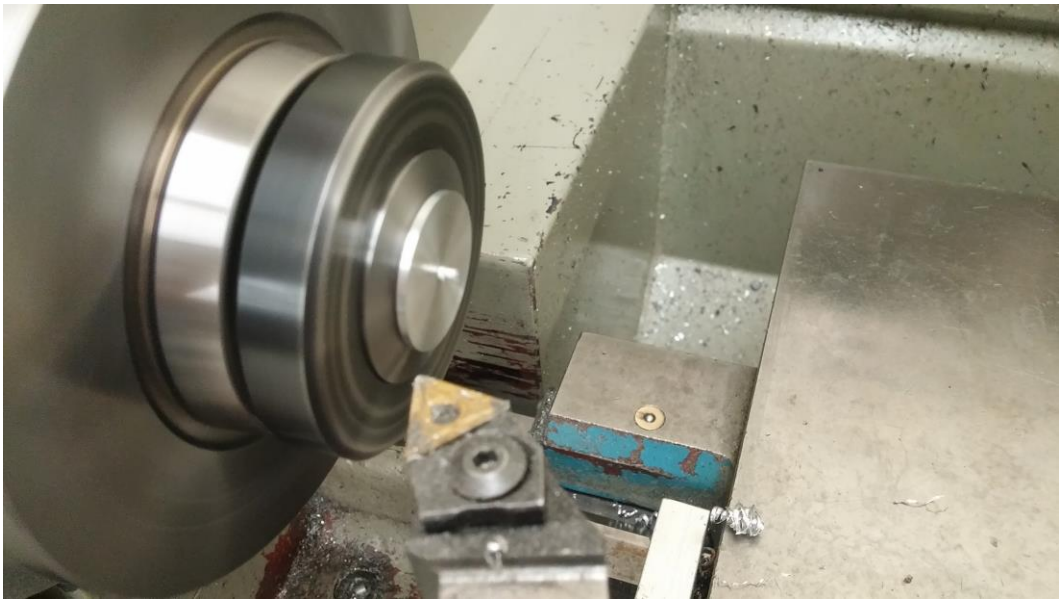

Figure A.49: Facing the parted surface to the desired flange thickness of 0.1”.

Another error made during the first two jack tubes’ manufacturing process was drilling the holes early. After the parts had been made, Eric Bramlett mentioned that welding can warp the tapped holes. This did not end up being an issue (both jack bars fit fine on the diffuser), but was noted for future welding projects. Tapping can be done by hand, made especially easy using a lathe to fixture the opposite end of the tap holder to ensure a centered hole.

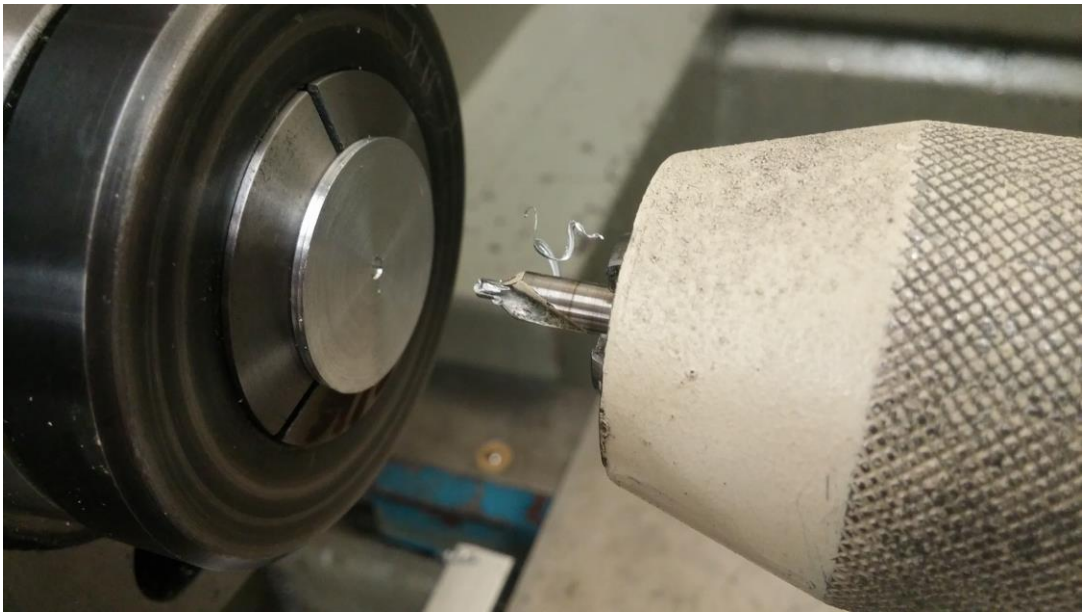

Figure A.50: Again, this should be saved for after the insert is welded. However, it shows the concept of using a center drill at the first stage of drilling and tapping the insert.

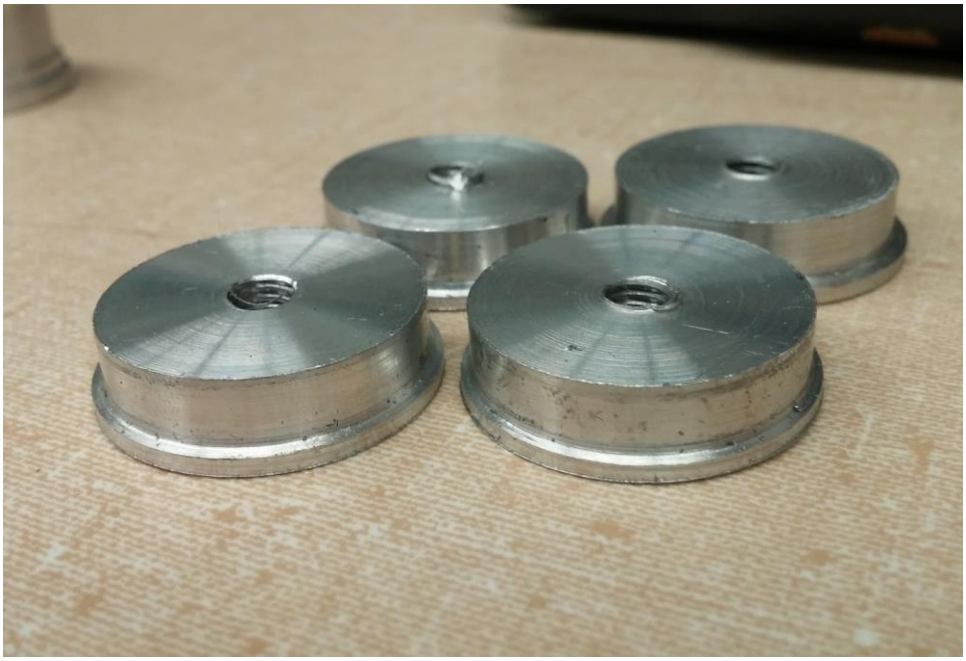

Figure A.51: Completed jack tube inserts.

Insert weight: 7g each.

Jack Bar - Tubes

Tubes were simply measured out to roughly 300mm. A little extra was given during cutting and then sanded down using the belt sander. To determine the length of tube needed, the fittings can be placed in (unless the fit is too tight to prevent removal) and the entire assembly measured. The initial cut can be done using a bandsaw, the cold saw, or even a lathe (though not recommended, as it was later found that a band

saw could give a much faster, though less accurate, cut). The rules state 300mm or 12” length. As 12” converts to roughly 305mm, the target was a total length of just over 300mm (remaining rules compliant with the metric value specified). The process of using a belt sander continued until the tubes were the desired length. Alternatively, the tube could be placed in a lathe to ensure a square end.

Figure A.52: Using the lathe to cut down the stock tube to length. This process is overall slower than using a bandsaw and placing the stock in a lathe to use a turning tool to square the end.

Combining into Jack Tube

To prepare the parts for welding, the area around the weld was rubbed with Scotch-Brite (a lathe set to a low speed makes this very easy) and cleaned up with acetone. The inserts were welded into the tube, using Eric’s improvised fixture. He used another metal rod to butt up against one end of a clamp, while having the other end of the clamp forcing the other end of the jack tube against it. This allowed him to weld near a surface that wouldn’t melt, as would the plastic tips of the clamp. Though this final method was not photographed, an earlier, similar setup can be seen in the following images.

Figure A.53: Another possible fixturing method for the jack tube, though has the disadvantage of only exposing about half the circumference of the tube end for welding. The tube would then need to be rotated to access the other side.

Figure A.54: A close up of the tube with insert pressed in and fixtured for welding.

Figure A.55: The resulting weld around the inserts.

Once welded, the jack tube can be placed in a jaw chuck lathe (very carefully, to avoid crushing the tube) in order to drill and tap holes in the inserts. Both are right hand threaded. It is worth using a center drill to first make a divot to avoid the bits from drilling off the center of rotation.

Once holes are tapped, the jack bars can be painted with orange spray paint. An easy way to do so is to use string of some sort (this year, safety wire was used) and tying it around a bolt bolted into one end of the jack bar. The bar can then be hung somewhere with access to all sides.

Welded jack bar weight: 75g each.

Linkage System

The linkage system consists of two arms, each of which is made up of four pieces. These pieces are the linkage insert, linkage tube, chassis tube, and chassis plate.

Linkage System - Insert

These parts are made in much the same manner as the jack bar inserts. To begin, a steel rod (4130) of diameter 0.5” is inserted into a lathe. As with the jack bar inserts, the stock is faced down at the end, then turned down along a length of 0.16” to the inner diameter of the rod they are to be inserted into. Again, the best way to gauge how much material to cut is to test it with a tube, ending when the insert fits snuggly. Once the part is turned down properly, the insert is parted such that the overall length is just over 0.275”, using the lathe to face down the larger diameter portion in a collet lathe to accurately hit the desired length. Completed inserts can be seen below.

Figure A.56: Eight completed linkage inserts.

Linkage System - Linkage Tube

The linkage tube is the main tube that extends from the jack bar to the chassis. The tube stock was cut slightly long, then welded with an insert (see discussion on jack bar welding for details). The tube could then be placed in a lathe in order to drill out and tap the insert. Tapping should be done using a hand tap with the lathe switched off (Figure A.57).

Figure A.57: Using a hand tap to tap the linkage insert in a lathe.

Once the insert was tapped, the tube was sufficiently prepared for coping. A print out of the unfolded tube can be used. The cope profile can be cut out and placed along the tube, using the distance from the end of the insert to a point along the profile that can be measured in CAD to determine the correct location along the tube. The coping process involves using angle blocks on a manual mill with an endmill matching the outer diameter of the tube (in this case, 0.5”). The cope profile acts as a guide for how far to cut into the tube.

Figure A.58: Coping the linkage tube.

Linkage System - Chassis Tube and Plate

The chassis tube was initially cut extra-long to help with welding, roughly 100mm long. One end was welded to a thin steel plate. To round off the plate after welding, the corners were sanded using a belt sander. The plate was finished off by placing the tube in a lathe and using a turning tool to turn down the plate until only a small amount of material was left bordering the weld around the tube. Finally, the tube/plate assembly was finished by drilling a 5mm hole in the lathe to create a through hole for an M5 bolt.

Figure A.59: Chassis tube welded to the chassis plate. This photo is after sanding two of the corners slightly, but before putting the tube in a lathe to round off the plate.

Welding the Linkage Together

To fix the linkage together, the simulator chassis was used as a welding fixture. The chassis tubes were bolted into their mounting positions on either side and the diffuser was mounted below with the linkage tubes bolted into the jack bar. The tubes were then adjusted by loosening or tightening the rod ends until they butted up against the chassis tubes at a suitable location, before being tack welded. Once tacked, the linkage assemblies were removed from the car before being fully welded.

Figure A.60: The linkage tube - chassis tube weld interface.

To reduce weight, the chassis tube can be cut down using an angle grinder, as long as the weld is not damaged around the tubes.

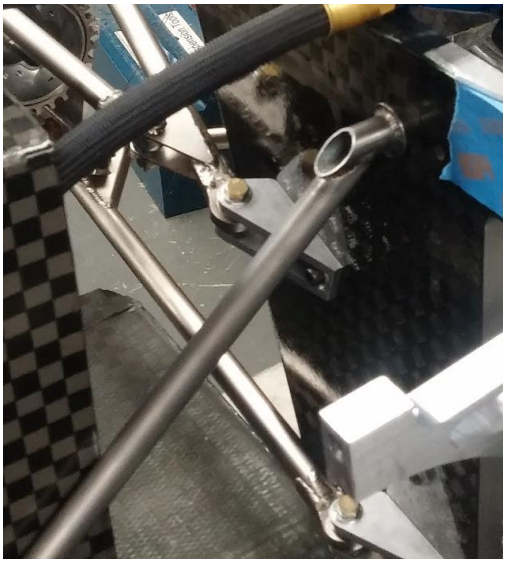

Figure A.61: Linkage tube as installed on the car, after having extra chassis tube removed with angle grinder.

Linkage tube assembly weight: 81g, each.

A3.2 Water Plumbing Elements

A3.2.1 Water Line

The water lines were made from aluminum 6061 tubing (0.75” outer diameter, 0.035” wall thickness) and bent by Elliott Bending. In order to prepare the tubes for bending, they were cut on a lathe to a slightly oversized length (around 1” extra). This was done in order to assist the bender, providing more material to grip in the bending device.

During assembly, the tubes had to be fit in the system to ensure they were the proper length. This was accomplished by mounting the diffuser and radiators, then holding the tube up where they were to be mounted. The engine outlet line was found to be somewhat long, so about half an inch of material was removed prior to installation. When the lengths were determined to be satisfactory, the ends of the tubes were beaded using a beading tool to prevent leaks at hose connection points.

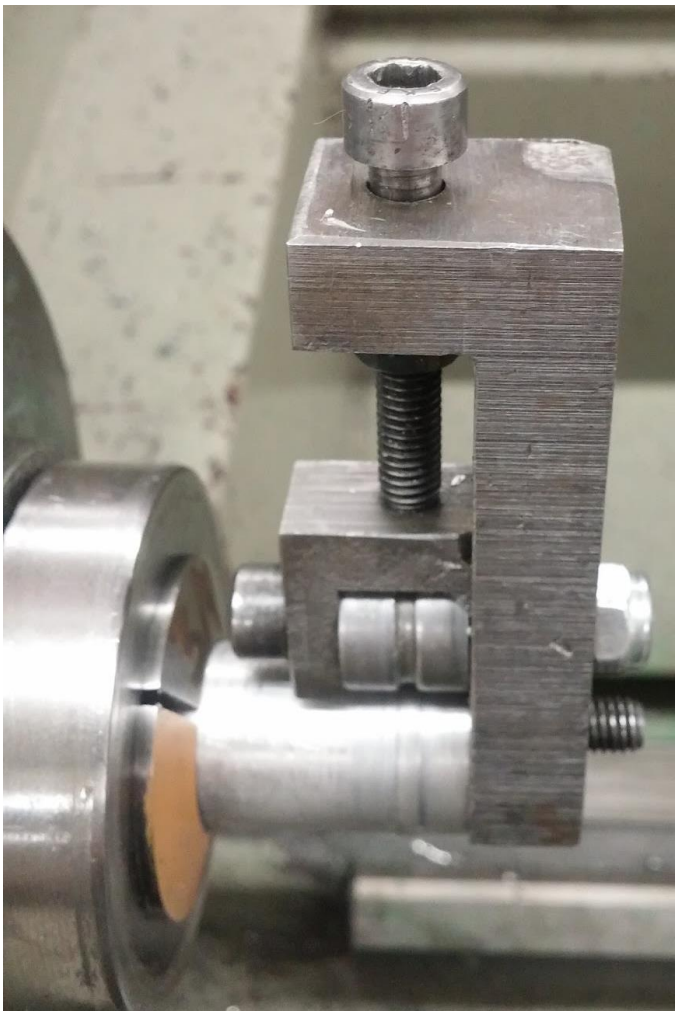

Figure A.62: Beading a straight tube using a lathe as a fixture.

The silicone hose was cut down in a similar fashion. The engine inlet and engine outlet lines were attached at the radiator ports using a small length of straight silicone hose. The opposite end was then held roughly in place and the silicone hose for the engine was held between the engine ports and the tubes. The desired

length was determined via observation and the line cut. Finally, the silicone hose was added to the system to ensure a proper fit, with further adjustments made as necessary. The line connecting the two radiators was far simpler; the line was attached to the first radiator with a short piece and a piece of oversized straight silicone hose was added at the second radiator and cut down until the desired fit was achieved.

Figure A.63: The black hose is attached to the water outlet on the engine.

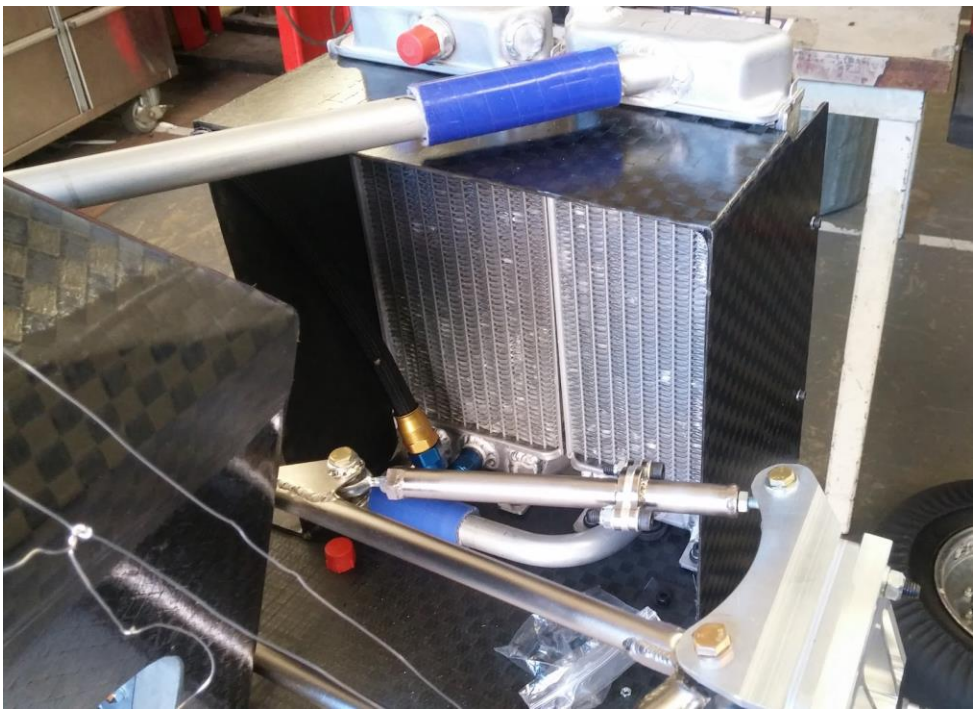

Figure A.64: Early water line fitting. Note the extra-long hose, prior to being cut down to a proper length.

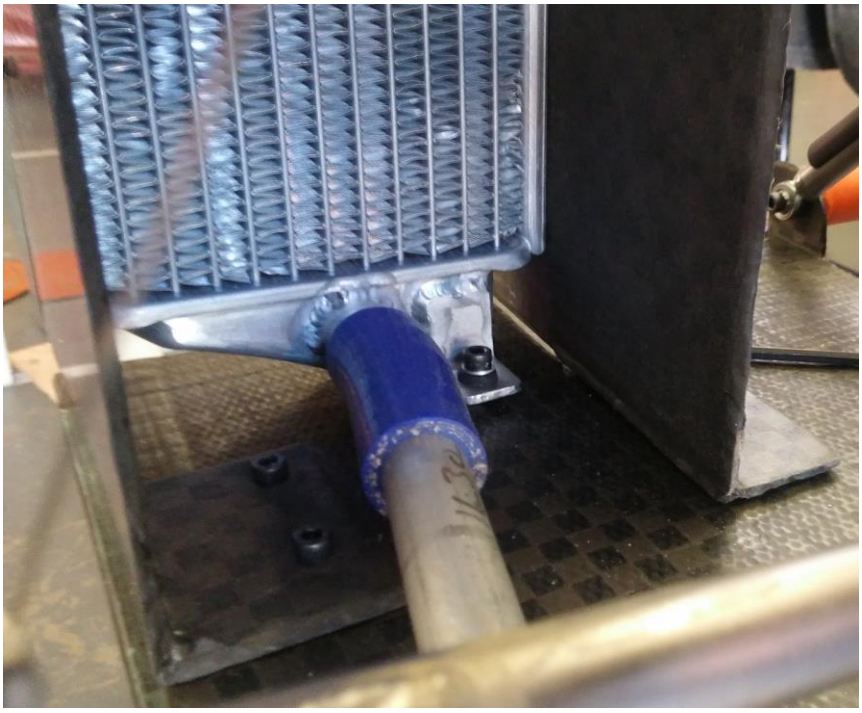

Figure A.65: Hose exiting the second radiator.

Figure A.66: To fit the connecting line, a small piece of silicone hose was attached to the outlet of the first radiator.

Engine outlet line: 79g
Radiator connection line: 65g
Engine inlet line: 83g

Note: above weights are just aluminum pieces, unfilled.

A3.2.2 Water Engine Ports

Engine Outlet

Due to the direction the water comes out of the engine, a stock part was used for the outlet water port. The only modification was to add a bung for taking temperature data.

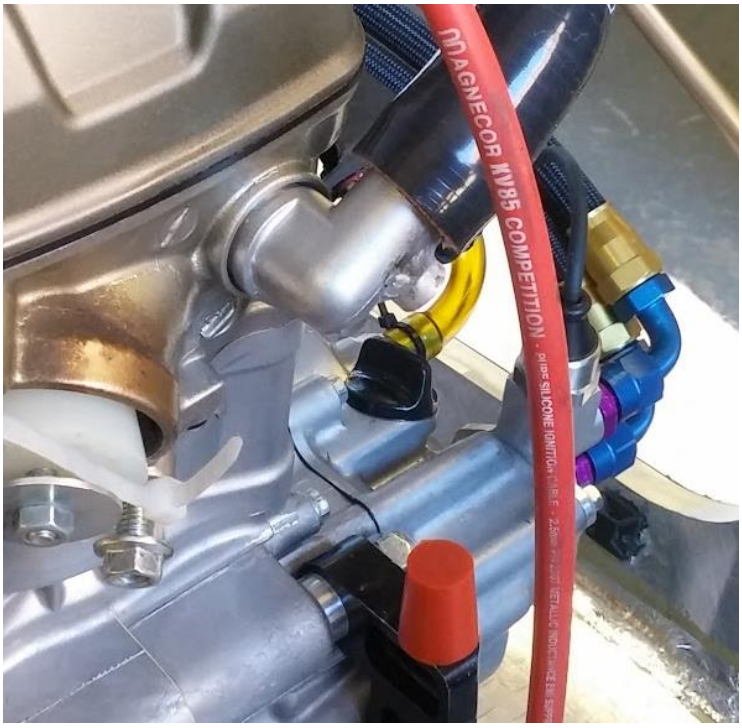

Figure A.67: Water outlet port installed in system, but before having temperature bung welded on.

Engine Inlet

The engine inlet was made by using two machines. Patrick Hinkle handled the initial steps on a CNC lathe and Sam Phelps finished the part on a manual mill. The last step was to weld a tube into the port.

The lathe was used to machine all the concentric features. This includes making the outer dome and boring out the center, as well as the recessed portion at the top for the temperature sensor. Figure A.68 shows most of the external features, with the exception of the o-ring groove on the bottom of the plate.

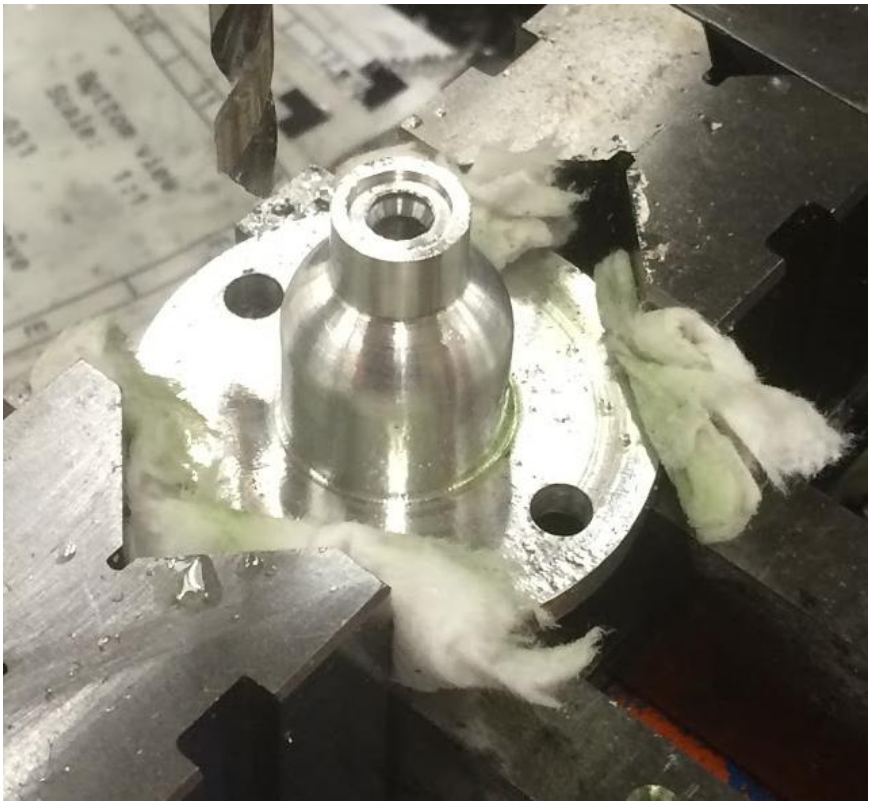

Figure 5.68: Inlet plate having its mounting holes drilled for mounting to the engine.

To finish the part, the holes in the plate were first drilled out. An error was made at this step. The center points of the inlet dome and two holes are not actually in line on the engine; rather, the dome needs to be offset slightly. This can be accounted for by measuring out how far the holes need to be spaced and shifting the piece when drilling them out.

Once the holes were drilled out, a block was made with the same holes as a fixture in order to mill out the side hole for the tube to be welded into. This is where good design is important: because the port was designed to come out at an angle at 90 degrees between the two bolts mounting the port to the engine, a flat block could be easily secured in a manual mill and bored out straight once the location was located.

Figure A.69: Fixture for the port.

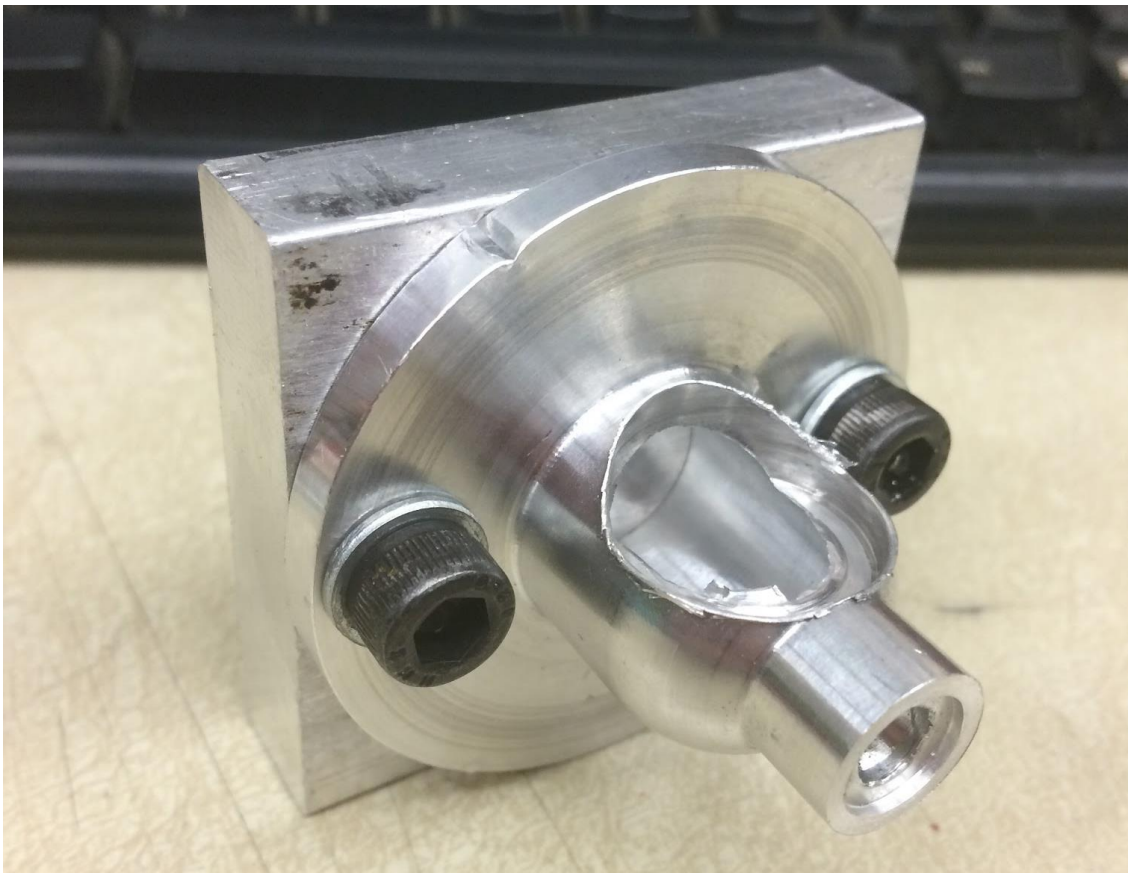

Figure A.70: The hole bored out of the side of the port for a ¾” tube.

Finally, extra material around the edges was removed to match the geometry of the engine. This is not an exact process, as the most important factor in sealing the port is the o-ring. The hole for the temperature sensor was tapped and a tube was welded into the port. The tube was made in the same manner as the tubes for the radiators.

Figure A.71: Bottom of the plates, showing an o-ring in the groove.

Figure A.72: Two port plates and accompanying tubes ready to be welded into the ports.

Before the tube is welded into the port plate, the bottom half should be coped to allow water to flow down the port. Otherwise, part of the port would be obstructed by the tube. This can also be done after welding, but may be harder to fixture the assembly.

Figure A.73: Coped tube inside the port, allowing water to flow through the tube and easily transition to flowing down the port.

Figure A.74: Engine inlet installed in the system and ready to be connected to silicone hose.

A3.2.3 Water Thermostat Housing

Based on a design from 2015 by Alex Yinger, the thermostat was housed in a basic set of two aluminum pieces attached via three M4 bolts. One of the pieces had already been partially manufactured by Alex Yinger, missing only the bolt holes and barbed end. However, the procedure for manufacturing it is similar to the other piece, perhaps even simpler due to lack of an o-ring groove.

The thermostat housing can either be made by hand or on a CNC lathe, depending on user skill. Alex managed to produce the first piece using the manual Hardinge lathe, while the second piece was made using the Haas CNC lathe with coding help from Jeff Sprenger. The lathe should contain the code used to make the part; unfortunately, it does not exist anywhere else. It is in two files as the part is made in two operations ("operation" being defined as the processes involved during machining for a single set up of the part).

Operation 1: General Shape

A stock piece of 7075 was used to make this part. However, this is only because it was what was on hand; 6061 would suffice. The stock diameter of the aluminum rod should be around 2.75" and machined down. The majority of the outer profile was made using a turning tool.

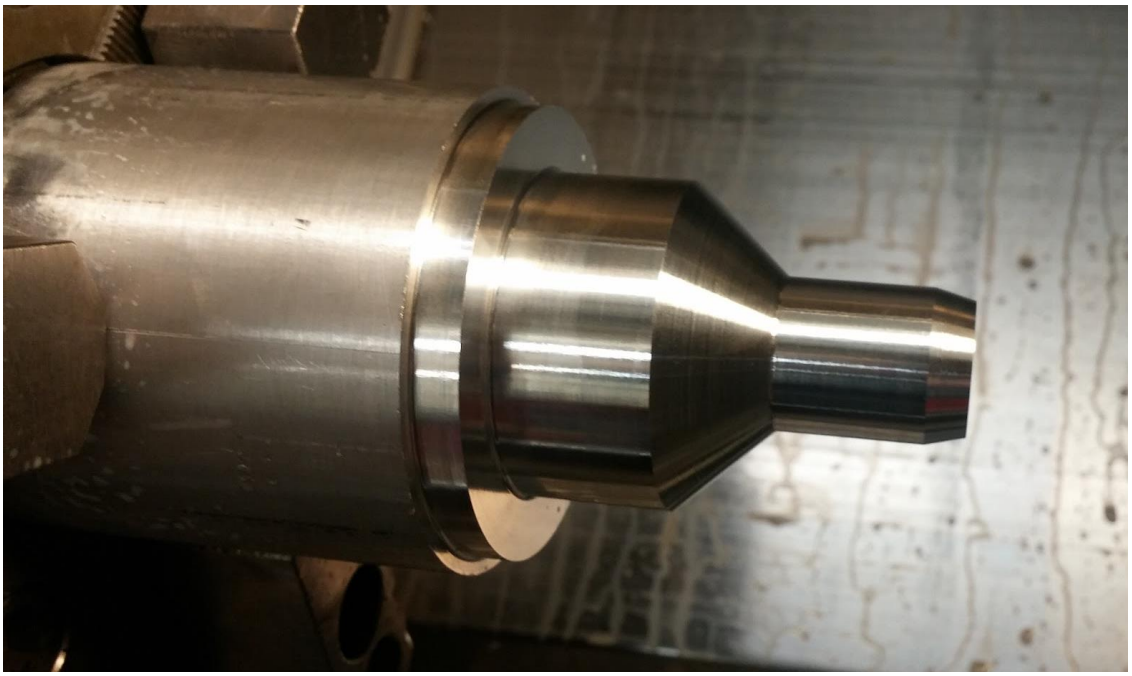

Figure A.75: Outer profile after turning tool used (first step).

Once the turning tool was finished running, a grooving tool was used to machine away material to make a barb. A grooving tool had to be used because a turning tool would introduce a radius at the barb and the silicone hose might not seal properly.

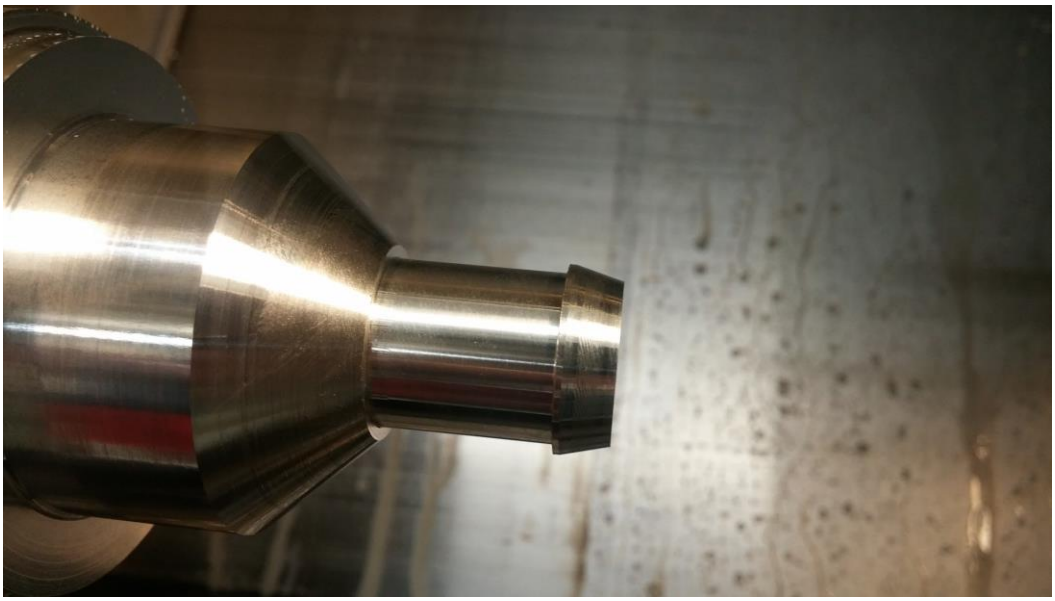

Figure A.76: A grooving tool was used to bring the diameter down to make a barb.

The final step during the first chunk of code was to drill out the center of the part. A center drill was first used to define the drill point. Then, a ⅝” drill bit was used to drill a hole through the entire part, tip to end. Cut depth was set to end at 3” to be sure that the whole diameter of the bit went the length of the part. A slow peck was used to keep the tool from deflecting or the part from breaking.

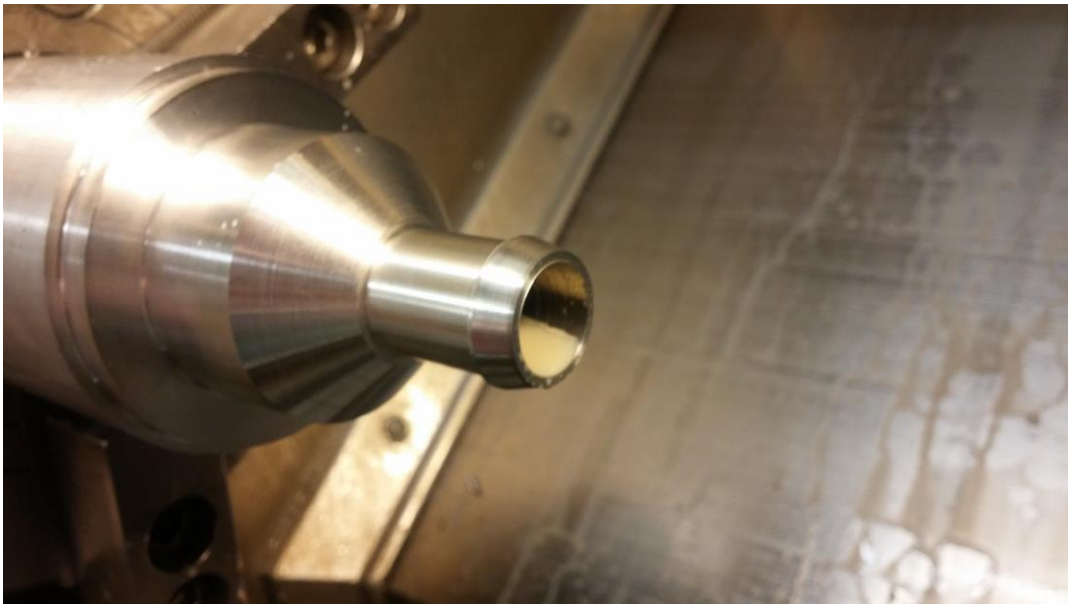

Figure A.77: Hole drilled through the part.

With the outer portion of the part machined and the hole created through the middle, the part was finally parted so that the inside could be bored out further in the second operation.

Figure A.78: The part after all CNC lathe steps were complete.

One important difference between the two pieces of the housing is that the piece Alex Yinger made does not have enough material to clamp at the base of the flange. Thus, that half of the thermostat housing should be made without the barb so that the neck can be used to fixture the part for drilling and boring. For that piece, adding the barb should be the last step.

Operation 2: Boring Out the Middle

The part was flipped around so that the barbed end was pointing towards the spindle. The code for the second operation only included boring out the inside using a boring bar, increasing the size of the hole from the drill bit until completion.

Figure A.79: Inside of the thermostat housing, showing the bored out section.

Figure A.80: Checking fit of the thermostat before making the o-ring groove and bolt holes.

Final Operations

To finish up the second piece of the thermostat housing, holes had to be drilled and an o-ring groove added around the thermostat. This was done on a manual mill using a rotary table with a three jaw chuck to fixture the two halves. Drilling the holes was done in the same manner for each, using coordinates to locate the bolt holes.

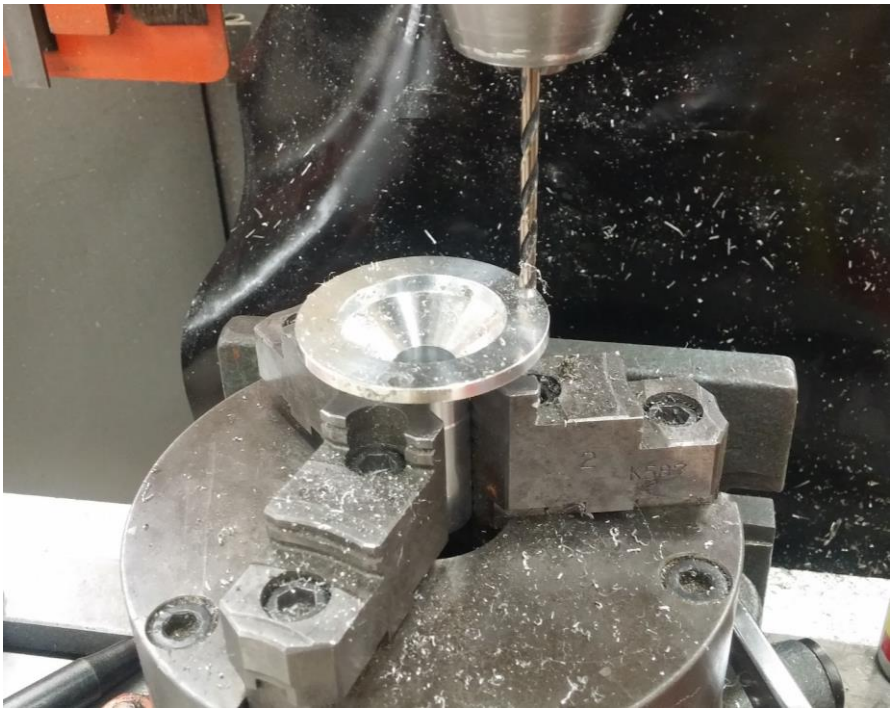

Figure A.81: A rotary table with a three jaw chuck used to fixture the two halves for drilling.

For the larger piece, an o-ring groove was added using a two step process of a center drill and drill bit. There are likely better methods that should be explored. However, time was of the essence and this worked reasonably well with what tools were available. First, the centerline of the groove was located on the mill. Then, the center drill was used to go around the part in 0.01" depth of cut passes until the desired groove depth was achieved. Then, the same was done with the closest drill bit size that could be found for the desired groove. If the groove from the center drill is not deep enough, the bit will deflect very easily during rotation! This was a huge problem this year and should be avoided in the future.

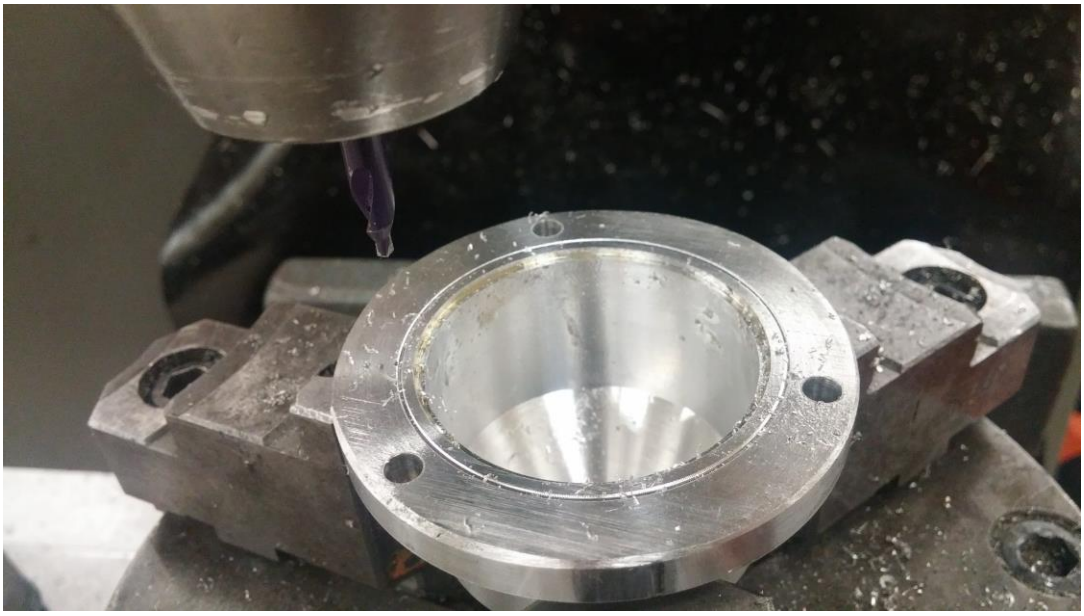

Figure A.82: Beginning the o-ring groove by using a center drill.

Assembly

The thermostat and o-ring were placed in the large half and the top was bolted on. Placing the assembly was the final challenge. Primarily constrained by space, it ended up being placed next to the engine right at the exit. This helps limit the amount of silicone hose needed as the 90 degree piece was already in place for the rest of the plumbing line.

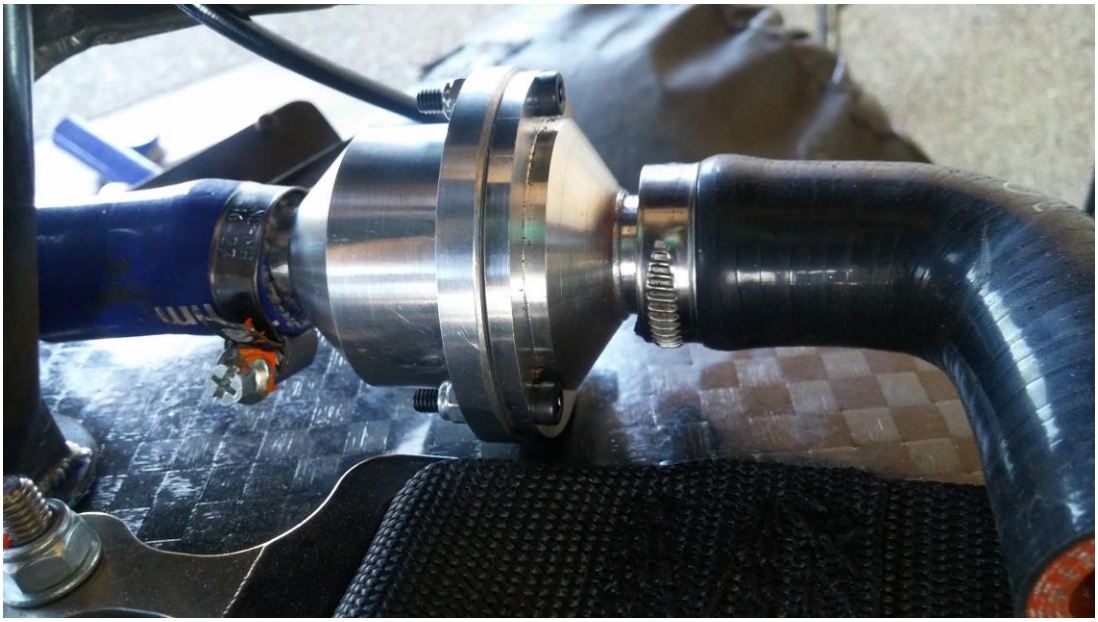

Figure A.83: Assembly bolted together and attached to hose, ready to install in the car.

Thermostat weight (assembled, with o-ring and housing): 196g.

A3.3 Oil Plumbing Elements

Main Lines

The oil lines were handled primarily by Caleb Cluster, Eric Bramlett, and other members of the cPowertrain subteam. The oil lines consist of braided lines from BMRS. The radiator has a weld in bung from Summit Racing at the inlet and outlet, with a straight AN -6 fitting at inlet and a 90 degree AN -6 fitting at outlet.

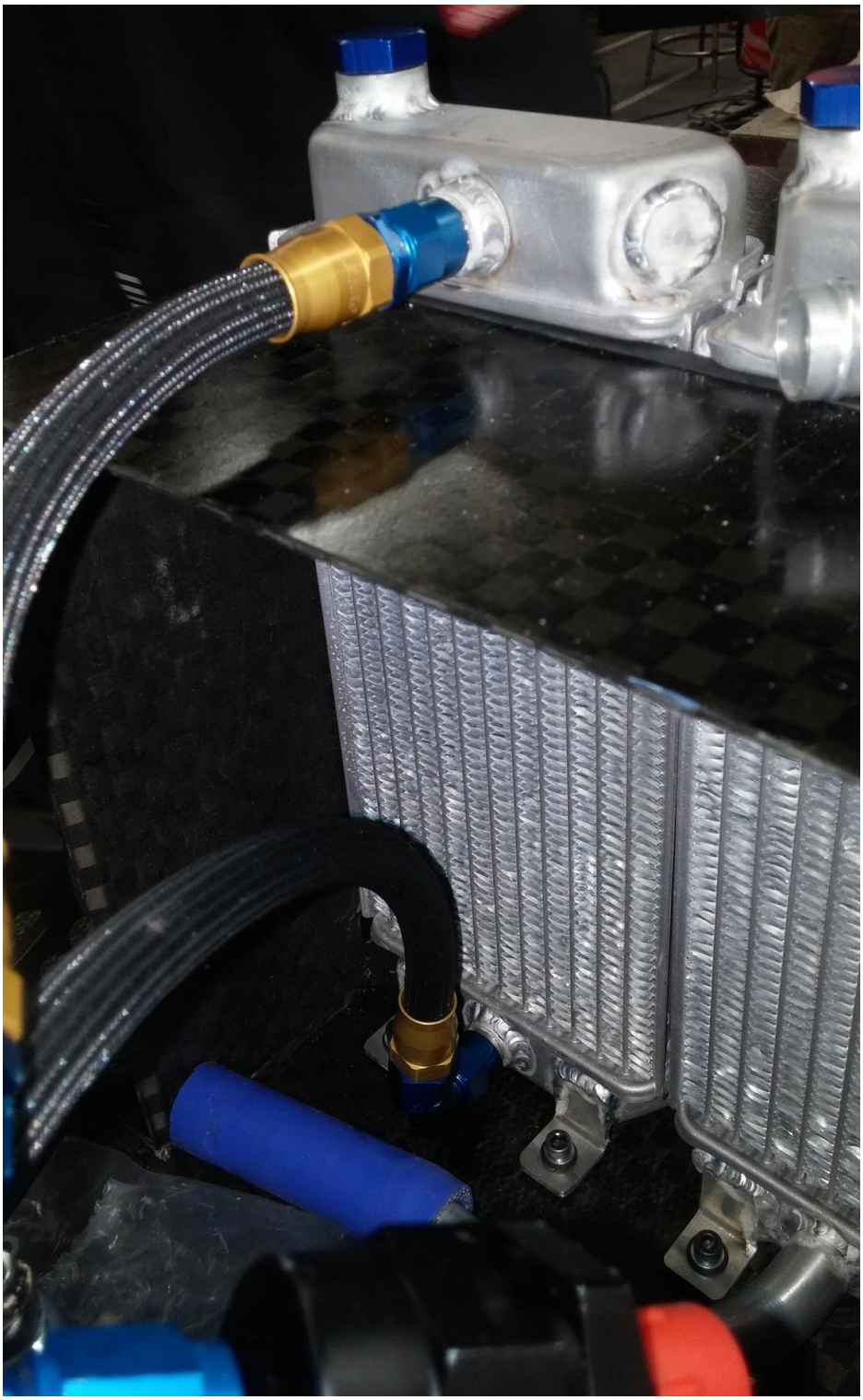

Figure A.84: Oil connections on the oil radiator.

The oil lines terminate on the engine at 90 degree AN -6 fittings.

Figure A.85: Oil fittings on engine.

While it was intended to manufacture in-house anti-siphon valves, due to time limitations and insufficient skill, purchased valves were used instead. These can be seen below in Figure A.86. One of each is mounted on a tee fitting along the oil lines between the engine and the radiators. The image is prior to final installation. By the time the car was driving, they were properly mounted with tubing coming out the top to an oil catch can.

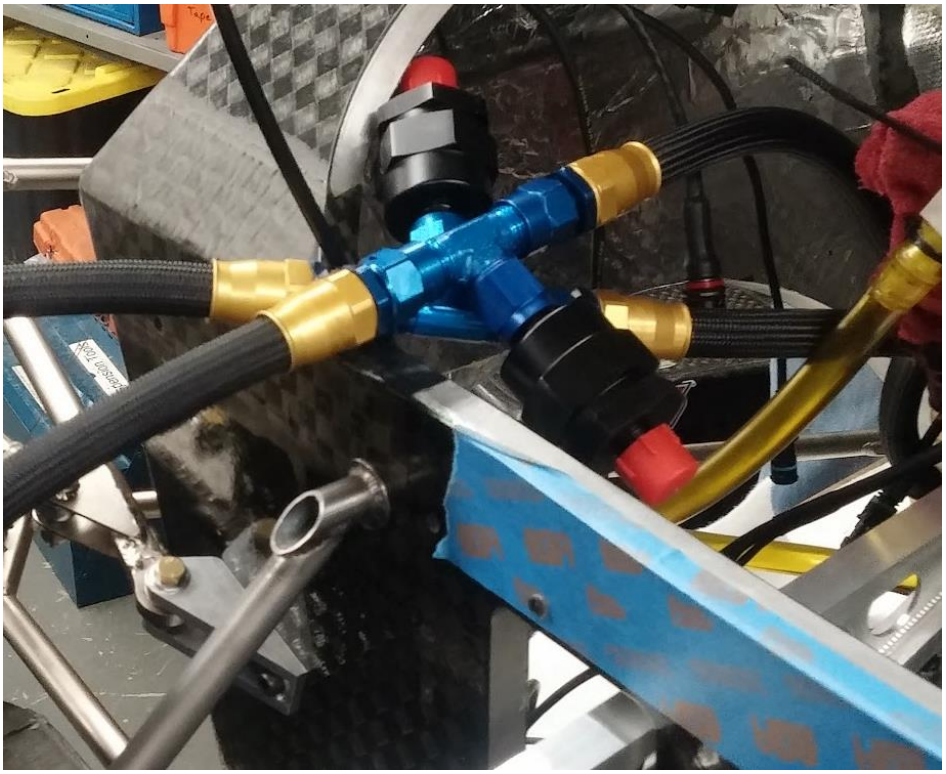

Figure A.86: Tee fittings and anti-siphon (or “check”) valves.

Catch Can and Overflow Lines

Once the oil catch can was completed (as explained in A3.4.2), it was mounted inside the engine bay. To hook it up to the system, the layout below was used. The two anti-siphon valves first connected together using a tee fitting, then, near the catch can, another tee fitting was used to add a short line of hose with a cover to act as a vent to atmosphere. The third leg of the tee connected to the catch can. Another inlet of the catch can connected to a line that linked the crankcase vent and transmission together. Finally, the catch can has an outlet leading back into the crankcase to keep oil in the system.

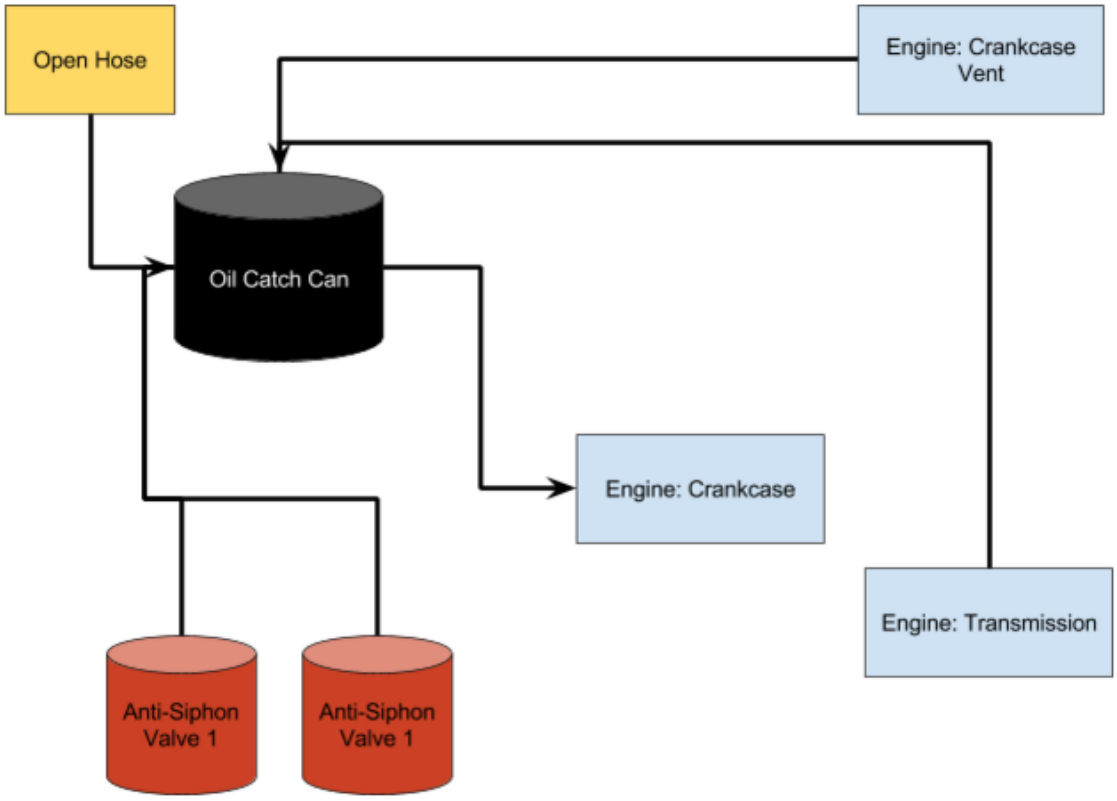

Figure A.87: Layout of the Tygon tubing lines (diagram contains a typo – valve on right should be labeled Anti-Siphon Valve 2).

A3.4 Other Parts

A3.4.1 Radiator Processing

Prep

Because the stock radiator ports were not oriented as desired, they were removed from all radiators using a vertical band saw. The holes corresponding to desired tube locations were then drilled out further using a step bit and finished with a ¾" drill bit. The holes that were unnecessary were left alone until being plugged. A couple more holes were needed in the radiators; these were added using a rotary broach.

Figure A.88: Example of a drilled out hole ready for a tube.

Tabs

Because the radiators need to be dampened in some fashion to isolate vibrations from the engine and avoid cracking, grommets needed to be placed in the holes for the tabs. Therefore, before welding tabs to the radiators, the holes were drilled out further to allow for a grommet and M5 bolt to mount the radiator to the diffuser. The grommets were sized based on what was available and allowed for an M5 bolt. To determine the proper size of the hole in the tab, calipers can be used to measure the outer diameter of the middle portion of the grommet. The process of drilling out the holes can be avoided if the holes are larger in the files sent to the laser cutting sponsor.

Once the holes were enlarged, the tabs were welded to the radiator using the diffuser and ducts as fixtures. The tabs were bolted into location on the diffuser, using washers to step it off the surface of the diffuser approximately as high as the grommet would be when compressed. The radiators were placed behind the tabs and a steel block was used to help prevent the radiators from slipping during welding.

Plugs

With the tabs in place, the focus shifted to plugging holes in the reservoir and adding tubes. For plugging the holes, small pieces of aluminum 6061 were turned down in a lathe. See Figure A.89 and Figure A.90 for the general design. Since a given port on the radiator may have different dimensions than the others, they need to be made specifically for each hole. The large diameter should be smaller than the outer diameter of the hole (Figure A.90) and the smaller diameter should just fit into the radiator; as with the jack bar and diffuser linkage inserts, a slight press fit is helpful when welding.

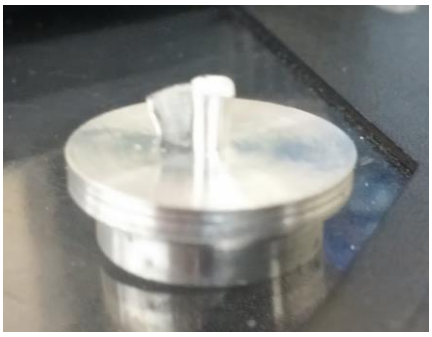

Figure A.89: Radiator plug. It is still excessively long, both on the flange side and the end that is placed inside the radiator. Both were sanded down in this case. Also, the top features material from parting that was removed.

Figure A.90: Plug resting in a radiator. Note that the radiator port was not drilled out completely; the tube was merely sawed off and the port sanded slightly for a smooth surface.

Figure A.91: Plug welded in and port sealed.

Tubes

Straight tubes were made out of ¾" outer diameter aluminum 6061, with 0.035" wall thickness. Lengths of approximately 50mm were cut off the tube. The smaller lengths were then placed in a lathe to use the turning tool to make sure the ends were squared off. Then, once the inside and outside were sanded until the material was smooth along the length of the tube, a beading tool was used to add a bead to the tube. This helps prevent water from leaking out where the tube interfaces with silicone hosing. Both sides should be beaded as the end that inserts into the radiator will have a lip to prevent the tube from falling inside.

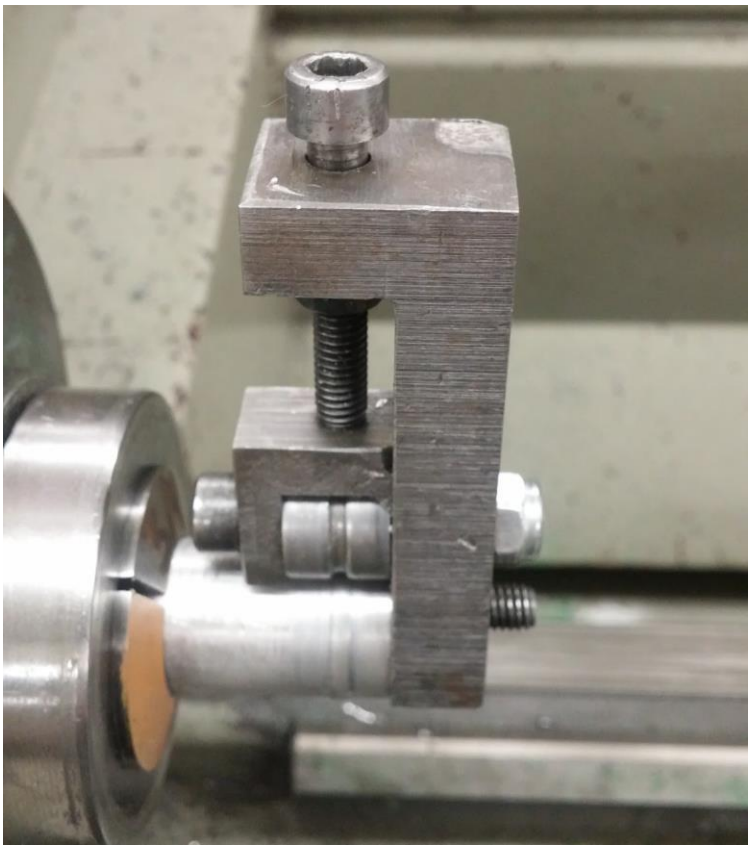

Figure A.92: Using a lathe helps to fixture the tube while beading.

Once beaded, the tubes were inserted into the desired ports. The first water radiator (driver's left) had some tricky geometry issues. In order to make it easier to get an angle relative to the face of the radiator reservoir where the tube was welded, the hole was drilled out further to allow the tube to come in at a tilt. The outlet of the radiator was made using a 90 degree piece that was found in the shop as attempts to bend new ones only resulted in tubes with deformations and flattening.

Figure A.93: Completed and installed radiator (second water radiator).

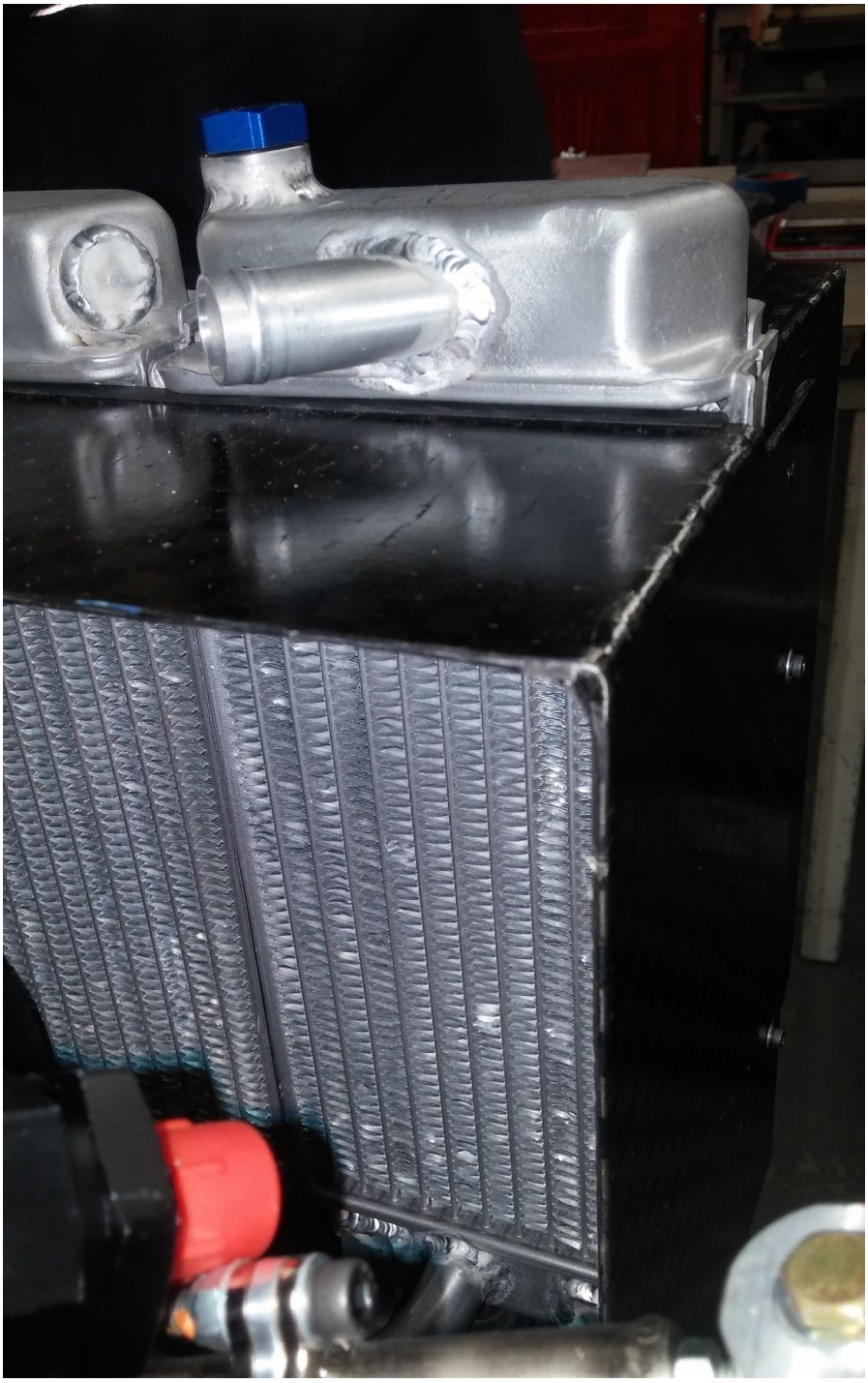

Figure A.94: Completed and installed radiator (first water radiator). The bottom of the image is obscured; a 90 degree piece of bent aluminum extends out of the radiator, pointing towards the oil radiator. The bend plane is parallel to the plane of the diffuser.

Oil Radiator

The only difference with the oil radiator is that rather than tubes, weld in bungs were used. This was primarily handled by Eric Bramlett. A portion of the bung was machined off (the side that welds onto the radiator). The bungs were then welded onto the radiator and AN fittings could then be screwed on.

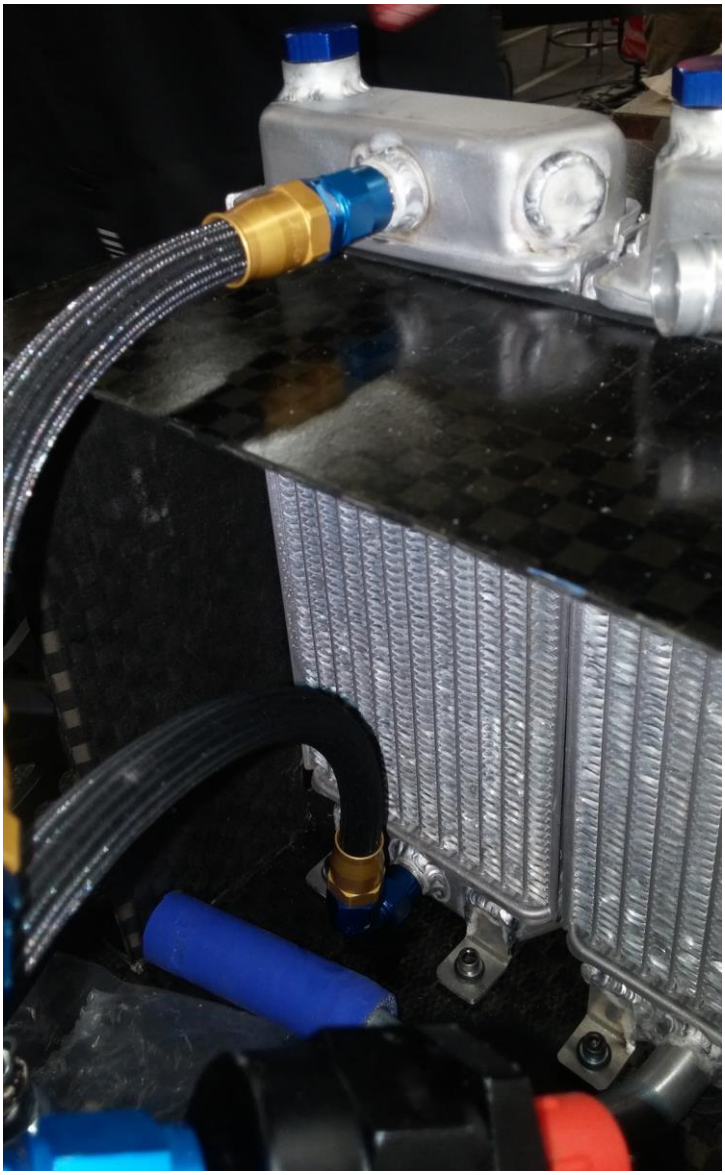

Figure A.95: Completed and installed radiator (oil radiator). The ports on the radiator are weld in bungs.

A3.4.2 Catch Cans

Both the oil and water catch cans were made using a cylinder approximately 115mm in diameter. As the cans both need to be able to hold 0.9 liters of fluid, the length would then need to be roughly 87mm. The cylindrical design helps to minimize the surface area of the can, and thus use less material. Less material leads to lower weight.

Fittings

The only constraint on fittings is that the vents must be at least ⅛” inner diameter hose. Thus, for the water catch can, two fittings were made: a ⅛” fitting to vent and a ¼” inlet port. The oil catch can was made with three ports, all ⅜”: two inlets and one outlet.

Each fitting was made by turning stock down on a lathe. The parts were not designed to hit any certain dimensions. Rather, the inner diameter of the ports were drilled to match the inner diameter of the hose. The stock was then turned down to an oversized diameter. Then, the majority of the stock was turned down further until a wall thickness of roughly 0.05” was achieved. However, the tip of the stock was not turned down at this point. Instead, the compound rest was used to create a barb at roughly 25 degrees. This helps the hose seal over the fitting. The carriage was moved further in in the X direction with a pass done using the compound rest each time until a piece of hose could be attached with relative ease over the barb, but still be secure on the fitting. The fittings were then parted with some material at the bottom still in stock diameter to provide a bonding surface.

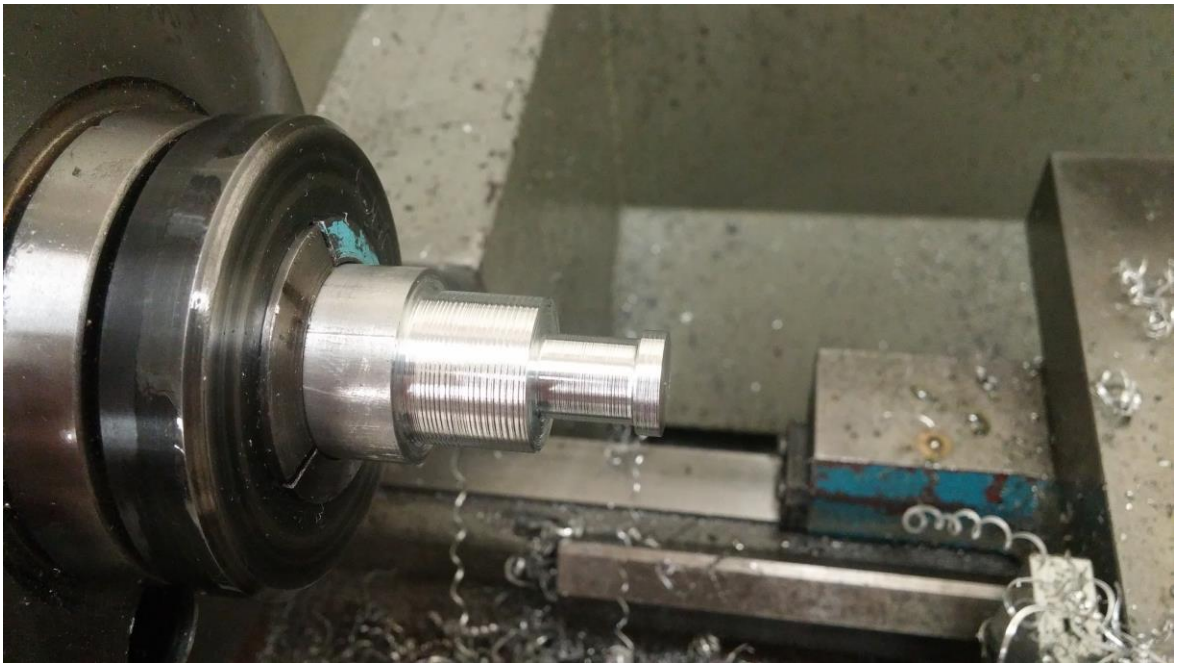

Figure A.96: Turning down the stock for one of the fittings. Note that at this step, the end has not yet been barbed.

Figure A.97: Completed fittings for the water catch can (⅛” vent, ¼” inlet).

Layup

As stated previously, the catch cans were made as cylindrical cans this year in an effort to lower weight. The layup for both cans follow a similar process, with some minor differences. To prep the mold for the catch cans, the first step was to lightly sand and clean the aluminum cylinder. Then, brown Airtech tape was used to create a smooth surface for laying up carbon without risking mechanical locking on the imperfect aluminum surface. This can be seen in Figure A.99. Wherever carbon was to be placed, the surface was covered with tape.

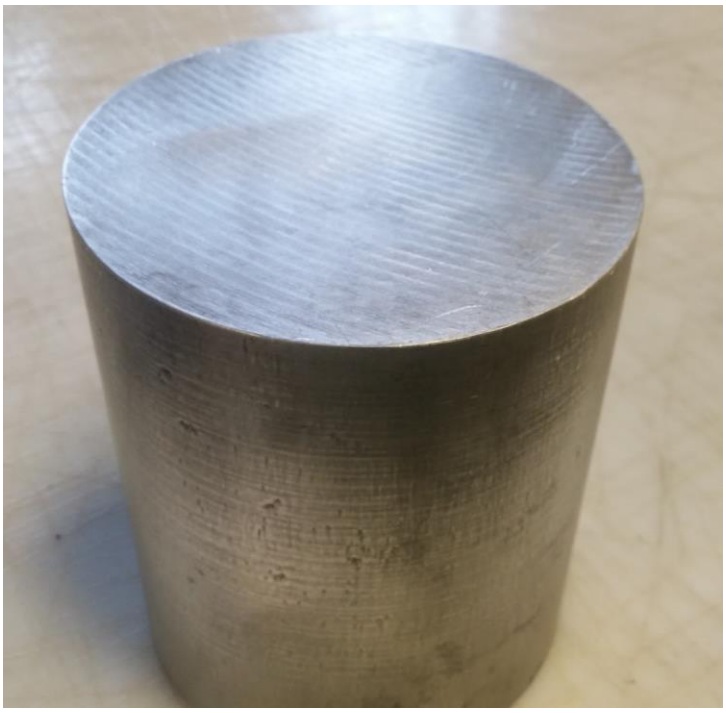

Figure A.98: Aluminum cylinder used as the mold for the catch cans.

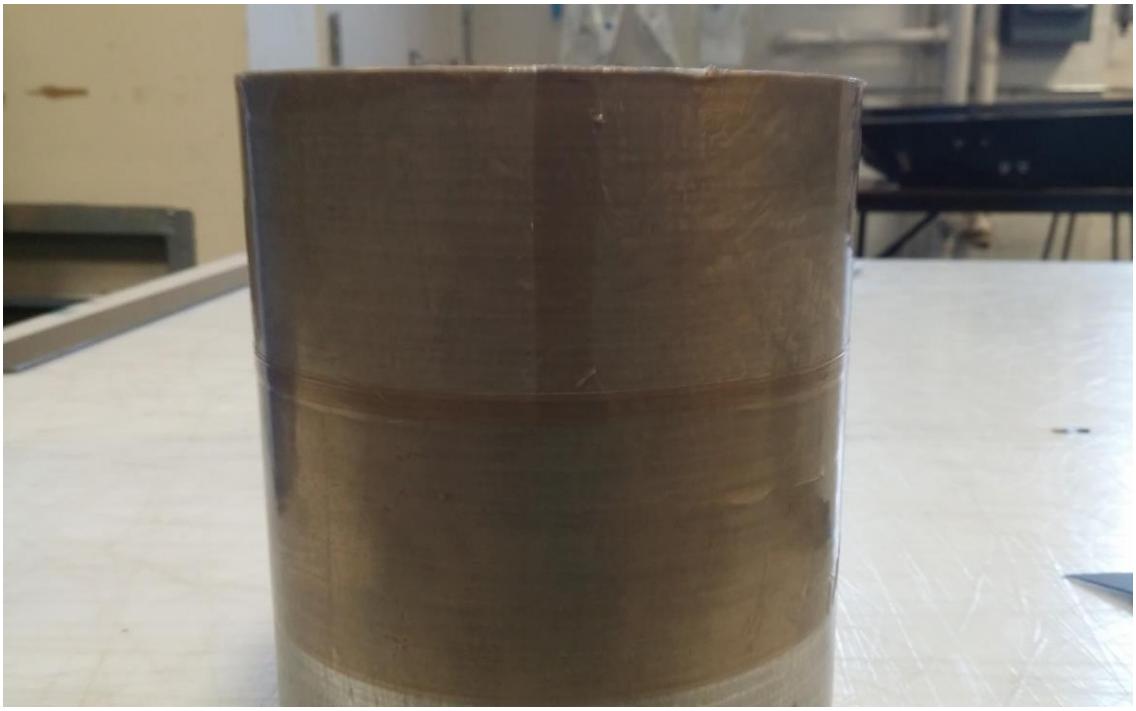

Figure A.99: Wrapping the catch can with tape to create a smooth layup surface.

Laying up the catch cans was straightforward compared to the ducts. The can has to be made of two parts and bonded together. The first piece made was the longer, “main body” of the catch can. The second is the cap. Layup is the same for both, with the mold being altered slightly and the rectangular pieces having different widths.

Layup began with the main body piece. The carbon was cut into two different shapes. A square of side length 130mm and a rectangle of 90mm by 400mm was cut for each layer. DIFFERENCE BETWEEN OIL AND WATER: the water catch can was made with only two layers of carbon. However, there were several leaks. It is recommended to use two layers of carbon as the added weight in epoxy ended up making both cans weigh roughly the same.

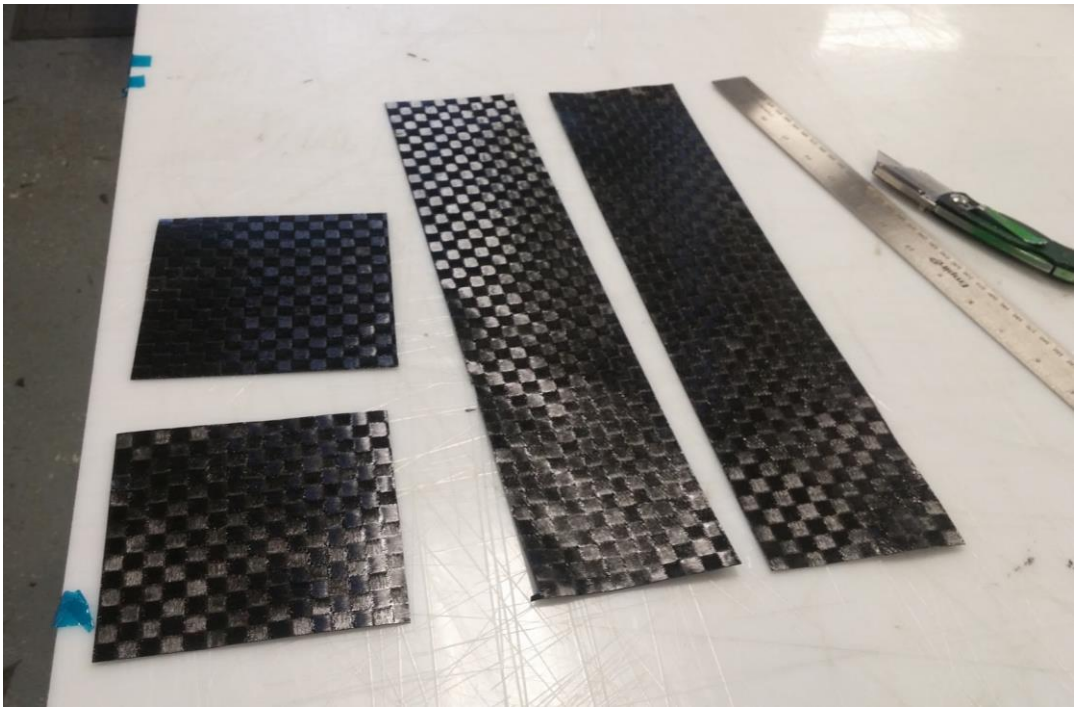

Figure A.100: Pieces used to make the main portion of the water catch can.

The rectangular pieces were oversized in length to ensure the strip would go all the way around the mold. The 90mm dimension was also oversized to be perfectly sure that the catch can volume would meet rules specifications.

The first piece to go on the mold were the squares. One square was placed, and the corners trimmed off. Then, relief cuts were made along the perimeter of the carbon from the edge to the mold to allow it to fold over the side of the cylinder. Then, a strip was placed on the edge of the mold, making sure to overlap the folds of the square piece. Once the first layer was on, the fittings were placed. For the water catch can, these were placed on the top surface of the main body, on opposite sides of the mold. See Figure A.102. For the oil catch can, only the outlet port was placed as the main body was the bottom of the oil catch can.

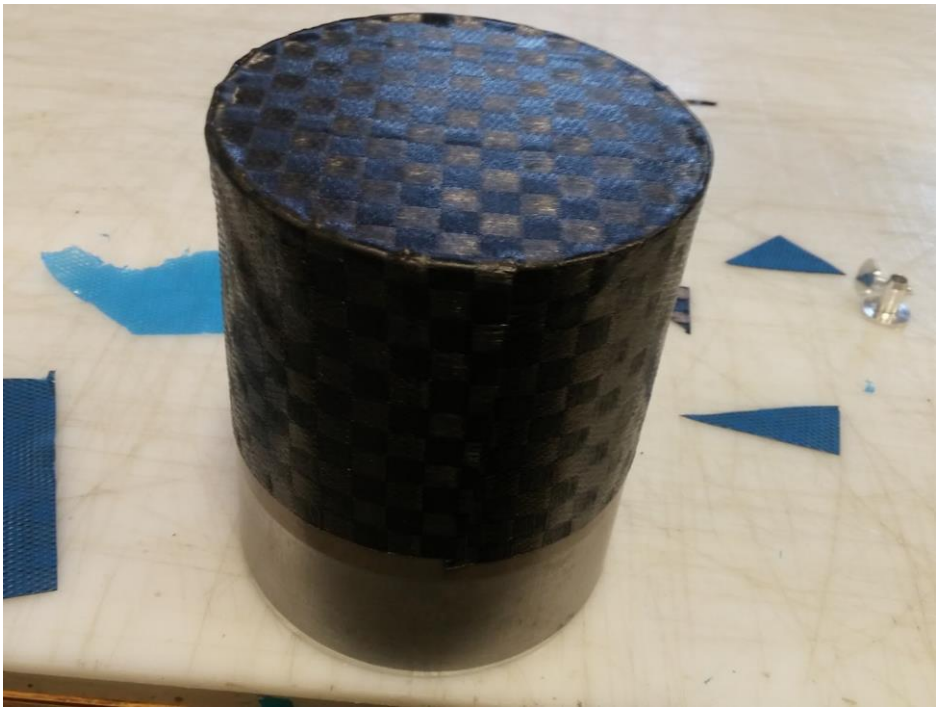

Figure A.101: First layer of carbon on the mold.

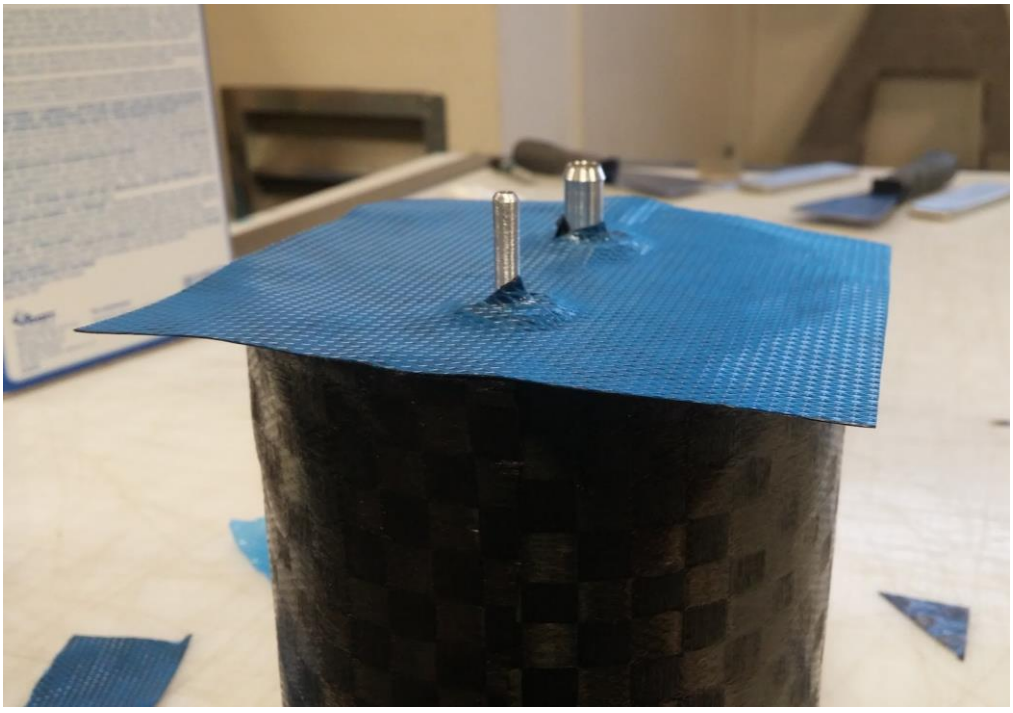

Figure A.102: Fittings sticking through the second piece of carbon on the top of the catch can.

The second layer of carbon was placed on the mold following the same procedure as the first layer, with cuts placed in the carbon for the ports. For the oil catch can, the third layer was added in the same fashion as the second layer.

In order to make the cap for the catch can, the mold had to be altered slightly by adding thickness so the cap could fit over the catch can. To determine how far out to space the layup surface, calipers were used to measure the cured carbon of the main body. Then, blue paint painter's tape was measured. The required number of pieces was found to be about 5 or 6 layers. The cylinder was wrapped in the blue tape until the spacing was correct, and a final layer of brown layup tape was used.

The layup procedure is the same as the main surface. The only difference is that the rectangular pieces that wrap around the mold were made to only be 25mm wide to create a bonding surface with the main body. For the oil catch can, the inlet and vent ports were placed on the cap surface on opposite sides.

Figure A.103: Completed catch can, prior to repairing holes.

The inner surface of the oil catch can pieces should be coated with Alpha Poxy to give it extra leak protection and prevent the oil from fouling the carbon.

Bonding

The catch cans were then bonded together using chemical resistant, high temperature epoxy. The outer surface of the main body was coated where the cap was to be placed. The caps were slid on and rotated in order to help spread epoxy. For the oil catch can, the inlet port was lined up with the outlet as the catch can was to be mounted at a tilt allowing the vent to be at the top of the can and the outlet at the bottom.

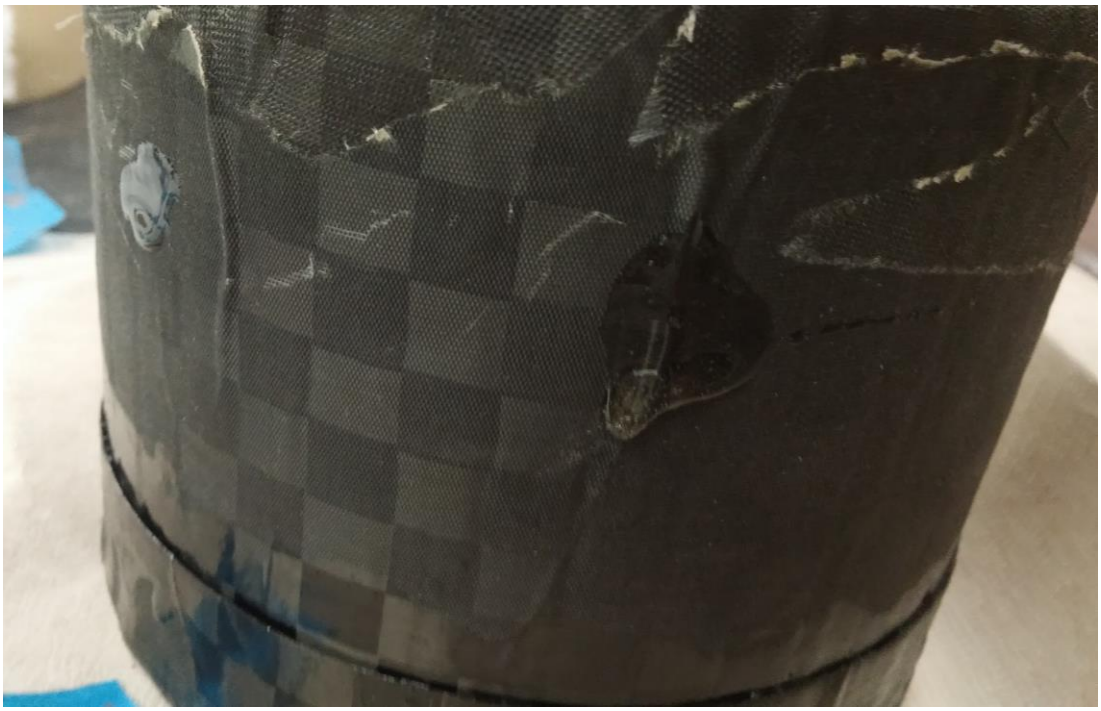

Figure A.104: Epoxy on water catch can to plug holes.

The water can showed signs of leaking. This may have been preventable with a third layer of carbon. To fix this issue, 5 minute epoxy was used to coat locations where leaks were found.

Figure A.105: The oil (left) and water catch cans.

Water catch can weight: 75g
Oil catch can weight: 75g

A3.4.3 Fan Mounting

Due to an oversight during design, the fan could not be mounted to the exit duct without special considerations to bolting it to the car. The solution selected was to epoxy bolts to the duct piece and then slide the fan on. Any extra bolt length can be cut off, as long as at least 2 threads are exposed when the fan is bolted onto the duct.

Figure A.106: Bolt head epoxied to inside of exit duct.

Figure A.107: The bolts now allow the fan to be fastened to the duct with just a nut. Access to the inside of the duct is no longer required.

Figure A.108: Fan mounting close up.

Figure 5.4.3.4: Fan mounted to exit duct on car.

Appendix B: Code

B.1 Heat Transfer Calculations for Radiator Configurations

```
clear
clc
clear all
```

```
dynoData = '7_19_2015_Grieshaber.mat'; % Name of the exported dyno data
file
load(dynoData);
flowConversion = 1.66667e-5; %1 l/min in m^3/s
% Water properties at 95 C
rho_water = 962; %kg/m^3
cp = 4.213; %kg/kg*K
% Data from flow test (dyno)
waterFlow = Eng_Coolant_Flow.Value*flowConversion; %water flow rate,
m^3/s
oilFlow = Eng_Oil_Flow_Supply.Value*flowConversion; %oil flow rate,
m^3/s
engRpm = Engine_RPM.Value; %engine speed, rpm
% Plot dyno data, water flow vs rpm
scatter(engRpm, waterFlow/flowConversion)
grid on, title('2014 Dyno Flow Test'), ylabel('Coolant Flow [l/min]')
xlabel('Engine Speed [rpm]')
figure()
% Endurance Data
fsg15Data = 'FSG15ENDURANCE.mat'; % FSG15 data, exported from Motec at
10Hz
fsa15Data = 'FSA15ENDURANCE.mat'; % FSA15 data, exported from Motec at
10Hz
load(fsa15Data); % Load desired data set
engRpmEnd = Engine_RPM.Value;
tempIn = Coolant_Temperature.Value;
tempOut = Engine_Temp.Value;
dT = tempOut - tempIn;
carSpeed = Corr_Speed.Value;
if length(carSpeed)<length(dT)
carSpeed(end+1) = 0;    %Comment out for FSA15
end
% Heat Transfered To Water - Third Degree Polynomial
coefWaterFlow = polyfit(engRpm, waterFlow/flowConversion, 3);
term1 = coefWaterFlow(1).*engRpmEnd.^3;
term2 = coefWaterFlow(2).*engRpmEnd.^2;
term3 = coefWaterFlow(3).*engRpmEnd;
waterFlowEnd = (term1+term2+term3)*flowConversion;
q_water = rho_water*waterFlowEnd*cp.*dT; % Heat transfered from engine
to water
scatter(engRpmEnd, q_water)
grid on, xlabel('Engine Speed [rpm]'), ylabel('Heat Transferred to
Water [kW]')
title('Heat Rejected to Coolant, FS Austria 2015')
figure()
% Radiator Cross Sections
Acur = 0.07475; %m^2
Asm = 0.039; %m^2
Alg = 0.057368; %m^2
rads = [Acur Asm Asm Alg 0.0266];
kalum = 207; % Aluminum conductivity
% Water properties at 97C, 150kPa
rhow = 960.6; % Density
Prw = 1.846; % Prandtl number
muw = 0.000291; % Viscosity
cpwater = 4213; % Specific heat
kw = 0.6641; % Conductivity
```

```
% Air properties @ 50C
rhoa = 1.092; % Density
Pra = 0.7221; % Prandtl number
mua = 0.00001963; % Viscosity
cpair = 1006; % Specific heat
nua = 0.00001798; % Kinematic viscosity
ka = 0.02735; % Conductivity
% Iterate through different radiator set ups
% First is baseline
% Second is small radiators in series
% Third is small radiators in parallel
% Fourth is a new, single, large radiator
% Last is a different small radiator, series
for j = 1:length(rads)
      Arad = rads(j);
      Afact = Arad/Acur; % This factor is used to scale radiator sizes
up or down

      Thi = tempOut;
      Tci = 30; % Ambient air temperature

      % Water flow
      % For parallel flow: split the mass flow rate in half
      if j==3
      Qwater = waterFlowEnd/2; % Parallel flow rate
      else
      Qwater = waterFlowEnd; % All other flow rates
      end
      mwater = Qwater*rhow; % Mass flow rate
      Cwater = cpwater*mwater;

      % Air flow
      if j==1
      baseair = 0.37; % Baseline
      elseif j ==4
      baseair = 0.39; % Single large rad
      else
      baseair = 0.22; % Each small rad
      end
      mair = baseair*carSpeed/65; % Scale the airspeed from CFM using
Motec car speed data
      Cair = cpair*mair;

      % Radiator tube dimensions - Measured from baseline radiator
      Ntube = 31*Afact; % Number of tubes; scaled to analyze
performance of other radiators
      Wtube = 0.023; % Tube width
      Htube = 0.0045; % Tube thickness
      Ltube = 0.2286; % Tube length

      Actube = Wtube*Htube; % Cross section of tube
      Ptube = 2*(Wtube+Htube); % Perimeter of tube

      % Radiator fin dimensions - Measured from baseline radiator
      Nfins = 288; % Number of fins along one tube
```

```
      Lfin = 0.006/2; % Length of fin (approximated as flat plate 1/2
the distance between tubes
      Wfin = 0.023; % Fin width (core thickness)
      Hfin = 0.00014; % Fin thickness

      Lc = Lfin+Hfin/2; % Corrected fin thickness

      Afin = 2*Wfin*Lc; % Surface area per fin
      Ab = 2*Ltube*Wtube - Hfin*Wfin*Nfins; % Base of tube area
      Afinbase = Nfins*Afin+Ab; % External surface area per tube

      Aint = 2*(Wtube+Htube)*Ltube*Ntube; % Total internal surface area
of all tubes
      Aext = Afinbase*Ntube; % Total external surface area of all tubes

      % Water-Side Calculations
      Dhwater = 4*Actube/Ptube; % Hydraulic diameter
      vwater = Qwater/(Ntube*Actube); % Water velocity
      Rewater = rhow*vwater*Dhwater/muw; % Reynolds number
      % Check for turbulence, apply proper correlation
      for i=1:length(Rewater)
      if Rewater(i) >5000
            % Turbulent - Use Gnielinski Correlation
            f(i) = (0.79*log(Rewater(i))-1.64).^(-2);
            Nuw(i) = (f(i)/8).*(Rewater(i)-
1000).*Prw/(1+12.7.*(f(i)/8).^(1/2).*(Prw^(2/3)-1));
      else
            % Laminar - Value from interpolating from table
            Nuw(i) = 4.96;
      end
      end
      hwater = Nuw*kw/Dhwater; % Convective heat transfer coefficient

      % Air calculations
      vair = mair/(rhoa*(Arad-Ntube*(Ltube*Htube+Nfins*Lc*Hfin))); %
Air velocity
      Reair = vair*Wfin/nua; % Reynolds number
      % The below equation assumes Re<5E5
      Nuair = 0.664.*Reair.^(1/2).*Pra^(1/3); % Nusselt number - flat
plate approximation
      hair = Nuair*ka/Wtube; % Convective heat transfer coefficient
      % Air convection efficiency calculations for fins
      m = (2*hair/(kalum*Hfin)).^0.5;
      etafin = tanh(m*Lc)/(m*Lc);
      etao = 1-Nfins*Afin/(Afinbase)*(1-etafin);

      % Epsilon - NTU (effectiveness - Number of Transfer Units)
calculations
      % Determine Cmin and Cmax
      for i=1:length(Cair)
      if Cair(i) >= Cwater(i)
            Cmin(i) = Cwater(i);
            Cmax(i) = Cair(i);
      else
            Cmin(i) = Cair(i);
```

```
            Cmax(i) = Cwater(i);
      end
      Cr(i) = Cmin(i)/Cmax(i);
      end
      UA = 1./(1./(etao*hair*Aext)+1./(hwater*Aint)); % Overall heat
transfer coefficient
      NTU = UA/Cmin; % Number of Transfer Units
      epsilon = 1-exp((1./Cr).*NTU.^0.22.*(exp(-Cr.*NTU.^0.78)-1)); %
Effectiveness
      q = epsilon.*Cmin.*(Thi-Tci); % Heat transfered from water to air

      % Check for additional processing
      if j==2
      % Small, series - Use same effectiveness, check heat rejected
from
      % second radiator and return sum
      Tho = Thi - q./(mwater*cpwater);
      q2 = epsilon.*Cmin.*(Tho-Tci);
      qtot(:,j) = q+q2;
      elseif j==5
      % Other small, series - Use same effectiveness, check heat
rejected
      % from second radiator and return sum
      Tho = Thi - q./(mwater*cpwater);
      q2 = epsilon.*Cmin.*(Tho-Tci);
      qtot(:,j) = q+q2;
      elseif j==3
      % Small, parallel - Double heat rejected, assuming equal rates
for
      % each radiator
      qtot(:,j) = q*2;
      else
      % Any other case, return the calculated heat rejected to air
      qtot(:, j) = q;
      end
end
% Plot the different heat rejection trends
plot(qtot(:,1)/1000, 'k')
hold on
plot(qtot(:,2)/1000, 'r')
plot(qtot(:,3)/1000)
plot(qtot(:,4)/1000,'m')
% Plot heat added to water for comparison
%plot(q_water, '-.')
% Plot alternative series radiator
%plot(qtot(:,5)/1000)
grid on
title('Heat Rejection Projections, FS Austria 2015 Data')
ylabel('Heat Rejected (kW)')
legend('2015 Baseline','Series Small', 'Parallel Small','Single Large')
%axis([3000 3500 0 20]) % Focus plot on an arbitrary range of values
hold off
```